NOAA Technical Memorandum NOS ORCA 121

National Status and Trends Program
for Marine Environmental Quality

Pollution History of the Chesapeake Bay

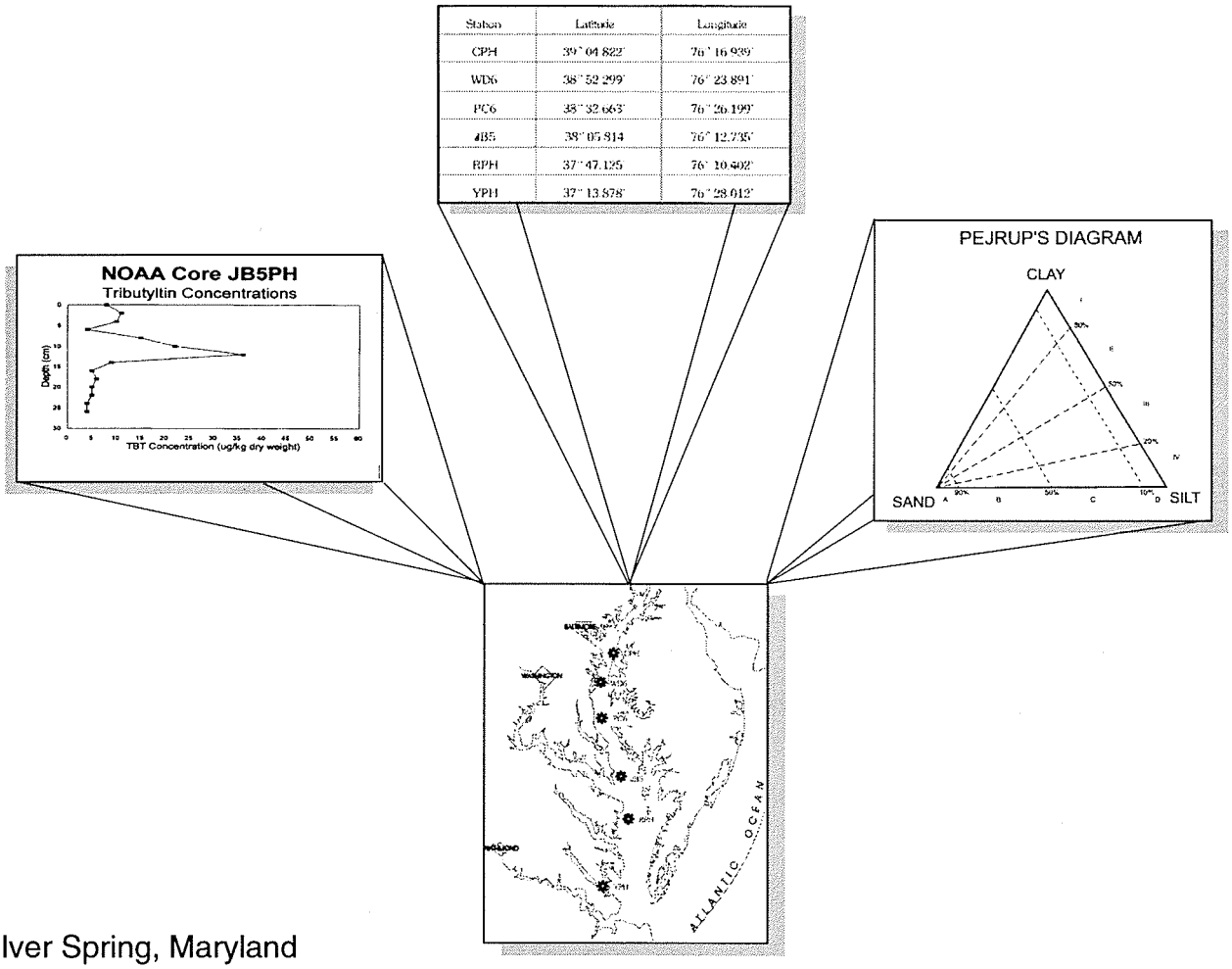

Silver Spring, Maryland
March 1998

US Department of Commerce

noaa National Oceanic and Atmospheric Administration

Coastal Monitoring and Bioeffects Assessment Division
Office of Ocean Resources Conservation and Assessment
National Ocean Service

Coastal Monitoring and Bioeffects Assessment Division
Office of Ocean Resources Conservation and Assessment
National Ocean Service
National Oceanic and Atmospheric Administration
U.S. Department of Commerce
N/ORCA2, SSMC4
1305 East-West Highway
Silver Spring, MD 20910

Notice

NOAA Technical Memorandum NOS ORCA 121

Pollution History of the Chesapeake Bay

Grace S. Brush
The Johns Hopkins University

James M. Hill
The Maryland Geological Survey

Michael A. Unger
The College of William and Mary

Silver Spring, Maryland
March 1998

United States
Department of Commerce

William M. Daley
Secretary

National Oceanic and
Atmospheric Administration

D. James Baker
Under Secretary

National Ocean Service

W. Stanley Wilson
Assistant Administrator

The National Oceanic and Atmospheric Administration
National Status and Trends Program
Core Project Report Series

Foreword
by Nathalie Valette-Silver

Historical trends in contamination of estuarine and coastal sediments:

The composition of surface waters in rivers, lakes, and coastal areas has changed over time. In particular, changes due to the Industrial Revolution, dating from the middle of the last century, are very well known. These changes are expressed by increased levels of components, such as trace metals and nutrients which occur naturally, but also by the increase of anthropogenic compounds, such as polychlorinated biphenyls (PCBs) and pesticides.

Since the early 1960's, regulatory measures have been taken to decrease the amount of pollutants entering our waterways, but the bulk of these environmental measures were not enacted until the 1970's. Because of the scarcity of accurate data, due to the lack of sensitive techniques or of regular data collection in the past, the extent of the past pollution and the effect of the recent legislative limitations is often difficult to assess.

The analysis of sediment cores presents a way out of this dilemma. Most pollutants have an affinity for and adsorb easily onto sediments and fine particles. Therefore, by analyzing cores of undisturbed sediments it is possible to assess the historic pollution of a given system. Sediment cores reflect not only the history of pollutant concentrations but also register the changes in the ecology of a water body. For example, changes in estuarine eutrophication are reflected in the concentration of organic matter, nitrogen, and phosphorous, while lake acidification is translated into changes in diatom assemblages.

The use of cored sediments to reconstruct the chronology of coastal and estuarine contamination is not, however, devoid of problems and caution must be exercised. Sediment mixing by physical or biological processes can obscure the results obtained by such studies, and sophisticated methods must be used in these cases to tease out the desired information.

The NS&T Core Project

Between 1989 and 1996, the National Status and Trends Program sponsored research that gathered information on long term trends in contamination of US coastal and estuarine sediments. In this project, ten areas have been targeted. They include:

1) On the East coast:
   - •Hudson/ Raritan estuary
   - •Long Island Sound marshes
   - •Chesapeake Bay
   - •Savannah Estuary

2) On the Gulf coast:
   - •Tampa Bay
   - •Mississippi River Delta
   - •Galveston Bay

3) On the West coast:
   - •Southern California Bight
   - •San Francisco Bay
   - •Puget Sound

Presently, all the studies are completed and reports are, or will soon be, directly available from the cooperators. One of the most important results of the NS&T studies and of other similar studies reported in the literature, is the observed decline in recent years of many organic and inorganic contaminants in the sediments. It is very encouraging to know that mitigating measures taken in the 1970's have been effective. This has shed a hopeful light on the potential success of future efforts to curb even more coastal and estuarine pollution.

In an effort to widely disseminate the results of these studies, the NS&T Prgram, in collaboration with the authors, is publishing some of the reports as NOAA Technical Memoranda. This study covering Chesapeake Bay is the third one to be published in this series.

POLLUTION HISTORY OF THE CHESAPEAKE BAY

Final Report
NOAA Project NA27OA0450

Submitted by

Grace S. Brush, The Johns Hopkins University
James M. Hill, The Maryland Geological Survey
Michael A. Unger, The College of William and Mary

August 9, 1997

POLLUTION HISTORY OF THE CHESAPEAKE BAY

TABLE OF CONTENTS

EXECUTIVE SUMMARY

Sediment cores were collected at six sites throughout the main stem of the Chesapeake Bay as part of the NOAA Status and Trends program. The sites were selected to encompass the range of geochemical environments found in the Bay, where high temporal resolution was expected. This multi-disciplinary project examined the historical record, focusing primarily on recently deposited sediments, to assess natural processes operating in the Bay, and the extent of human influences on these processes. The scope of this project was to measure a range of physical properties and inorganic chemical species as indicators of natural and anthropogenic processes within the sediment column.

The two northernmost cores are strongly influenced by input from the Susquehanna River, both in regard to physical transport based on terrigenous carbon loading, and geochemical processes indicated by variations in sulfur and iron speciation. In addition, the cores' geochemistry differs from normal marine sediments in that gas is present. The presence of gas tends to preserve acid volatile sulfides (AVS) and organic carbon, and alter the suite of diagenetic minerals that may form.

The two mid-Bay cores also have gas present, and because they are located in paleochannels are characterized by high sedimentation rates. Fluvial influence appears negligible; the primary source of carbon is plankton. The diagenetic processes within the last 30 years appear well-behaved and show little variation in carbon and sulfur chemistry.

Cores in the southern part of the Bay have lower sedimentation rates. Gas is not present in the southernmost core, while gas in the second southern core is present over a meter into the sediment As a result, organic carbon from plankton is not well preserved and the fraction of AVS sulfur is low. Diagenetic processes within the last 30 years appear well-behaved.

There is little change in the enrichment factors of trace metals analyzed over the past 30 years. Generally, variations in metal behavior follow environmental conditions with regard to fluvial influence or variations in geochemical conditions. There is a trend of increasing metal concentrations in the northernmost site, starting in the mid 1960s, peaking ~1981, and then decreasing rapidly in the mid 1980s. Metals showing this trend are lead, zinc and copper.

Zinc and copper are significantly elevated throughout the Bay when compared with "pristine" sediments collected at the same site. Lead is elevated to some extent in 4 of the 6 cores.

Comparisons of variations in Baywide loading of recent sediments with pristine sediments show the influence of the Susquehanna River. Manganese, zinc, nickel, chromium and copper have elevated levels in the northernmost samples and decrease to

background levels in mid-Bay. South of this point, enrichment factors of manganese, nickel and chromium close to 1, indicate that compared to pristine sediments recent sediments are not enriched. On the other hand, enrichment factors of 2 to 2.5 throughout the Bay for both copper and zinc indicate anthropogenic loading of these metals. The ubiquitous nature of the loading suggests atmospheric loading as a possible source of these metals, and that atmospheric loading is equivalent in magnitude to background loading.

Concentrations of PCB, pesticides, butylins and PAH analyzed from 3 box cores were very low. The core data indicates that regulations imposed in the late 1980s to reduce tributyltin are having an effect in the Bay. Because of high sedimentation rates, it was not possible to get a history of contaminants over a long enough period to compare the period of pre-contaminants with later times when contaminants were used. It is recommended that longer cores be analyzed to get a more complete picture.

INTRODUCTION

The Chesapeake Bay is a complex environmental system made up of dynamic geological and biological processes influenced by human activities. Effective stewardship of the Bay's resources requires an understanding of processes governing estuarine natural dynamics in order to assess and regulate the extent of human influences. This requires examining temporal dynamics preserved in the sedimentary record in order to correlate human activities with observed historic changes. This project is part of the NOAA Status and Trends program, the mission of which is to examine the historical record, focusing primarily on the past 30 years, in order to determine the extent of human influence on the Bay system. Human impact is assessed by measuring a wide range of chemical species, biological markers, and physical parameters, and comparing the state of these parameters with the period of time when human influence was minimal.

Sample locations

Six sites were selected in the main stem of the Chesapeake Bay for the study. The criteria for site selection were:

(1) Subbottom profiles based on shallow seismic data (Coleman et al. 1990; Halka et al. 1993). This provides information on the geologic setting of the sediments.

(2) Existing sedimentation rate data, including changes in historic bathymetry (Kerhin et al. 1988) and Pb^{210} and pollen dating analyses (Brush 1989). Selecting areas of high deposition ensures maximum temporal resolution.

(3) Sediment type (Kerhin et al. 1983). Fine-grained sediments provide the best record for chemical species which are affected by human activities, because trace elements, nutrients and trace organic compounds are associated with fine-grained sediments (Forstner and Wittman 1979). In addition, these sediments are more easily penetrated thus providing ready access to older sediments.

(4) Representative coverage of different environmental settings in the Bay. There are four geochemical reservoirs in the main stem of the Bay (Hill 1984; Hill 1988). Three of these are in fine-grained sediments - River Dominated, Transitional and Near Marine, and the fourth is in sandy sediments - Quartzose. These reservoirs reflect not only different sources of sediment, but also differences in geochemical environments.

The sites selected are shown in Fig. 1. Latitude and longitude based on differential global positioning system (DPGS) are also shown on Fig. 1.

Environmental Setting

CPH is located in the main stem of the Chesapeake Bay off the mouth of the Chester River. This site is within the southern portion of the River Dominated reservoir of the Bay. The reservoir is dominated by input from the Susquehanna River. The water column in this area is characterized by the lowest salinities in the main stem of the Bay, ranging from fresh water at the mouth of the Susquehanna to a seasonal average of ~15 ‰ at a latitude of 39°00'. Seasonal anoxic events do not generally occur in the water column of this reservoir.

Sediments in this area are the deposited sediment load from the Susquehanna River. They are fine sediments with a general seaward fining sequence, with the highest metal and carbon concentrations in the main stem of the Bay. Diagenetically, the bacterial decomposition processes in this area are carbon and sulfate limited sulfate reduction and methane formation. Within the upper meter of sediment, sulfate is entirely reduced; however, there are no free sulfide species in the interstitial waters. Methane is ubiquitous in this reservoir year round, which interferes with obtaining seismic records.

WD6 and PC6 are located near the mouths of the West River and Parker Creek respectively. These sites bracket the northern and southern portion of the Transitional Reservoir. This reservoir encompasses the northernmost extent of seasonal anoxia, and the southernmost extent of the fluvial influence of the Susquehanna. Trace metal levels are strongly influenced by the Susquehanna River (Sinex and Helz 1981; Cantillo 1982). On the other hand, carbon and sulfur contents reflect a marine influence based on Sulfur:Carbon ratios (Berner and Raiswell 1984). Both erosion and deposition occur in the bottom sediments of the reservoir with an overall net erosion.

Diagenetically, the bacterial decomposition processes alternate between carbon limited and carbon and sulfate limited sulfate reduction, depending upon the seasonal extent of mixing of fresh water from the Susquehanna. Free sulfide species occur in the interstitial waters during periods of higher salinity. Methane formation occurs in this reservoir, but is limited to sediments within the paleochannels. Gas saturated cores tend to preserve variations in the geochemical environment, specifically in regard to variations in water column conditions.

JB5, RPH AND YPH are located within the Near Marine reservoir in Maryland and Virginia. JB5 is situated near the mouth of Jerome Creek, north of the Potomac River. RPH is near the mouth of the Rappahannock River, while YPH is within the mouth of the York River. Within the Near Marine reservoir, the interstitial water chemistry is relatively stable due to the reduced influence of freshwater input. Free sulfide is present in the sediments year round as a result of carbon-limited sulfate reduction. Methane is found in this reservoir in sediments confined to infilled paleochannels. JB5 and RPH are located within a paleochannel.

Trace metals are at their lowest levels in the fine-grained sediments at these locations in the Bay. Because of the low levels, atmospheric deposition is postulated as a significant source of some of the metals. Carbon occurs in lower concentrations than in the other two reservoirs. The relationship between carbon and sulfur reflects marine environmental conditions.

Sample Collection

Field

Samples were collected from the Maryland Department of Natural Resources R/V Discovery research vessel, using three different coring systems - box core, gravity core, and piston core. Box core samples were collected using a stainless steel box core with a

8x16 cm area capable of collecting samples to a depth of 30 cm. Samples collected from the box core were designed to obtain a large amount of sample in depths expected to include the last 30 years of deposition. Analyses performed on these samples were: grain size, water content, trace metals Hg and As, total C, N and S, trace organic compounds, and organo-tin speciation. Trace metal and physical parameters were measured on samples taken from the core by subcoring the box core with a cellulose acetate butyrate (CAB) core liner. Samples for trace organics and organo-tin speciation were collected immediately upon retrieval of the cores. Sediment samples were collected at a distance no closer than 1 cm to the CAB liner in order to prevent organic contamination, and at depths of 2 cm intervals using stainless steel sampling utensils. These samples were refrigerated at 4°C upon collection. Upon return to the dock, samples were immediately transported to the Virginia Institute of Marine Sciences (VIMS) for analyses. Sampling of the sediment in the CAB subcore was performed at the Maryland Geological Survey's laboratories.

Gravity cores were collected using a Benthos type corer with a CAB core liner. The penetration of this sampling device is ~ 1 meter. The purpose of collecting this core was to assure continuity between the box core and the piston core. Collection and transportation of the piston cores *can* disrupt the upper 0.5 meter, near the sediment water interface, effectively homogenizing the sedimentary record. If this should occur, it would be difficult to place the box core sample in context with the deeper sediments. The intent was that the gravity core could bridge the record between sediments in the box core and the piston core. However, this was not necessary, because the piston cores were not disrupted during sampling and transportation, based on X-rays and Optical Scans.

Piston cores, with CAB liners, were collected at each site to provide an historical framework for the more recent changes observed in the shallow sediments collected in the box cores. These cores had penetrations of ~ 5 meters at each site.

All cores were transported back to the laboratory at the end of each day, and stored at 4°C in walk-in refrigerators, until the cores were processed.

Laboratory

All cores were X-rayed using a Med-Torr X-ray unit, modified to accept core samples. Images were processed using a Xeroradiographic developing system. Following this, the cores were extruded from the core liners, split in half lengthwise using an electro-osmatic core cutting device, and sealed in clear polyethylene sheeting. Cutting the core in this manner provides a flat, undisturbed surface, and the polyethylene prevents oxidation and drying of the sediment. One-half of the split core was sealed, labeled, and sent to Johns Hopkins University for pollen, carbon^{14} and lead^{210} dating. The other half was optically scanned using a modified Gilford spectrophotometer (see Hill et al. 1992). Optical scanning measures the reflectance of light at a specific wave length (in this case 520nm), from the core's surface. Spatial resolution of the optical scanning system is 3 mm. Subsequent to X-ray and optical scanning, samples were collected. Samples from the subcore taken from the box core, were collected at 2 cm intervals, corresponding to

the intervals collected for trace organics and organo-tin analyses. Samples were collected from the gravity and piston cores based on features observed in the X-rays and optical scans. Descriptions of the cores based on optical scans, X-rays and visual examination are given in Appendix I.

SEDIMENT CORE CHRONOLOGIES AND SEDIMENTATION RATES

Methods

Dating cores

Three methods were used for dating the sediment cores, lead-210, carbon-14 and pollen analysis. Lead-210 has a half-life of 21 years, and therefore has the potential for dating sediments deposited within the last century. Carbon-14 has a half-life of 5,770 years and is capable of providing dates ranging from 500 to 50,000 years. Pollen analysis is used in two ways for dating sediments. Historically dated changes in vegetation represented by changes in the pollen assemblage allow dating of horizons in the cores whic show those changes (Table 1).

Table 1. Pollen horizons used for dating sediment cores in CB. The history of land use differed geographically, so that the date assigned to a horizon with a particular percentage of ragweed is not similar for all cores throughout the area; hence the different dates given for one category of land use change.

Date of horizon	Change in vegetation/land use	Pollen indicator
1930 (1923-1927)	demise of American chestnut	decrease in chestnut pollen to <1%
1910 (1908-1912)	decline of chestnut (disease)	decrease in chestnut pollen
1840 (1820-1860) or 1780 (1760-1800)	40-50% land cleared	% ragweed pollen >10; oak to ragweed pollen ratio <1 - <5
1650 (1640-1660) or 1730 (1720-1740)	<20% (often <5%) land cleared for initial and tobacco farming	% ragweed pollen >1 to <10; oak to ragweed pollen ratio >1->5
pre-European	Indian agriculture	% ragweed pollen <1 or 0

The pollen concentration method (Brush 1989) was used to calculate sedimentation rates for individual samples within a core from which dates for those samples can be extrapolated.

Sedimentation rates

Average sedimentation rates between dated horizons (the length of the core between dated horizons/the length of time spanned by that interval of the core) can be used to construct chronologies by dividing each 1 cm sample of the core by the average sedimentation rate, which gives the number of years in which the sample was deposited. However, average sedimentation rates between dated horizons are not useful for developing chronolgies in estuarine sediment cores, because of the high variability in sedimentation rates within and between cores, related to estuarine dynamics. To overcome this difficulty, sedimentation rates can be calculated for each sample in the core,

by adjusting the average sedimentation rate between dated horizons to the pollen concentration for each sample (Brush 1989), using the equation

$R_{0\text{-}1} = (n/n_{0\text{-}1})R$

where $R = d/t$ = average sedimentation rate between 2 dated horizons,

n = average pollen concentration between 2 dated horizons,

$n_{0\text{-}1}$ = pollen concentration in an individual sample,

d = depth

t = number of years between dated horizons.

The method assumes that when vegetation cover and species composition are similar, total pollen rain is more or less uniform and that most pollen in the sediment is wind-transported and enters the estuary from the atmosphere. Pollen grains are small particles that have transport properties similar to fine silt and clay. If the majority of the pollen introduced into the estuary is wind blown from terrestrial vegetation and thus independent of sediment (silt and clay mainly) introduced with river runoff, and if pollen influx is more or less uniform (no significant change in species composition and cover), the pollen concentration in any sample in the core will reflect the rate of accumulation of the other particles that make up the sediment. If the rate of sediment accumulation increases, the concentration of pollen will be correspondingly less and if sediment accumulation decreases, pollen concentrations will be correspondingly greater. Using these assumptions, sedimentation rates for each sample in a core can be calculated. Once a sedimentation rate is derived for different samples in a core, the number of years required for the deposition of that layer can be calculated by dividing the sedimentation rate for the particular sample by the depth of the sample. The method has been verified by comparing pollen-derived chronologies of fires, storms and other events with historical chronologies of the same events (Brush 1989). The resolution of the resulting chronology depends on the rate of sediment accumulation and the sampling interval of the core. The chronology for the last century can be compared with lead-210 derived dates to check for discrepancies. However, lead-210 dating must be used with caution in estuarine sediments, because of its propensity for migrating in silty sediments without much clay or organic material.

Lead-210 measurements were made at the University of Maryland Environmental Laboratories. Lead-210 measurements were used to obtain sedimentation rates for the box cores and to check pollen derived dates for the piston cores.

Carbon-14 measurements were made by accelerator mass spectrometry of the lowermost sediment in each core. Analyses were done at the University of Arizona AMS Facility.

Pollen was extracted from the cores by treating samples with hydrochloric acid, hydrofluoric acid and an acetolysis mixture of acetic anhydride and sulfuric acid. The samples are washed in distilled water and alcohol and stored in a fixed volume of tertiary butyl alcohol. All pollen in measured aliquots are counted in order to obtain the concentration of pollen per cm^3 of sediment.

Sedimentation rates are expressed as linear rates and mass rates. Mass rates are obtained by multiplying the grams of dry sediment/cm^3 by the linear sedimentation rate (cm/yr).

Results and Discussion

Table 2 contains a summary of dates and sedimentation rates for the cores collected at each station.

Table 2. Dates and sediment accumulation rates for cores

Station CPH

Box core: not analyzed

Piston core: Length 427 cm., radiocarbon date: 427 cm: 2740±50 ybp; European settlement horizon 377 cm: 290 ybp.

Sedimentation rates: Average for entire core: 2740/427 = ~0.15 cm yr^{-1}
Lead-210 for to 30 to 130 cm: ~0.5 cm yr^{-1}
Average post-European: 377/290 = ~1.3 cm yr^{-1}
Average pre-European: 50/2450 = ~0.02 cm yr^{-1}

Station WD6

Box core: not analyzed

Piston core: Length 531 cm., radiocarbon date 531 cm: 1495±50 ybp; European settlement horizon: 450 cm: 290 ybp

Sedimentation rates: Average rate for entire core: 531/1495 = ~0.35 cm yr^{-1}
Lead-210 for top 120 cm: ~3 cm yr^{-1}
Average post-European: 450/290 = ~1.5 cm yr^{-1}
Average pre-European: 81/1205 = ~0.07 cm yr^{-1}

Station PC6-PH

Box core: Lead 210 sedimentation rate of 1.0 cm/yr

Piston core: Length 409 cm., radiocarbon date: 409 cm: 1820±55 ybp; European settlement horizon 300 cm: 290 ybp.

Sedimentation rates: Average for entire core: 409/1820 = ~ 0.22 cm yr^{-1}
Lead-210 for 30 to 110 cm: >>> 3 cm yr^{-1}
Average post-European: 300/290 = ~1.0 cm yr^{-1}
Average pre-European: 109/1530 = ~ 0.07 cm yr^{-1}

Station JB5-PH

Box core: Lead 210 sedimentation rate of ~1.0 cm/yr

Piston core: Length 448 cm., radiocarbon date: 448 cm: 13,725 ±95 ybp; European settlement horizon could not be identified; the ragweed profile is more or less constant throughout the core.

Sedimentation rates: Average for entire core: 448/13,725 = ~0.03 cm yr^{-1}
Lead-210 for to 60 cm: > 3 cm yr^{-1}

Station RPH

Box core: Lead 210 sedimentation rate of 0.5 - 1.0 cm/yr

Piston core: Length 435.5 cm., radiocarbon date: 435.5 cm: 2,540±75 ybp; European settlement horizon 380 cm: 350 ybp.

Sedimentation rates: Average for entire core: 435.5/2,540 = ~0.17 cm yr^{-1}

Average post-European: 380/350 = ~1.1 cm yr^{-1}

Average pre-European: 55/2190 = ~0.025 cm yr^{-1}

Station YPH

Box core: not analyzed

Piston core: Length 502.5 cm., radiocarbon date: 502 cm: 9,995±95 ybp; European settlement horizon could not be identified, because there appears to be no ragweed pollen.

Sedimentation rates: Average for entire core: 502/9,995 = ~0.05 cm yr^{-1}

Lead-210 for 30 to 120 cm: 0.5 - 1.0 cm yr^{-1}

Average pre-European sedimentation rate: ~0.07 cm yr^{-1}

All of the cores with the exception of YPH show very high sedimentation rates. The carbon-14 date of 13,725 ybp for JB5-PH is believed to be inaccurate because of the high sedimentation rate obtained from lead-210 analysis and the presence of ragweed throughout the core, indicating that the entire core represents sediment deposited since European settlement. Because of the high sedimentation rates, it was not possible to date all samples of each core using the pollen concentration method, which requires counting the total pollen in aliquots of similar size from each sample. Therefore, selected samples were counted and both average and individual linear rates were used to obtain mass rates of sedimentation throughout the cores.

Sedimentation rates for each of the cores are presented in tabular form. Linear and mass sedimentation rates are plotted against depth and linear rates plotted against depth and time.

In addition to high sedimentation rates, there is a great deal of variability in accumulation rates in the different cores. Because storms could be an important distributor of sediment, attempts were made to estimate the coincidence of high sedimentation peaks in the different cores with the historical record of storms.

Core CPH

Table 3. CPH: average sedimentation rate for entire core: ~0.15 cm yr^{-1}; average post-European sedimentation rate ~1.2 cm yr^{-1}; average pre-European sedimentation rate ~0.02 cm yr^{-1}

Depth	cm/yr	approximate chronology	g/cm2/yr
10	1.85	1985	2.957
20	4.80	1983	6.263
30	4.36	1981	6.9625
40	2.29	1977	2.8758
50	3	1974	3.6408
60	3.2	1971	5.9406

	70	1.5	1964	2.4855
	80	9.6	1963	19.081
	90	1.66	1957	3.2737
	100	1.55	1951	2.8472
	110	5.33	1949	7.7146
	118	1.85	1944	3.3441
	129	2.67	1939	3.7505
	141	1.37	1930	2.7604
	154	1.5	1921	2.0778
	166	1.09	1910	2.1368
	179	2.67	1905	4.1057
	191	0.81	1890	1.6398
	204	1.6	1882	1.9789
	216	0.98	1870	1.9302
	229	1.78	1863	2.4835
	241	0.92	1850	2.0128
	254	1.26	1840	1.3642
	265	0.73	1825	1.428
	277	0.8	1811	0.7463
	290	0.54	1787	0.6443
	303	0.54	1763	0.5934
	318	0.56	1736	0.6124
	333	0.58	1710	0.6424
	347	0.7	1690	0.8105
290±20 ybp				
	361	0.61	1667	0.6554
	375	1.12	1654	1.2041
	377	1.12	1652	
	390	0.02	737	0.0228
	405	0.03	293	0.0325
	418	0.01	-586	0.0114
	424	0.02	-842	0.0233
2740±50 ybp	427			

Sedimentation rates are plotted against depth in Fig. 2 and the sediment accumulation rate in cm/yr is plotted against depth and time in Fig. 3. High sedimentation rates synchronous (allowing for some degree of error) with historically recorded storms are noted in Fig. 3.

The stratigraphy of this core seems to be relatively undisturbed. As in all of the cores, sedimentation rates are very high and highly variable. At CPH, rates range from <1 cm/yr to >5 cm/yr in the post-European period. The highest sedimentation rates occur at approximately the time of the 1905 storm, 1946 storm, 1960 and 1961 storms and David which occurred in 1979.

Core WD6

Table 4. WD6: average sedimentation rate for entire core: ~0.35 cm yr^{-1}; average post-European sedimentation rate ~1.5 cm yr^{-1}; average pre-European sedimentation rate ~0.07 cm yr^{-1}

Depth	cm/yr	approximate chronology	g/cm2/yr
1	1.37	1991	1.084
5	1.37	1988	2.137
6	2.46	1988	3.929
7	1.5	1987	2.124
8	1.5	1987	2.001
9	1.5	1986	2.167
10	1.5	1985	1.694
11	1.5	1985	1.764
12	1.5	1984	2.181
13	1.5	1983	2.107
14	1.5	1983	2.548
15	1.5	1982	2.493
16	1.5	1981	1.860
17	1.5	1981	2.238
18	1.5	1980	2.308
19	1.5	1979	2.191
20	2.67	1979	3.351
21	0.8	1978	0.992
22	0.74	1976	0.983
23	0.47	1974	0.877
24	1.75	1974	2.462
25	1.5	1973	2.375
26	1.81	1972	2.947
27	0.89	1971	1.460
28	2.67	1971	3.750
29	1.5	1970	2.359
30	1.5	1970	2.417
40	1.5	1963	2.561
45	1.5	1960	1.600
50	1.5	1956	1.031
56	1.5	1952	1.638
63	1.5	1948	1.581
70	1.5	1943	1.836
72	1.5	1942	2.186
84	1.5	1934	1.496
95	1.5	1926	1.178
105	1.5	1920	2.219
116	1.5	1912	1.576
128	1.5	1904	2.254
140	1.5	1896	1.292
151	1.5	1889	2.161
162	1.5	1882	2.348
173	1.5	1874	2.761
185	1.5	1866	1.769
195	1.5	1860	1.122
204	1.5	1854	2.329

	213	1.5	1848	2.448
	221	1.5	1842	2.924
	226	2.74	1840	3.336
	238	2.74	1836	3.577
	246	2.74	1833	2.040
	250	1.07	1829	1.823
	259	1.07	1829	0.988
	269	1.45	1822	2.677
	276	1.45	1818	1.357
	282	1.37	1813	2.223
	291	1.37	1807	1.180
	294	1.5	1805	2.293
	296	1.5	1803	1.197
	301	1.5	1800	1.621
	306	1.22	1796	2.377
	312	1.22	1791	1.590
	318	1.6	1787	2.626
	330	1.5	1779	2.823
	336	1.5	1775	1.950
	341	1.5	1772	1.521
	346	1.5	1768	1.122
	354	1.32	1762	2.633
	360	1.32	1758	1.435
	366	2.18	1755	4.700
	371	1.08	1751	1.680
	396	2	1739	1.728
	399	2	1737	3.000
	416	1.96	1729	1.709
	417	1.96	1728	2.864
	446	3.84	1721	3.524
300 ± 20 ybp				
	466	0.15	1587	0.166
	496	0.05	987	0.032
1495 ± 50 ybp	531			

Sedimentation rates are plotted against depth in Fig. 4 and the sediment accumulation rate in cm/yr against depth and time in Fig. 5. High sedimentation rates more or less synchronous with historically recorded storms are noted in Fig. 5.

As at CPH, the long core collected at station WD6 is characterized by high sedimentation rates ranging from slightly <1 cm/yr to slightly <4 cm/yr. The agricultural horizon was located at 450 cm based on the presence of ragweed pollen. Because the horizon was so deep, many of the samples were assigned the average sedimentation rate of 1.5 cm/year. Individual sedimentation rates show high variability here also, with extreme rates often correlatable with historical records of major storms. At this location, the storms that appear to be recorded in the stratigraphy are those that occurred in 1760, 1786, 1805, 1905, Agnes in 1972 and David in 1979.

Core PC6-PH

Table 5. PC6-PH: average sedimentation rate for entire core: ~0.22 cm yr^{-1}; average post-European sedimentation rate ~1.0 cm yr^{-1}; average pre-European sedimentation rate ~0.07 cm yr^{-1}

	Depth	cm/yr	approximate chronology	g/cm2/yr
	0	0.81	1990	0.420
	9	0.64	1972	0.331
	18	0.65	1954	0.530
	27	0.73	1945	0.490
	36	1.58	1936	1.125
	43	1.00	1929	0.532
	52	1.07	1920	0.742
	61	0.81	1911	0.504
	70	0.88	1902	0.565
	79	0.61	1884	0.471
	88	0.73	1875	0.369
	97	0.56	1857	0.363
	110	0.77	1844	0.384
	122	2.14	1844	1.122
	134	1.88	1836	1.349
	147	1.76	1823	1.088
	160	1.07	1810	0.998
	173	1.67	1797	1.517
	186	1.36	1784	1.155
	199	1.20	1771	0.864
	212	0.75	1758	0.614
	225	0.91	1745	0.799
	238	1.07	1732	1.051
	251	1.76	1719	1.465
	264	0.94	1706	0.710
	279	1.36	1693	0.948
	294	0.97	1678	0.636
300±20 ybp	300	0.97	1672	0.053
	307	0.70	1300	
	320	0.70	925	0.053
	335	0.70	550	0.060
1820±55 ybp	409	0.70	170	0.050

Sedimentation rates are plotted against depth in Fig. 6 and the sediment accumulation rate in cm/yr against depth and time in Fig. 7. High sedimentation rates synchronous with historically recorded storms are noted in Fig. 7.

Sedimentation rates are not quite as high at this location as at the previous 2 locations. The range here is 0.56 to 2.14 cm/yr. Again the variability is extremely high, with periods of high sedimentation correlated with the 1781, 1786, 1825 and 1936 storms.

JB5-PH

Table 6. JB5-PH: average sedimentation rate for entire core: ~3.0 cm yr^{-1}; the entire core is believed to represent sediment deposited within the last 150 years.

	Depth	cm/yr	approximate chronology	g/cm2/yr
	5	1.85	1988	2.010
	14	1.85	1980	2.928
	25	1.85	1973	3.177
	45	2.87	1966	3.666
	66	2.87	1959	3.337
	85	2.05	1950	3.591
	105	2.05	1940	3.623
	125	3.96	1935	5.774
	140	3.96	1931	8.037
	141	9.23	1931	13.684
	154	9.23	1930	18.063
	167	20.78	1930	41.550
	180	20.78	1930	43.950
	193	2.25	1924	3.307
	206	2.25	1918	3.799
	219	2.25	1912	3.879
	232	2.25	1906	4.532
	245	2.97	1901	5.866
	258	2.97	1896	5.366
	271	3.54	1892	6.567
	294	3.54	1888	3.257
	297	2.28	1887	2.498
	310	1.79	1880	2.480
	323	1.81	1873	2.496
	336	1.46	1864	1.581
	349	2.37	1859	3.268
	362	2.34	1854	4.419
	376	2.31	1848	5.568
	389	4.26	1845	13.906
	402	5.36	1843	15.015
	415	11.87	1842	35.728
	428	41.55	1841	116.315
	438	10.39	1840	
13,275 ± 95 ybp*	448			

* based on lead-210 and pollen analysis, the carbon-14 date is considered incorrect

Sedimentation rates are plotted against depth in Fig. 8 and the sediment accumulation rate in cm/yr against depth and time in Fig. 9. High sedimentation rates synchronous with historically recorded storms are noted in Fig. 9.

The occurrence of ragweed pollen throughout the core and lead-210 analysis support a high sedimentation rate ranging around 3 cm/yr. Therefore, the carbon-14 date of over 13,000 years must represent contamination from older carbon. Sedimentation rates based on pollen stratigraphy and lead-210 analysis show extremely high sedimentation rates at this location ranging from 1.85 to >20 cm/yr. There are two

periods of highest sedimentation. One of these correlates with the 1930,1931 storms. The earlier high sedimentation rate occurs in 1841, but the error in dating could allow correlation with storms which occurred in the early 1850s.

Core RPH

Table 7. RPH: average sedimentation rate for entire core: ~0.17 cm yr^{-1}; average post-European sedimentation rate ~1.1 cm yr^{-1}; average pre-European sedimentation rate ~0.025 cm yr^{-1}

	Depth	cm/yr	approximate chronology	g/cm2/yr
	1	0.72	1991	0.759
	40	0.82	1944	0.703
	60	1.05	1925	1.426
	80	1.52	1912	1.788
	100	1.84	1901	2.502
	125	1.34	1882	1,729
	137	0.83	1868	0.968
	167	1.22	1843	1.708
	207	0.84	1805	1.145
	210	1.42	1803	1.939
	225	0.78	1780	1.080
	240	1.16	1767	1.432
	246	1.16	1761	1.261
	260	0.96	1747	1.364
	275	1.10	1733	1.547
	282	1.10	1719	1.358
	295	1.10	1715	1.353
	297	1.20	1711	1.883
	302	0.72	1708	0.984
	322	1.14	1692	1.553
	335	0.80	1675	1.218
	336	0.80	1674	1.099
	340	1.45	1672	2.347
	344	1.75	1670	1.953
	348	1.12	1666	1.209
	352	1.84	1664	2.105
	356	1.39	1661	1.841
	361	1.55	1658	2.042
	363	0.87	1654	1.121
	365	0.87	1653	1.130
	367	1.95	1652	2.375
	369	1.95	1650	2.848
	372	0.85	1648	1.085
	374	2.20	1647	2.797
	375	0.96	1647	1.206
	376	0.60	1644	0.833
350±20 ybp	380	2.01	1643	
	382	0.025	1563	
	383	0.025	1523	
	424	0.025	-117	
2540±75 ybp	435	0.025	-557	

Sedimentation rates are plotted against depth in Fig. 10 and the sediment accumulation rate in cm/yr against depth and time in Fig. 11. High sedimentation rates synchronous with historically recorded storms are noted in Fig. 11.

Sedimentation rates are less high at this more southern locations but are still relatively high compared with sediment deposited in shallower water (Brush 1990). Rates range from<1 to >2 cm/yr. There is high variability with peaks coincident with the 1786, 1805, 1850 and 1933 storms.

Core YPH

Table 8. YPH: average sedimentation rate for entire core: ~0.05 cm yr^{-1}; average post-European sedimentation rate ~0.5 cm yr^{-1}; average pre-European sedimentation rate ~0.07 cm yr^{-1}

	Depth	cm/yr	approximate chronology	g/cm2/yr
	3	1	1988	1.359
	8	1	1983	1.117
	13	0.4	1968	0.537
	18	0.4	1958	0.653
	'23	0.9	1953	1.453
	28	1.1	1948	1.981
	33	0.5	1938	
	38	0.2	1913	0.284
	43	0.5	1903	0.686
	48	0.5	1893	0.994
	52	0.5	1885	0.720
	56	0.5	1877	0.688
	60	0.5	1869	0.802
	72	0.5	1853	0.583
	85	0.5	1827	0.650
	97	0.5	1803	0.756
	110	0.5	1777	0.644
	122	0.5	1753	0.648
	135	0.5	1727	0.676
	147	0.5	1703	0.691
300 ± 20 ybp	150			
	160	0.036	1339	0.050
	172	0.036	1003	0.068
	185	0.039	66	0.056
	197	0.036	329	0.060
	203	0.036	161	0.089
	217	0.036	-231	0.078
	231	0.036	-623	0.074
	245	0.036	-1015	0.063
	259	0.036	-1407	0.040
	273	0.036	-1799	0.079
	287	0.031	-2247	0.093
	301	0.036	-2639	0.095
	315	0.036	-3031	0.078
	329	0.036	-3423	0.097

	343	0.036	-3815	0.081
	350	0.039	-3997	0.079
	357	0.036	-4193	0.103
	369	0.036	-4529	0.106
	381	0.036	-4865	0.081
	393	0.036	-5201	0.085
	405	0.036	-5537	0.066
	417	0.036	-5873	0.067
	429	0.036	-6209	0.082
	441	0.036	-6545	0.064
	453	0.036	-6881	0.086
	465	0.036	-7217	0.076
	477	0.036	-7553	0.101
	489	0.036	-7889	0.072
9,995 ± 95 ybp	501			

Sedimentation rates are plotted against depth in Fig. 12 and the sediment accumulation rate in cm/yr against depth and time in Fig. 13. High sedimentation rates synchronous with historically recorded storms are noted in Fig. 13.

The absence of ragweed pollen in numerous samples in the uppermost part of this core necessitated the use of lead-210 analysis for sedimentation rates and dating. Linear sedimentation rates are therefore average rates based on lead-210 and carbon-14 dating. However, mass sedimentation rates do not show much variability in this core. Three peaks in sediment accumulation in the top part of the core coincide with the 1946 storm, Agnes in 1972 and David in 1979. These are the only anomalously high peaks in the core.

Seasonal sedimentation

The very high average sedimentation rates and the erratic distributions of ragweed pollen led to the realization that the 1 cm sampling might be capturing seasonal sedimentation. Since most trees flower and pollinate in spring and ragweed pollinates in late summer, not all samples would contain ragweed if this were the case and there should also be a majority of pollen in sediments deposited in spring. An experiment was conducted to see whether or not the pollen distributions supported the hypothesis of seasonal sedimentation. All pollen in consecutive samples from one section of a core were counted. The results (Fig 14) show that pollen increases to >200 grains per aliquot in 2 to 3 levels (presumably spring), then decreases to <50 (presumably late spring and early summer), increases to ~ 100 (presumably late summer) and decreases again. The distributions of oak and pine are dramatically higher in the sections where the total pollen is highest (spring), and ragweed shows 2 peaks one when the total pollen is highest and the largest peak in late summer. The "ragweed" peak in spring may actually represent pollen of marsh elder which pollinates in spring and is difficult to distinguish from ragweed pollen. The potential of differentiating sediments deposited in different seasons is very promising for analysis of the history of seasonal chemical and biological processes in the estuary.

TRACE METALS AND NUTRIENTS

Laboratory Analyses

Physical Parameters

Samples were analyzed in the laboratory for water content and grain size composition (sand-silt-clay content). Values of these four measured physical characteristics - Water Content, Sand, Silt, and Clay - are reported in Appendix I.

Water content was calculated as the percentage of the water weight to the total weight of the wet sediment:

$$Wc = \frac{Ww}{Wt} \times 100, \text{ where}$$

Wc = water weight (%), Ww = weight of water (g), Wt = weight of wet sediment (g). Water weight was determined by weighing the wet sample, drying the sediment at 65°C, and reweighing it. The difference between total wet weight (Wt) and dry weight equals water weight (Ww). Bulk density was also determined from water content measurements.

The relative proportions of sand, silt, and clay were determined using the sedimentological procedures described in Kerhin et al. 1988. The sediment samples were pre-treated with hydrochloric acid and hydrogen peroxide to remove carbonate and organic matter respectively. Then the samples were wet sieved through a 62μm mesh to separate the sand from the mud (silt plus clay) fraction. The finer fraction was analyzed using the pipette method to determine the silt and clay components (Blatt et al. 1980). Each fraction was weighed; percent sand, silt and clay were determined; and the sediments were categorized according to Pejrup's (1988) classification (Fig. 15).

Elemental Analyses

The elements analyzed for this study, the methodology and the samples on whcih the analyses were performed are listed in Table 9. Results are in Appendices III and IV.

Table 9. Elements and chemical species analyzed.

Element/Chemical Species	Methodology	Box core	Gravity core*	Pis
MAJOR				
Si, Al	Lithium Borate Fusion/Flame AA	x	x	
Fe	Microwave Digestion/ICP	x	x	
MINOR				
Mn, Ni, Cu, Zn, Cr, Cd, Pb	Microwave Digestion/ICP	x	x	
Hg, As**	HNO_3 Digestion/Cold Vapor AA	x		
OTHER				
Total C,N,S	Total Combustion/GC	x	x	
AVS	HCl Digestion/Iodometric Titration	x	x	
Soluble Fe	Conc. HCl Digestion/Flame AA	x	x	

* - Data not presented in this report

** - Analyzed by Artesian Laboratories, DE

All analyses, except As and Hg, were performed in the Maryland Geological Survey (MGS) Laboratories. The following section outlines the procedures used at MGS.

Major Elements

Sediment solids were analyzed for Al and Si using a lithium metaborate fusion technique, followed by standard flame atomic absorption spectrophotometry. This procedure, based on methods developed by Suhr and Ingamells (1966) for whole rock analysis, was refined specifically for the analysis of Chesapeake Bay sediments (Sinex et al. 1980; Sinex and Helz 1981; Cantillo 1982).

The MGS Laboratories followed the steps listed below in handling and preparing trace metal samples:

1. Samples were homogenized in the "Whirl-Pak" bags in which they were store and refrigerated.
2. Approximately 10 g of wet samples were drawn into a modified "Leur-Loc" syringe fitted with a 1.25 mm polyethylene screen, used to remove shell material and large pieces of detritus.
3. Sieved samples were disaggregated in high-purity water and dried overnight at 110°C in Teflon evaporating dishes.
4. Dried samples were then hand-ground with an agate mortar and pestle and stored in "Whirl-Pak" bags.
5. Samples were weighed (0.25±0.0002 g) into a drill-point graphite crucible (7.8 cc vol.) and mixed with $LiBo_2$ (0.75±0.01 g).
6. The crucibles were placed in a highly regulated muffle furnace at 930±5°C for 20 min.
7. The molten beads produced by heating were poured directly into Teflon beakers containing 100 ml of a solution composed of 4% HNO_3, 1000 ppm La (from $La(NO_3)_3$), and 2000 ppm Cs (from $CsNO_3$), and stirred for 10 min. If dissolution did not occur within 30 min, the solution and bead were discarded and the sample re-fused.
8. The dissolved samples were transferred to polyethylene bottles and stored for analysis.

All surfaces that came into contact with the samples were acid washed (3 days 1:1 HNO_3; 3 days 1:1 HCl), rinsed six times in high-purity water (less than 5 mega-ohms), and stored in high-purity water until use.

The dissolved samples were analyzed with a Perkin-Elmer atomic absorption spectrophotometer (Van Loon 1980). The instrumental parameters used to determine the solution concentrations of Al and Si were the standard settings recommended by Perkin-Elmer for the acetylene-nitrous flame. Blanks were run every 12 samples, and standard reference materials were run five times every 24 samples

Results of the analyses of three standard reference materials (National Institute of Standards and Technology SRM # 1646 - Estuarine Sediment; NIST-SRM # 2704 -

Buffalo River Sediment, National Research Council of Canada # PACS-1 - Marine Sediment) compared to certified values are excellent; ≥98% recovery for both Al and Si for all of the SRMs.

Minor/Trace Elements

Sediment solids were analyzed for trace elements using a microwave digestion technique, followed by analysis of the digestate on an Inductively Coupled Argon Plasma unit (ICAP). The microwave digestion technique is modified from EPA Method # 3051, in order to achieve total recovery of the metals analyzed, in compliance with the guidelines of the NIST program and the EPA-EMAP program.

The steps in microwave digestion are outlined below:

1. Samples were homogenized in the "Whirl-Pak" bags in which they were stored and refrigerated (4°C).
2. Approximately 10 g of wet sample were transferred to Teflon evaporating dishes and dried overnight at 105-110°C.
3. Dried samples were then hand-ground with an agate mortar and pestle, powdered in a ball mill, and stored in "Whirl-Pak" bags.
4. 0.5000±0.0005 g of dried, ground sample was weighed and transferred to a Teflon digestion vessel.
5. 2.5 ml concentrated HNO_3 (trace metal grade), 7.5 ml concentrated HCl (trace metal grade), and 1 ml ultra-pure water were added to the Teflon vessel.
6. The vessel was capped with a Teflon seal, and the cap was hand tightened. Between 4 and 12 vessels were placed in the microwave carousel. (Preparation blanks were made by using 0.5 ml of high-purity water plus the acids used in Step 5.
7. Samples were irradiated using programmed steps appropriate for the number of samples in the carousel. These steps have been optimized based on pressure and percent power. The samples were brought to a temperature of 175°C in 5.5 minutes, then maintained between 175-180°C for 9.5 minutes. (The pressure during this time peaks at approximately 6 atm for most samples).
8. Vessels were cooled to room temperature and uncapped. The contents were transferred to a 100 ml volumetric flask, and high-purity water was added to bring the volume to 100 ml. The dissolved samples were transferred to polyethylene bottles and stored for analysis.
9. The samples were analyzed.

Samples were analyzed using a Thermo Jarrel-Ash Atom-Scan sequential ICAP. The wavelengths and conditions selected for the elements of interest were determined using digested bottom sediments from the vicinity of Hart-Miller Island and standard reference materials from the National Institute of Standards and Technology (#1646-Estuarine Sediment: #2704-Buffalo River Sediment) and the National Research Council of Canada (PACS-1-Marine Sediment).

The wavelengths and conditions were optimized for the expected metal levels and the sample matrix. Quality control was maintained by routinely including blanks, replicates and standard reference materials in the analysis. Blanks were run every 20 samples; one sample in every ten was replicated; and a standard reference material was analyzed after every ten samples. Table 10 shows the recovery of this method using the NIST Buffalo River SRM. For a comparison, the recoveries for the unmodified EPA method #3051 are given. The recoveries are excellent for the elements measured.

Table 10. Comparisons of Recoveries between the EPA Method #3051 and the modified EPA method used by MGS based on the NIST Buffalo River SRM #2704

	Cr	Cu	Fe	Mn	Ni	Zn
NIST certified value	1.35	98.6	41100	555	44.1	438
EPA Method #3051	82.3±1.3	86.6±2.1	29162±554	463±7	36.2±0.7	390±10
% Recovery	62	87	71	83	82	89
Modified EPA Method	136±6.3	95.7±2.5	39600±30	552±22	41.1±2.4	424±12
% Recovery	101	97	96	99	93	97

Other Analyses

Total Carbon, Nitrogen and Sulfur

The sediments were analyzed for total nitrogen, carbon and sulfur (CNS) content using a Carlo Erba NA1500 analyzer. This analyzer uses complete combustion of the sample followed by separation and analysis of the resulting gases by gas chromatographic techniques employing a thermal conductivity detector. The NA1500 Analyzer is conFig.d for CNS analysis using the manufacturer's recommended settings. As a primary standard, 5-chloro- 4-hydroxy- 3-methoxy- benzylisothiourea phosphate is used. Blanks (tin capsules containing only vanadium pentoxide) are run at the beginning of the analyses and after 12 to 15 unknowns (samples) and standards. Replicates of every fifth sample are run. As a secondary standard, a NIST reference material (NIST SRM #1646-Estuarine Sediment) are run after every 6 to 7 sediment samples. The recovery of the SRM is excellent as seen in Table 4. There is excellent agreement between the NIST values and MGS's results. Generally, the carbon measured is in the form of organic carbon; inorganic carbon occurs as shell material which is physically separated from the sample (Hennessee et al. 1986).

Table 11. Results of nitrogen, carbon and sulfur analyses of NIST-SRM #1646 - Estuarine Sediment compared to the certified or known values. MGS values were obtained by averaging the results of all SRM analyses run with the unknowns.

Element Analyzed	Certified Weights* (% by weight)	MGS Results
Nitrogen	0.18	0.17±0.01
Carbon	1.72	1.69±0.08
Sullfur	0.96	1.04±0.08

* The value for carbon is certified by NIST. The sulfur value is the non-certified value reported by NIST. The value for nitrogen was obtained from repeated analyses in-house and by other laboratories (Haake Buchler Labs and U.S. Dept. of Agriculture.

Soluble Fe

Iron is an important element in many diagenetic and biological reactions in the sediment. The speciation of Fe as either soluble (also called labile or reactive) or bound Fe is an indicator of geochemical environmental conditions. Soluble/labile iron when coupled with sulfur speciation has been used as an environmental indicator (Raiswell and Berner 1985).

Soluble Fe was measured on all samples using the method of Berner (1970). This method places a weighed amount of dried ground sample in a test tube with a fixed volume of concentrated HCl, the sample is boiled for one minute, diluted and analyzed by standard Flame AA or ICP methods.

Acid Volatile Sulfides

Acid volatile sulfides (AVS) are another indicator of the geochemical environment, and are currently investigated as indicators of pollution when analyzed with simultaneously extracted metals (SEM; USEPA 1994). Sulfides in the sediments are metabolic products resulting from bacterially mediated decomposition of organic matter. The free sulfide species, generated by this bacterial action, are sequestered in the sediments as metal sulfides. The primary minerals formed are Fe sulfides, which are either acid soluble, such as FeS, or acid insoluble in the form of pyrite (FeS_2). The formation of pyrite has FeS as an intermediate. Conversion of FeS to FeS_2 requires an excess of sulfur in the system as well as specific geochemical conditions. Thus AVS is a strong indicator of geochemical conditions and availability of sulfur (as sulfate) to the sediments.

The AVS method used is a modification of standard iodometric sulfide determinations (Ayres 1968). The procedure used is outlined as follows:

1. Wet sample is collected in an open ended syringe to minimize contact with the air. The weight of the wet sample is determined by difference and corrected for water content, measured during grain size measurement, to determine the dry weight.
2. The syringe is fitted into an arm of a two-armed round bottom flask purged with nitrogen, from a bubbler, and containing a stirred solution of HCL and stannous chloride. The system is further purged to remove all air prior to

injection of the sample.

3. The sample is injected and allowed to react. The hydrogen sulfide released is purged from the solution by the nitrogen bubbler, and is swept into a flask containing an ammoniacal zinc sulfate solution, which traps the hydrogen sulfide as zinc sulfide.
4. The trapping solution is acidified with HCl and immediately titrated using standard iodometric techniques.

The recovery of this technique is 98% based on analyses of spectroscopic grade FeS from Aesar Specialties.

Discussion

Historical changes in trace metals in the Chesapeake Bay are the primary concern of this phase of the Pollution History Study for the NOAA Status and Trends project, specifically identifying anthropogenic loading to the Chesapeake Bay. The metal concentrations found in the sediments reflect three primary factors: natural background loading, anthropogenic loading and geochemical environment, which contributes to the stabilization or remobilization of metals. In order to assess the anthropogenic component, the other two components must be addressed.

Geochemical Environment

The cores collected for this project are fine grained organic-rich sediments extending spatially through the different environments of the Chesapeake Bay. The geochemical signature of these environments is recorded in chemical species which reflect the diagenetic processes of these environments. Two related, well-documented processes are the microbial decomposition of carbon and the formation of metal sulfides. Organic carbon reacts through bacterial mediation with a variety of oxidants based on the free energy yield of the reaction (Krumbein 1984). The sequence of oxidants used, in order of preference is oxygen, nitrate, Mn and Fe oxides, sulfate and finally internal conversion (methane formation). Within organic-rich sediments, the first three oxidants are rapidly depleted, because of their low availability and high energy yields which account for higher reaction rates (Krumbein 1984). Sulfate is more slowly depleted from the sediments by bacterial action because of its low energy yield, with a corresponding lower reaction rate, and greater availability from the overlying water column in marine and estuarine environments. The oxidation (removal) of carbon from the sediment, as a result of sulfate reduction, forms dissolved sulfide species as a by-product. These sulfides react with labile or soluble Fe to form iron sulfide minerals. Iron monosulfides are the first sulfides formed; these minerals are the source of acid volatile sulfides (AVS). Subsequent to the formation of monosulfide minerals is the formation of pyrite, which is acid insoluble. Pyrite is formed through the conversion of iron monosulfides, which requires time and the presence of excess dissolved sulfide. Bacterial sulfate reduction and the formation of authigenic sulfides involve reactive carbon, sulfur, labile iron, and AVS. Therefore, their behavior within the sediments can be used as indicators of environmental conditions. The best approach to using these chemical species as indicators is to use them in ratios to one another. The use of ratios minimizes variations due to grain size induced variability (Trefrey and Presley 1976; Sinex and Helz 1981; Hill, in preparation), and emphasizes the

processes occurring in the sediment. The ratios used here are C/Al, N/Al, S/C, AVS/total S, and Soluble Fe/total Fe. Discussion of the behavior of the ratios below refers to Fig. 16 unless otherwise noted, which plots all of these ratios for each of the cores as a function of the date of deposition.

C/Al & N/Al - These ratios together indicate the source and amount of carbon preserved in the sediment. There are two primary sources of organic carbon to the Bay - planktonically derived carbon and terrigenous carbon. Planktonically derived carbon is the detrital remains plankton. It is composed of carbon, hydrogen, oxygen, nitrogen and phosphorus; these occur in a fixed ratio (Redfield et al. 1966). Terrigenous carbon is derived from erosion and runoff from the land's surface, and is composed of complex polymers, cellulose and coal/lignite. This material is depleted in the nutrients nitrogen and phosphorus (Shimoyama and Ponnamperuma 1975).

Organic carbon content in surficial sediments of the Bay is linearly related to the clay size fraction south of latitude 39° (Hill 1984; Hennesee et al. 1986). Thus, since the occurrence of Al is restricted to the clay fraction (Hill 1984), the ratio of C/Al would be expected to be a constant in surficial sediments. With depth into the sediment, assuming a uniform geochemical environment and uniform sedimentation rate, the ratio of C/Al would be highest near the sediment-water interface and decrease with depth into the sediment. This reflects the microbial oxidation/removal of the carbon with time. In addition, where the only source of carbon is planktonically derived, the ratio of N/Al would parallel the behavior of carbon. This ideal behavior in the ratios is seen to a limited extent in core YPH. The other cores show behavior which is either more complicated indicating variation in input (CPH, WD6, JB5), or show little variation with time (PC6 and RPH). A comparison of the carbon vs nitrogen ratios indicates input of terrigenous carbon, which is most noticeable in core CPH and less so in cores WD6 and JB5. The variation in the C/Al ratio, as in cores WD6 and JB5, indicates either changes in the geochemical conditions which either favor oxidation or preservation, or changes in the amount of carbon entering the sediment. Based on the AVS/S and labile Fe behavior, the variations in WD6 are related to variations in the geochemical environment, while the variations in JB% are related to changes in the input of carbon (see below).

S/C - The S/C ratio has been used as an indicator of paleosalinity (Berner and Raiswell 1984). Through the reactions outlined above, sulfur is preserved in the sediments at the expense of carbon. In uniformly deposited sediments, the ratio varies with depth into the sediment, with the lowest S/C ratio near the sediment-water interface and increasing with depth in the sediment. This simple variation with depth can be seen in cores PC6 and YPH. The ratio also changes with availability of sulfate; the greater the availability of sulfate for the bacteria, the greater the amount of metal sulfides formed and less carbon preserved. This assumes an abundance of labile iron to form sulfides. Availability is controlled by several factors; two of which are sedimentation rate and salinity, and is inversely related to sedimentation rate. High sedimentation rates effectively isolate the sediment from the source of sulfur and reduce the extent of conversion; similarly the lower the sedimentation rate the higher the availability because of the longer time in proximity with the source of sulfate. Salinity /sulfate concentration is directly related to availability.

That is in fresher water, where the available sulfate is low, the ratio is low, and conversely, in highly saline waters the ratio is high. This has been clearly shown in the S/C ratio in different environments around the world (Berner and Raiswell 1984; Raiswell and Berner 1985). The average S/C ratio (Fig. 17) clearly reflects the salinity pattern in the Bay, with CPH, the lowest salinity station, having the lowest ratio, increasing monotonically towards the mouth of the Bay with the highest ratio at station YPH. Although the Baywide trend mirrors the salinity distribution in the Bay,, the behavior at any site can vary as a function of geochemical conditions, sedimentation rate, and variations due to carbon input. These variations can be seen in cores CPH, WD6, JB5 and RPH.

AVS/S - The ratio of AVS/S reflects the availability of sulfur to the sediment, sedimentation rate and salinity, and the geochemical conditions in the sediments. AVS is converted to pyrite, which is acid insoluble, in the presence of excess dissolved sulfide which is partially oxidized to produce the -I oxidation state of sulfur in pyrite. Excess sulfide species increase with increasing availability. Variation in this pattern occurs in sediments which are highly gas charged. The gas is an alternate source of carbon, which can change the kinetics of biologically mediated reactions, and alter the redox state of the system. As a consequence, the conversion to pyrite can be inhibited.

As before, in a uniform situation, the fraction of AVS would be the highest near the sediment-water interface and diminish with depth as it is converted to pyrite. This is seen in PC6, JB5, RPH and YPH. However, the rate of change and the fractions of AVS present varies substantially between each of the cores. These variations are due to differences in sedimentation rates and the geochemical environment. PC6 and JB5 have higher sedimentation rates and have gas present. Both factors tend to preserve AVS and retard conversion to pyrite. On the other hand, RPH and YPH have lower sedimentation rates and no gas present near the sediment-water interface, and in the case of YPH gas is absent throughout.

CPH and WD6 both have large variations in the fraction of AVS sulfur present. These variations are induced by changes in the geochemical environment, specifically due to freshwater input from the Susquehanna River. Fresh water input affects both the salinity and anoxic conditions in the main channel of the Bay.

Soluble Fe/Total Fe (SolFe/Fe) - Iron exists in the sediments either as soluble Fe, which is readily available for diagenetic reactions or as insoluble Fe which is trapped in mineral grains and does not undergo diagenetic reactions readily. Soluble Fe occurs as iron oxyhydroxide grain coatings, monosulfides,, carbonates and/or phosphates; insoluble Fe is found in silicates, pyrite, and certain heavy minerals. The conversion of monosulfides to pyrite sequesters soluble iron into an insoluble mineral phase. Thus the fraction of soluble Fe follows the conversion of AVS in uniform settings. This behavior occurs in all of the cores to a greater or lesser extent, confirming the diagenetic conditions inferred by the AVS/S behavior.

Summary of Environmental Indicators

CPH and *WD6* are strongly influenced by input from the Susquehanna, both in regard to physical transport based on terrigenous carbon loading and geochemical processes, indicated by the variations in AVS/S and SolFe/Fe. In addition, the cores' geochemistry varies from normal marine sediments with gas present to fresher environments. The presence of gas tends to preserve AVS and organic carbon, and alter the suite of diagenetic minerals that may form.

PC6 and *JB5* also have gas present and have high sedimentation rates, as a result of their location in paleochannels. However, fluvial influence appears negligible, and the primary source of carbon is plankton. The diagenetic processes within the last 30 years appears well-behaved, showing little variation in carbon and sulfur chemistry.

RPH and *YPH* have lower sedimentation rates. Gas is not present in YPH and does not occur until over a meter into the sediment at RPH. As a result, organic carbon from plankton is not well preserved and the fraction of AVS sulfur is low. Diagenetic processes within the last 30 years appears well-behaved.

Recent Trends in Metal Loading

In order to evaluate the loading of metals to the sediment, natural variability in metal loading due to grain size needs to be accounted for, and reference levels are required in order to place the data in a meaningful context. The use of enrichment factors is one method commonly employed to satisfy both of these requirements. An enrichment factor is defined as:

$$E.F._{Al}(X) = \frac{(X/AL)_{measured}}{(X/AL)_{reference}} \qquad (1)$$

where: $(X/Al)_{measured}$ is the ratio of any element to Al measured in the sample;
$(X/Al)_{reference}$ is the ratio of the same element to Al in a reference material.

Here the normalizing element is Al, although any element which is unaffected by anthropogenic loading could be used (iron is also frequently used). The reference value for each core was determined by averaging samples from the core dated prior to European settlement (Hill et al. 1996). This was done to eliminate potential natural variations in source of material due to different locations in the Bay, and to provide a comparison between recent metal loadings and "pristine" Bay sediments from the same location.

Fig. 18 shows the enrichment factors for the Mn, Zn, Cr, Cu and Pb for all of the cores. Enrichment factors are not shown for:

Hg and *Cd*, because most of the data were near or below detection;

Fe, because the ratio of Fe/Al varied little throughout the Bay for all samples (0.61±0.03);

As was not included due to the lack of a comparable reference

In addition, As showed little temporal or spatial variability with an average enrichment factor of 0.8±0.25 (referenced to an average shale) for all of the samples. Within each core enrichment factors showed only minor variations.

There are several features to note in Fig. 18.

(1) For most of the metals for all of the cores there is little change in the enrichment factor over a 30-year period.

(2) Variations in metal behavior follow environmental conditions outlined in the previous section, in regard to fluvial influence or variations in geochemical conditions.

(3) Pb is elevated to some extent in all of the cores except YPH and JB5. Enrichment factors are not shown in WD6 or RPH because the Pb concentrations in the "pristine" sediments were below detection, so no reference level could be determined. However, measurable values of Pb were measured in recent sediments with average Pb/Al ratios of 3.1 and 2.14 in WD6 and RPH respectively. The average shale has a ratio of Pb/Al = 2.5. This value is not appropriate to use considering the measured ratios of the "pristine" sediments of the other cores: 0.091, 1.93 and 1.08 for CPH, PC6 and YPH, respectively. The highest measurable enrichment occurs in CPH. The right-hand Y-axis in the diagram shows the enrichment value of Pb peaking at ~130 in 1981. WD6 and RPH (not shown) also have high degrees of enrichment but the amount of enrichment cannot be quantified without a reference. PC6 has lower levels of enrichment.

(4) In core CPH, there is a trend of increasing metal concentrations, starting in the mid-60s and peaking around 1981, then decreasing rapidly in the mid 1980s. The metals which show this trend are Pb, Zn and Cu.

(5) Other temporal variations are seen in cores WD6 for Mn and PC6 for Pb. The change in Mn in core WD6 mirrors the behavior of AVS/S, suggesting a linkage between Mn enrichment and changes in the geochemical environment (Fig. 18). On the other hand, the other temporal variations noted including those seen in core CPH do not show a linkage either to changes in the geochemical environment or changes in loading of organic carbon from planktonic or terrigenous sources. Consequently they are most likely due to anthropogenic loading.

(6) Zn and Cu are significantly elevated throughout the Bay compared to "pristine" sediments collected at the same site.

Comparison of Baywide variations in loading of recent sediments with pristine sediments can be made by averaging the enrichment factors for each of the metals for all of the cores for the 30 year period. This comparison is shown in Fig. 19. The most prominent feature is the influence of the Susquehanna River. All of the elements in the Fig. have elevated levels in the northernmost samples decreasing to background levels at PC6, located near the southernmost extent of the Susquehanna's influence (Hill 1984). The cores PC6 and south have enrichment factors close to 1 of Mn, Ni and Cr, indicating that recent sediments are not enriched compared to pristine sediments. On the other hand, both Cu and Zn show an enrichment factor of 2 to 2.5 throughout the entire Bay, indicating anthropogenic loading of these metals. The ubiquitous nature of the loading suggests atmospheric loading, equivalent to background loading, as a possible source of these metals additional to fluvial input from the Susquehanna River.

Recommendations for future studies

Future studies should be directed at placing the recent changes observed in this study into a long-term historical perspective. Ranges of natural variations in metal and nutrient loadings as a function of environmental changes need to be documented throughout the Bay within all the geochemical settings. Work on the older portions of the piston cores collected for this study is well underway using the relationships presented in this report. Additional cores taken in transitional environments, and sampling the entire Holocene, would be invaluable for documenting natural changes which could be used as benchmarks in interpreting modern conditions.

ORGANOTINS, PAH AND ORGANOCHLORINES

Methods

Sample Collection and Preparation

Cores were sectioned on board ship and samples placed in precleaned quart glass jars. Sample jars were washed, acid rinsed, baked and solvent rinsed prior to use. Samples were stored on ice in the field and immediately frozen when returned to the laboratory. Core sections contained in quart mason jars with Teflon lined lids were stored in a -15 C freezer until used. The samples were transferred to a refrigerator overnight to thaw prior to processing. Once the sample was thawed and homogenized with a stainless steel spatula, an aliquot was transferred to a clean solvent rinsed mason jar for chemical desiccation or to a centrifuge bottle for butyltin analysis.

The aliquots transferred to a mason jars for organics analysis were chemically desiccated with a 2:1 ratio of desiccant to wet sample, by weight. The preignited desiccants (4 hours at 550 C)were added in a 9:1 ratio of sodium sulfate to QUSO® and then mixed thoroughly. After mixing, the samples were stored in the freezer overnight to aid in the desiccation process. The desiccated samples were quantitatively transferred to glass fitted thimbles and placed in soxhlet apparatus. All core section samples were processed with a desiccant blank and a NIST SRM 1941 aliquot to demonstrate QA/QC performance. An aliquot for percent total solids was weighed into a pretared aluminum weigh boat, dried at 110 C overnight, equilibrated at room temperature for 20 minutes, then weighed and reweighed to verify constant weight and the percent total solids calculated.

Analytical Methodology

General Procedures

All solvents used were chromatography grade (Burdick and Jackson) and blank samples were extracted with each batch of environmental samples to account for any contamination if it occurred during the analytical procedures. Replicate extractions were performed on at least 10% of the environmental samples and a standard estuarine sediment sample was analyzed to demonstrate the accuracy of the methodology. All laboratory glassware was thoroughly cleaned with soap and water, followed by oven drying and multiple solvent rinses. Performance of gas chromatographs was checked daily by injection of a standard mix which included the internal standard. Satisfactory performance was verified by a check of retention times, response factors and peak shape.

Gel permeation chromatography (GPC) Procedure

Sample extracts for PAH and organochlorine analysis were fractionated using size exclusion chromatography on a gel permeation chromatograph (ABC Laboratories, Autoprep 1000 2-B) to remove large molecular weight biogenic material. The GPC column was packed with 60 g of SX-3(ABC Laboratories) in a 50:50 cyclohexane/dichloromethane solvent regime. The GPC flow rate was 5 mL/min and the sample loop volume was 5.0 mL from an 8 mL total. The column calibration and analyte separation protocols are regularly performed, verified and entered into the instrument daily maintenance logbook by the operator.

PAH Analysis

Surrogate standards consisted of several deuterated PAH and 1,1'-binaphthyl for GC/MS and were spiked into the samples immediately prior to extraction. Extracts were rotary evaporated to ~4 mL and transferred to 15 mL centrifuge tubes along with DCM rinsings of the extraction flask. The volume was adjusted to 4 mL on a water bath using a gentle stream of prepurified nitrogen gas. Four mL of cyclohexane was added to the sample to give a final volume of 8 mL which was then injected onto the GPC.

After GPC, the extracts (P2) were run over activated copper powder to remove elemental sulfur and the samples were solvent-exchanged to hexane and concentrated under N_2 to ~0.1 mL. Internal standard (p-terphenyl) as added and the final volumes were adjusted to 0.2 mL. PAH were identified and quantified using GC-MS with selected ion monitoring in the electron ionization mode.

Three ions were monitored for each target, surrogate and internal standard. The extracted ion current profile of one ion for each compound was used for quantitation. A 5pt calibration curve was generated for quantitation from 25 to 1000 ng/ml. A mid-range continuing calibration standard was analyzed with each batch of samples to check on the accuracy of the curve. Quantitation was based on a linear fit to the curve using response factors for each compound relative to the internal standard (p-terphenyl). Table 1. shows mass spectrometer conditions and ions selected for these analyses.

Polychlorinated Biphenyls and Organochlorine Analyses

The surrogate standards PCB 30, PCB 65, and PCB 204 (concentrations 127.20 ng/mL, 104.10 ng/mL, and 119.10 ng/mL respectively) were added to each sample, blank, and QA/QC sample prior to extraction. Samples are extracted for 48 hours with 350 mL of dichloromethane. Following extraction the sample volumes were reduced to 4 mL using a rotary evaporator and then gentle nitrogen blowdown with low temperature water bath (39 C). Sample volumes were adjusted to 8.0 mLs with cyclohexane for introduction to the GPC. The GPC eluant, the aromatic fraction (P2) of 150 mLs, was reduced in volume to 1 mL using the rotary evaporator and then gentle nitrogen blowdown. Sulfur removal was performed on the P2 fractions by eluting the samples over a column of activated fine granular copper (Mallinckrodt). The samples were then solvent exchanged to hexane, spiked with the internal standard pentachlorobenzene, and analyzed on a gas chromatograph with electrolytic conductivity detection (GC-ELCD). Gas chromatography conditions are presented in Table 1.

The data from the GC-ELCD were collected via an analog to digital converter interfaced with Hewlett-Packard 1000 Laboratory Data System. Data were analyzed using software on the HP 1000 and the results were imported into Quattro Pro spreadsheets for interpretation.

The above protocol follows the "Analytical Protocol For Hazardous Organic Chemicals In Environmental Samples" by the Division of Chemistry and Toxicology at The Virginia Institute of Marine Science.

Butyltin Analyses

Sediment samples were processed by an adaptation of the methodology published earlier for butyltins in environmental water samples (Unger et al, 1986). Ten grams of wet sediment were placed into a tared 250 mL Teflon centrifuge bottle and spiked with the internal standard, tripentyltin chloride. The samples were then mixed with 20 mL of acidified (pH2) deionized water and 100 mL hexane containing 0.2% tropolone. Samples were shaken on a Burrell© wrist action shaker for 60 min. After settling, the organic layer was removed and an additional 100 mL hexane/tropolone was added to the samples and they were shaken for an additional 60 min. The resulting extracts were decanted from the samples and combined with the first in a round bottom flasks, reduced in volume by rotary evaporation and transferred to a centrifuge tubes. Extracts were then passed over a small pipette column of activated copper to remove excess sulphur. The extracts were adjusted to 10 mL in 50 mL centrifuge tubes and derivatized for 30 min with excess Grignard reagent (n-hexyl magnesium bromide) at room temperature. Remaining Grignard reagent was neutralized with 6 N HCl and the hexane layers were then cleaned up by open column chromatography with florisil. Extracts were reduced in volume under dry nitrogen and analyzed by gas chromatography with flame photometric detection. Table 1. lists gas chromatography conditions used for these analyses.

Table 12. Gas Chromatography and Mass Spectrometry Conditions

Gas Chromatography-Electrolytic Conductivity Detection (ELCD)

- Column: DB-5; 60m x 0.32 id. x 0.25um
- Injector temperature: 320°C
- Detector temperature: 320°C
- Detector reaction temperature: 814°C
- Initial column oven temperature: 90°C
- Final column oven temperature: 320°C
- Temperature program rate: 4°C min^{-1}
- Final column oven temperature hold time: 20 min.
- Injection technique: solute focusing

Gas Chromatography-Mass Spectrometry Negative Chemical Ionization

- Column: DB-5; 60m x 0.32 id. x 0.25um
- Injector temperature: 310°C
- Initial column oven temperature: 75°C
- Final column oven temperature: 310°C
- Temperature program rate: 6°C min^{-1}

Final column oven temperature hold time: 10 min.
Injection technique: solvent effect
Source temperature: 100°C
Transfer line temperature: 280°C
Scan Range: 100-700
Ionization energy: 300 eV moderator gas=methane at 0.7 Torr

Gas Chromatography-Mass Spectrometry Selected Ion Monitoring
Column: DB-5; 30m x 0.32 id. x 0.25um
Injector temperature: 310°C
Initial column oven temperature: 75°C
Final column oven temperature: 310°C
Temperature program rate: 6°C min^{-1}
Final column oven temperature hold time: 10 min.
Injection technique: solvent effect, splitless-split
Source temperature: 200°C
Transfer line temperature: 280°C
Ionization energy: 70 eV, EI

Gas Chromatography-Flame Photometric Detection (FPD)
Filter: 600 nm band pass
Column: DB-5; 30m x 0.32 id. x 1.00um
Injector temperature: 280°C
Detector temperature: 280°C
Initial column oven temperature: 135°C
Final column oven temperature: 300°C
Temperature program rate: 10°C min^{-1}
Final column oven temperature hold time: 5 min.
Injection technique: solute focusing

Results and discussion

Three box cores, RPH, JB5PH and PC6PH were analyzed for PCB, pesticides, butyltins and PAH. Overall, contaminant concentrations were very low in all samples. Individual compounds were typically in the low to sub part per billion (μg/kg) concentration range and are reported on a dry weight basis. These low levels agree with previous studies that examined the distribution of contaminants in surface sediments in Chesapeake Bay (Unger et al, 1991).

PCB in all samples were near the quantitation limit for individual congeners of 0.1 μg/kg. Small sample size afforded by core section samples, detection limits for the ELCD detector, and difficulty with low level background contamination prevented lower quantification of PCB. Analysis of PCB in NIST standard reference material SRM 1941(estuarine sediment) showed that results from the methodology were generally in good agreement with reported values (Table 2).

Total PAH concentrations in the cores ranged from 400 to 1200 μg/kg. Concentrations are reported as dry weight and are corrected for surrogate recovery.

Measured concentrations in NIST SRM 1941 are presented in Table 3 for comparison to certified values.

Butyltin concentrations were highest in the most northerly cores (JB5PH and PC6PH) analyzed and ranged up to 35 µg/kg for TBT. All butyltin concentrations are reported as µg/kg dry weight of the cation. To demonstrate the accuracy of the method, the standard reference sediment PACS-1(National Research Council, Ottawa Canada) was analyzed and the results are reported in Table 3. Sample chromatograms from PCB, PAH and butyltin analyses are shown in Fig.s 20-22.

Core PC6-PH

Sedimentation Rate: 1-3 cm yr^{-1}.

PCB and Organochlorines

PCB totals for the selected 20 congeners ranged from 2-9 µg/kg throughout this box core (Table 4). There is no obvious trend to the PCB concentrations which are near the detection limit for these compounds (Fig. 23). Previous analysis of surface sediments at a nearby station MCB4.3C (38°33'24"/76°26'12", Lat/Long) in 1991 found total PCB concentrations to be below 1 µg/kg (Unger et al, 1992). OCDD concentrations were constant with depth and averaged near 1 µg/kg (Fig. 24).

Butyltins

TBT concentrations in this core ranged from a low of 5 µg/kg at the surface to a maximum of 25 µg/kg at 18-20 cm (Table 5, Fig. 25). Radio dating of this core was problematic with estimates between 1-3 cm/yr. This would put the maximum TBT value between 1973 and 1987. TBT rapidly sorbs to estuarine sediments, so concentrations in core samples should reflect water column concentrations at time of burial (Unger et al, 1988; Leguille, F. et al, 1993). Based on known temporal trends in TBT concentrations in Chesapeake Bay (Unger et al, 1995), the 1987 date for a maximum is more reasonable and supports the rapid sedimentation rate for this core. A similar decrease in TBT concentrations during this time period was also seen in shellfish monitoring data as part of the NOAA Status and Trends program (O'Connor et al, 1995). The similarity in trends for all three data sets is shown in Fig. 26. TBT maximums in core profiles may prove to be valuable for identifying the late 1980's in cores where rapid sedimentation rates makes radio dating difficult. Analysis of additional samples at greater depths is needed to document trends prior to TBT legislation. The DBT concentration trends followed that shown for TBT. The ratio of DBT to TBT is constant throughout the core (Fig. 27) which suggests that little degradation of TBT is occurring after burial or TBT and DBT degradation rates are similar. Laboratory studies (Dowson et al, 1993) have shown that in anaerobic sediments, degradation rates for TBT are quite slow ($t_{1/2}$=years).

PAH

PAH concentrations ranged from 400 to 1170 µg/kg (Table 6) . No obvious trends in concentration with depth are evident in the data (Fig. 28). Concentrations are within the same range as those found in surface sediments during Chesapeake Bay mainstem sediment monitoring at a nearby station, MCB4.3C (38°33'24"/76°26'12", Lat/Long) (Unger et al, 1992). During this work surface sediments were analyzed for total PAH in

1984,1986 and 1991 and fluctuated around 1000 µg/kg. These core data appear to be in good agreement with historical surface sediment data.

Core JB5-PH

Sedimentation Rate: 3 $cmyr^{-1}$ or greater?

PCB and organochlorines

Individual PCB congener concentrations in this core were again near detection limits with totals for the selected congeners ranging from 2-15 µg/kg (Table 7). No consistent trend with depth is evident with an average concentration near 8 µg/kg (Fig. 29). This total corresponds well with surface sediment concentrations measured south of this station in 1991(Unger et al, 1992). During this previous study total PCB concentrations in surface sediments were estimated at 8.31 µg/kg at station MLE 2.3 (38°01'18"/76°21'00") located near the mouth of the Potomac river. OCDD concentrations were constant with depth and averaged near 1 µg/kg (Fig. 30).

Butyltins

Tributyltin concentrations in this core ranged from 5 to 37 µg/kg (Table 8). A maximum concentration of 37 µg/kg occurred at mid depth (12-14 cm) with decreasing values towards the surface (Fig. 31). Measured DBT concentrations in the core showed a similar trend. Lead-210 radio dating of this core suggests that sedimentation rates are 3 cm/yr or greater. This would put the maximum TBT concentration in the core at approximately 1988-1989 and corresponds well with TBT regulatory action enacted in 1988 restricting the use of TBT in antifoulant paints. Water column monitoring of TBT in Chesapeake Bay has demonstrated a similar decrease in TBT concentrations since regulatory action (Fig. 26).

PAH

Total PAH concentrations in this core showed no trend with depth and ranged from 400 -800 µg/kg (Table 9, Fig. 32). Previous analysis of surface sediments at a station near the mouth of the Potomac (MLE 2.3 at 38°01'18"/76°21'00") ranged between 1000-2000 µg/kg from 1984 to 1991 with no obvious trend in the data (Unger et al, 1992).

Core RPH

Sedimentation Rate: 0.5-1.0 $cmyr^{-1}$

PCB and Organochlorines

Individual PCB congener concentrations in core RPH were again near the detection limit and totals ranged from 1-6 µg/kg with no evidence of trends with depth (Table 10, Fig. 33). OCDD concentrations were constant with depth and averaged near 1 µg/kg (Fig. 34).

Butyltins

Tributyltin concentrations in core RPH were less than 3 µg/kg in all sections (Table 11). Dibutyltin was below the detection limit of 1 µg/kg in all sections. Some sections were below the analytical detection limit of 1 µg/kg for TBT. The low levels in this core are not unexpected as previous work comparing TBT concentrations in shellfish

from various regions of the Bay has shown that TBT levels in the Rappahannock River are some of the lowest measured in the southern Chesapeake Bay (Unger et al, 1992). The low TBT concentrations in this core prevents any trend analysis (Fig. 35).

PAH

Total PAH concentrations in this core ranged from a low of 500 µg/kg at the surface to approximately 800 µg/kg at 22 cm (Table 12, Fig. 36). There is a trend of decreasing PAH concentrations towards the surface suggesting decreasing PAH input at this site over the length of the core. Based on Lead-210 dating, this core has the slowest sedimentation rate of those analyzed for PAH and represents a 20 to 40 year span.

Conclusions

PCB and Organochlorines

Individual organochlorine compounds in these three cores were mostly sub part per billion in concentration. These low levels are in agreement with previous work that analyzed surface sediments in the mainstem of the Chesapeake Bay for organic contaminants (Unger et al, 1992). At low concentrations (near the detection limits for the sample size and techniques used here) it is difficult to analyze spatial trends within a core. If future work is planned to look at trends in PCB concentration in mainstem Chesapeake Bay sediments, it is recommended that analytical techniques capable of precise quantification of PCB at low part per trillion concentrations in estuarine sediment samples be employed. In areas where high sedimentation rates occur, long cores should be used for organic analysis and adjacent core sections should be combined to produce larger size samples for chemical analysis. This will lower detection limits to some extent without compromising resolution in cores with high sedimentation rates.

Butyltins

Tributyltin is one of the few pollutants in this country that has been regulated on the basis of a concern for adverse environmental impacts. Most environmental regulations are based on human health issues and environmental clean-up is a byproduct of decreasing human exposure to these compounds. The extreme toxicity of TBT to aquatic organisms and early monitoring efforts in coastal environments led to rapid regulation in the late 1980's. The core data presented here indicates that these regulations are having an impact on reducing TBT in the water column and sediments of Chesapeake Bay. Due to the high sedimentation rates of the cores analyzed, samples from longer cores need to be examined to document trends prior to TBT regulations in the late 1980's. The trends in these data also demonstrates that TBT does not readily degrade once buried in estuarine sediments so that sediments can act as a sink for TBT. This must be considered when estimating the risk when contaminated sediments are exposed to the water column either through natural disturbances such as storm events or by dredging. TBT regulations were national in scope so similar trends should be detected at other locations across the country. As additional data is gathered from other sites, the peak in TBT concentrations may prove to be a valuable chemical marker for the late 1980's in estuarine sediments. This may be particularly valuable for areas where high sedimentation rates makes radio dating difficult in recent sediments.

PAH

The core (RPH) with the slowest sedimentation rate (0.5-1.0 $cmyr^{-1}$)showed a trend of decreasing PAH concentrations in recent years (20-40 years). To identify if this trend is evident throughout Chesapeake Bay, additional work is needed to look at PAH concentrations at other sites and in deeper cores with lower sedimentation rates. Future work in the mainstem of Chesapeake Bay should again target longer cores and thicker core sections for PAH analyses.

REFERENCES

Ayres, G. 1968. Quantitative Chemical Analysis: second edition. Harper and Row Publishers: 709 pp.

Berner, R. A. 1970. Sedimentary pyrite formation. American Journal of Science 268: 1-23.

Berner, R. A. 1981. A new geochemical classification of sedimentary environments. Journal of Sedimentary Petrology 51: 359-365.

Berner, R. A. and R. Raiswell. 1984. C/S method for distinguishing fresh water from marine sedimentary rocks. Geology 12: 365-368.

Blatt, H., G. Middleton and R. Murray. 1980. Origin of Sedimentary Rocks. Prenctice-Hall Inc., Inglewood Cliffs, New Jersey: 782 pp.

Brush, G. S. 1989. Rates and patterns of estuarine sedimentation. Limnology and Oceanography 34: 1235-1246.

Cantillo, A. Y. 1982. Trace elements deposition histories in the Chesapeake Bay. Ph. D. dissertation. Chemistry department, University of Maryland: 298 pp.

Colman, S. M., J. P. Halka, C. H. Hobbs III, R. B. Mixon and D. Foster. 1990. Ancient channels of the Susquehanna River beneath Chesapeake Bay and the Delmarva Peninsula. Geological Society of America Bulletin

Daskalakis, K. and T. P. O'Connor. 1995. Normalization and elemental sediment contamination in the Coastal United States. Environmental Science and Technology 29 (2): 470-477.

Dowson, P. H., J. M. Bubb, T. P. Williams and J. N. Lester. 1993. Degradation of Tributyltin in Freshwater and Estuarine Marina Sediments. Wat. Sci. Tech. Vol. 28, No. 8-9, pp. 133-137.

Forstner, U. and G. T. W. Wittman (eds). 1979. Metal Pollution in the Aquatic Environment. Springer-Verlag: 486 pp.

Halka, J. P., S. M. Colman and C. H. Hobbs III. 1993. Distribution of gas in surficial sediments of the Chesapeake Bay. U. S. Geological Survey Miscellaneous Investigation Map MF-1948-E: 3 sheets.

Halka, J. P. and D. L. Gardner. 1987. Acoustic investigation of paleo-drainage networks in central Chesapeake Bay. Journal of the Acoustic Society of America 82: S123.

Hennessee, E. L., P. J. Blakeslee and J. M. Hill. 1986. The distribution of organic carbon and sulfur in surficial sediments of the Maryland portion of the Chesapeake Bay. Journal of Sedimentary Petrology 56: 674-683.

Hill, J. M., J. P. Halka, R. D. Conkwright, Koczot and S. Coleman. 1992. Distribution and effects of shallow gas on bulk estuarine sediment properties. Continental Shelf Research 12 (10): 1219-1230.

Hill, J. M. 1984. Identification of biogeochemical reservoirs in Chesapeake Bay. Ph. D. dissertation. Northwestern University, Evanston, Illinois: 354 pp.

Hill, J. M., G. S. Brush and J. Park. 1996. Geochemical history of the Chesapeake Bay: natural and anthropogenic influences. Society of Environmental Toxicology and Chemistry. abstract 1996 meeting.

Kerhin, R. T., J. P. Halka, D. V. Wells, E. L. Hennessee, P. J. Blakeslee, N. Zoltan and R. H. Cuthbertson. 1988. The surficial sediments of Chesapeake Bay, Maryland: physical characteristics and sediment budget. Maryland Geological Survey Report of Investigations No. 48: 82 pp.

Krumbein, W. (ed.). 1983. Microbial Geochemistry. Blackwell Scientific Publications: 330 pp.

Leguille, F., A. Castetbon, M. Astruc and R. Pinel. 1993. Study of the Tributyltin water-Solid Partitioning. Environ. Technology, Vol. 14, pp. 949-955.

O'Connor, T. P., B. Beliaeff. 1995. Recent Trends in Coastal Environmental Quality: Results from the Muscle Watch Program. National Oceanic and Atmospheric Administration, Coastal Monitoring and Bioeffects Assessment Division, NOAA/NOS, N/ORCA2, SSMC4, 1305 East-West Highway, Silver Spring, MD, 20910-3281.

Pejrup, M. 1988. The triangular diagram used for classification of estuarine sediments: a new approach. In: deBoer, P. L., A. van Gelder and S. D. Nio (eds.). Tide-influenced Sedimentary Environments and Facies. D. Reidel Publishing Company, Dordrecht, Holland: 289-300.

Raiswell, R. and R. A. Berner. 1985. Pyrite formation in euxinic and semi-euxinic sediments. American Journal of Science 285: 710-724.

Redfield, A. C., B. H. Ketchum and F. A. Richards. 1966. The influence of organisms on the composition of seawater. In: Hill (ed.) The Sea: Vol. II: Wiley-Interscience, New York.

Shimoyama, A. and C. Ponnamperuma. 1975. Organic material of recent Chesapeake Bay sediments. Geochemistry Journal 9: 85-90.

Sinex, S. A., A. Y. Cantillo and G. R. Helz. 1980. Accuracy of acid extraction methods for trace metals in sediments. Analytical Chemistry 52: 2342-2346.

Sinex, S. A. and G. R. Helz. 1981. Regional geochemistry of trace metals in Chesapeake Bay sediments. Environmental Geology 3: 315-323.

Spiker, E. C., J. L. Glenn and M. M. Nichols. 1982. Carbon isotopes studies in the Chesapeake Bay estuarine system. American Geophysical Union: abstract for spring meeting, Philadelphia, Pa.

Suhr, N. H. and C. O. Ingamells. 1966. Solution techniques for analysis of silicates. Analytical Chemistry 38: 730-734.

Trefrey, J. H. and Presley. 1976. Heavy metals in sediments from San Antonio Bay and the northwest Gulf of Mexico. Environmental Geology 1: 282-292.

Turekian, K. and K. Wedepohl. 1961. Distribution of elements in some major units of the Earth's crust. Geological Society of America Bulletin 72: 175-192.

Unger, M. A., W. G. MacIntyre, J. Greaves and R. J. Huggett. 1986. GC Determination of Butyltins in Natural Waters by Flame Photometric Detection of Hexyl Derivatives with Mass Spectrometric Confirmation. Chemosphere 15(4):461-470.

Unger, M. A., W. G. MacIntyre and R. J. Huggett. 1988. Sorption Behavior of Tributyltin on Estuarine and Freshwater Sediments. Environmental Toxicology and Chemistry, Vol. 7, pp. 907-915.

Unger, M. A., C. L. Smith, J. Greaves and G. W. Rice. 1992. 1991 Chesapeake Bay Mainstem Sediment Monitoring. Report. Prepared for Virginia State Water Control Board as part of the EPA Chesapeake Bay Mainstem Water Quality Monitoring Program. 55 pp.

Unger, M. A., E. T. Travelstead and G. G. Vadas. 1995. Measurement of Trends in Tributyltin Concentrations in Virginia Shellfish: An Assessment of the Effectiveness of

Tributyltin Legislation. Final Report. Prepared for Virginia Environmental Endowment. Richmond, Virginia. 13 pp.

USEPA. 1994. Assessment and Remediation of Contaminated Sediments (ARCS) Program: Assessment Guidance Document EPA 905-B94-002. Great Lakes National Program Office, Chicago, Ill.: 247 pp.

Van Loon, J. C. 1980. Analytical Atomic Absorption Spectroscopy: Selected Methods. Academic Press,, New York: 337 pp.

LIST OF FIGURES

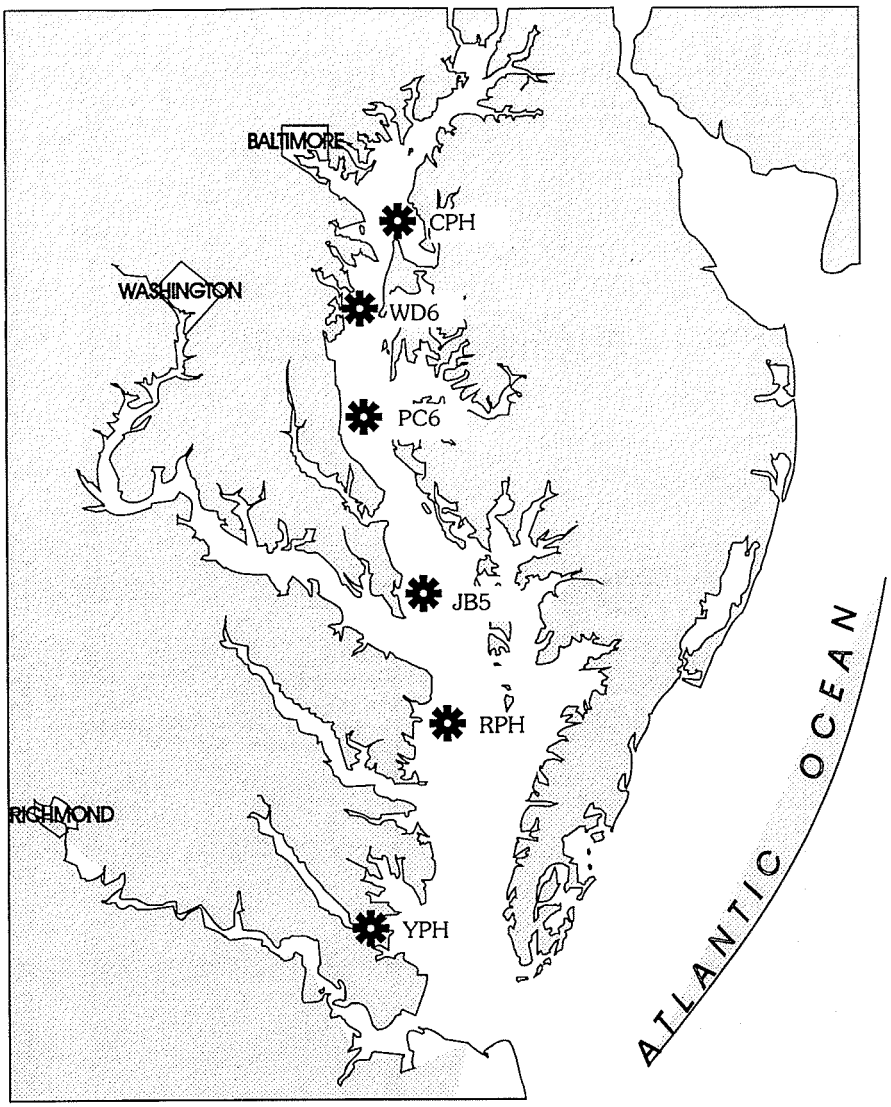

Station	Latitude	Longitude
CPH	39° 04.822'	76° 16.939'
WD6	38° 52.299'	76° 23.891'
PC6	38° 32.663'	76° 26.199'
JB5	38° 05.814	76° 12.735'
RPH	37° 47.125'	76° 10.402'
YPH	37° 13.878'	76° 28.012'

Figure 1. Location of cores.

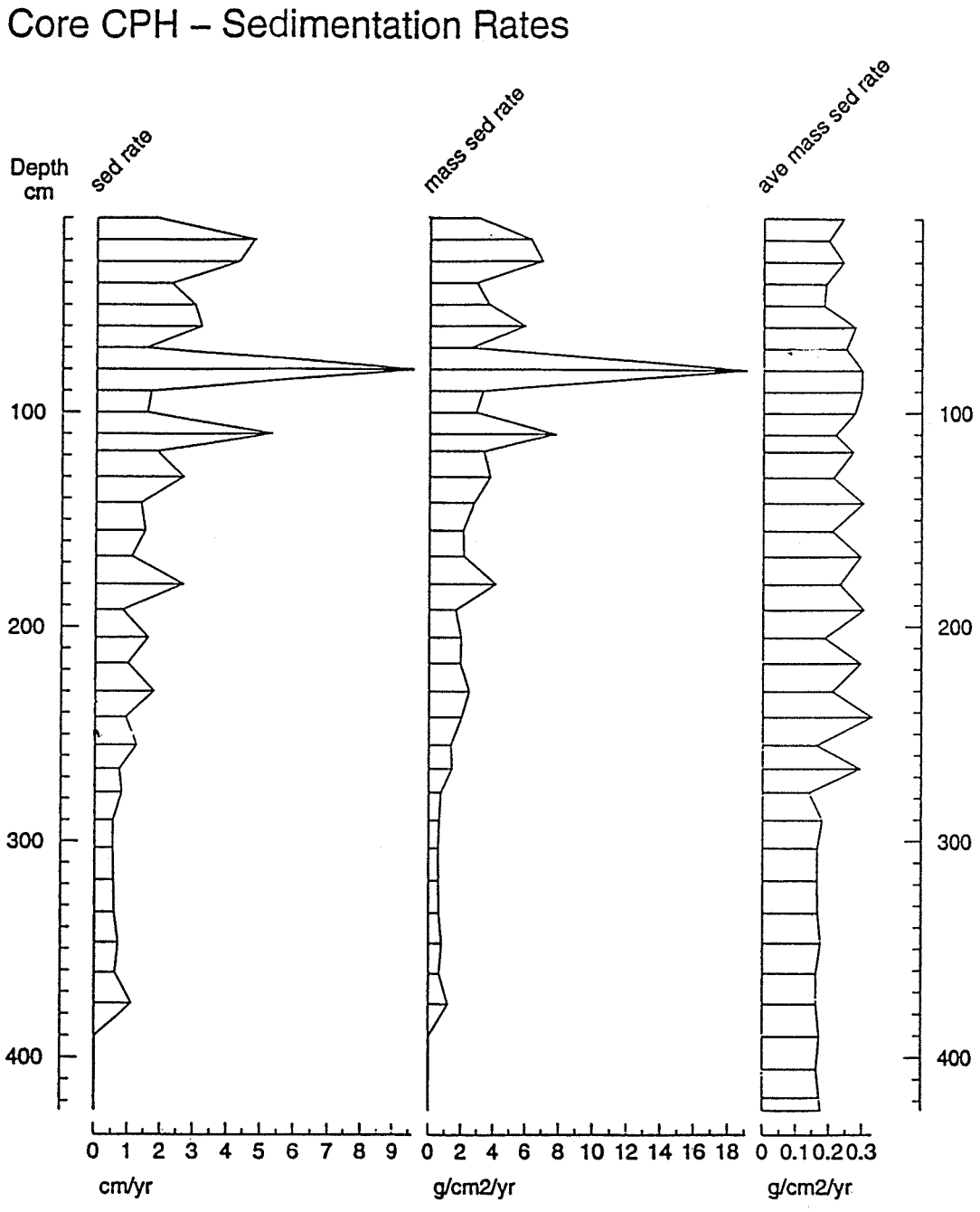

Figures 2. Sedimentation rates in Core CPH.

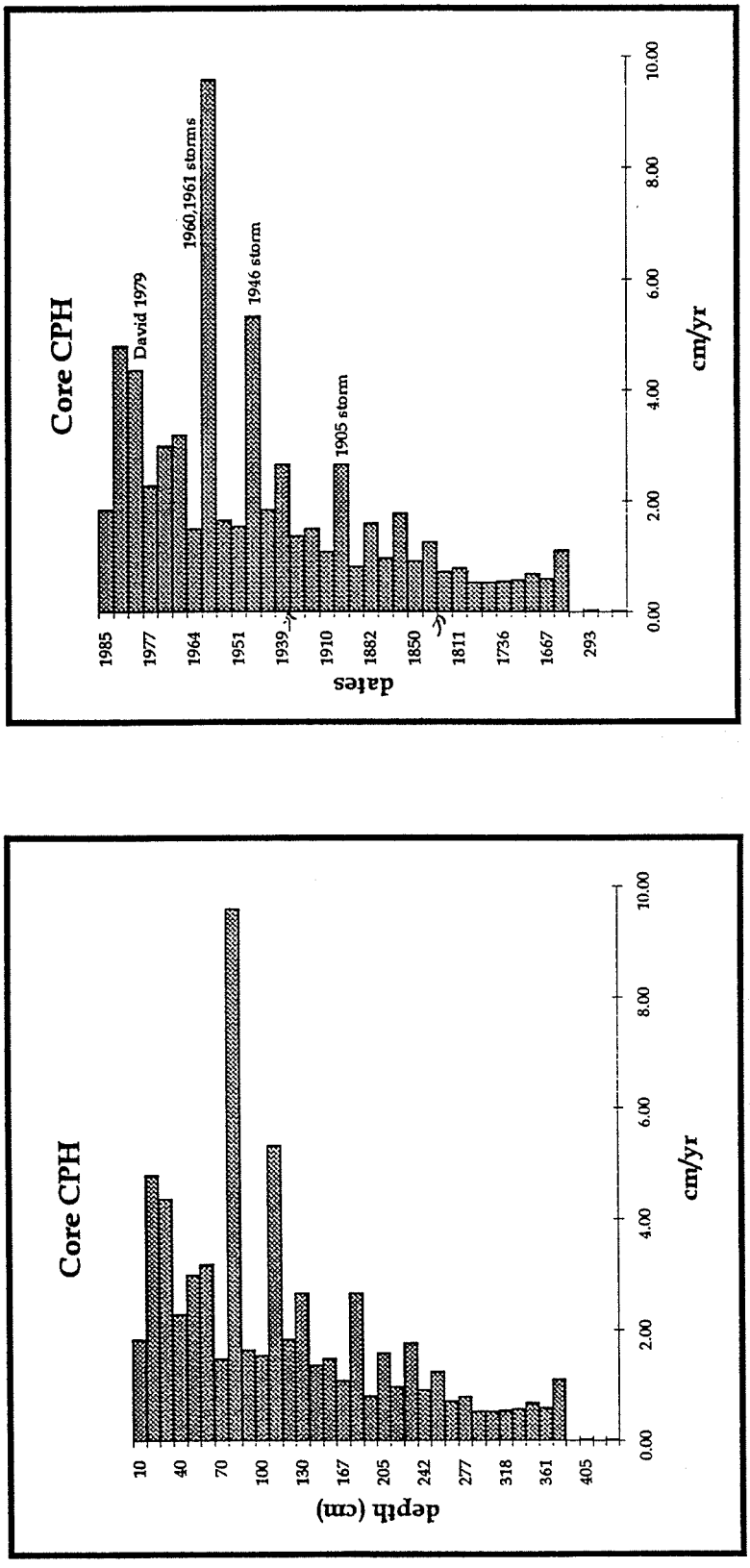

Figure 3. Sedimentation rates vs. depth and time with storm records for Core CPH.

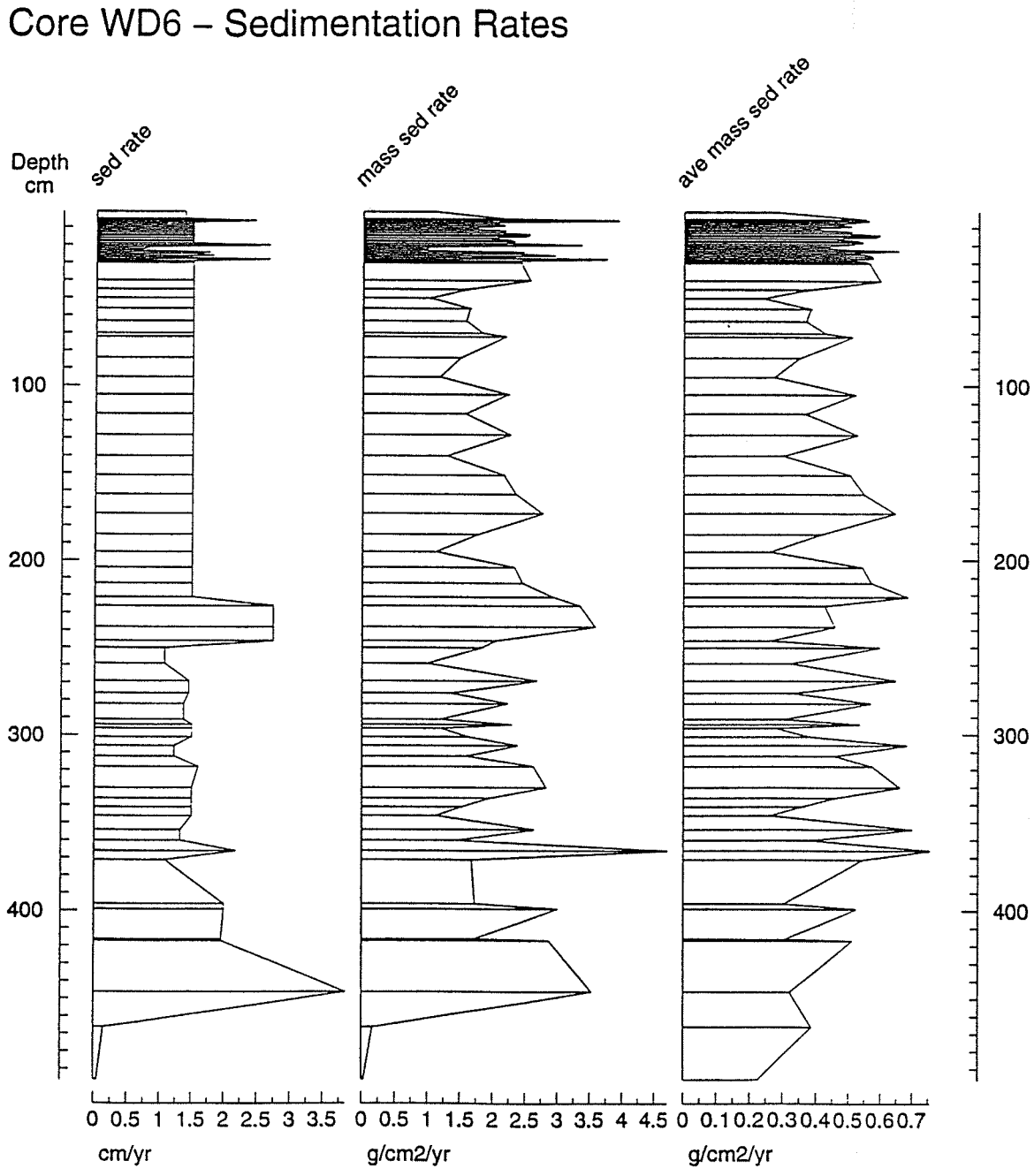

Figure 4. Sedimentation rates in Core WD6.

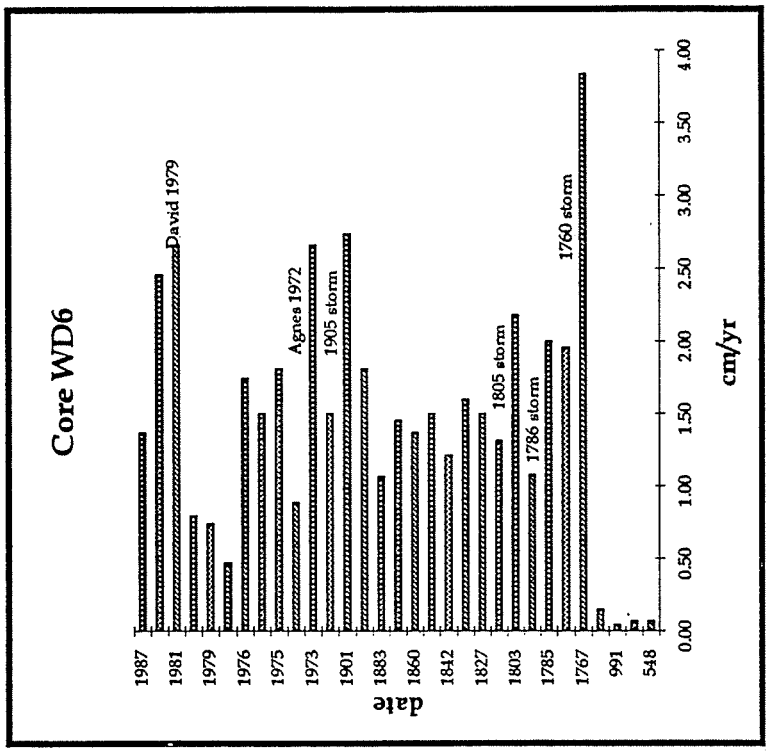

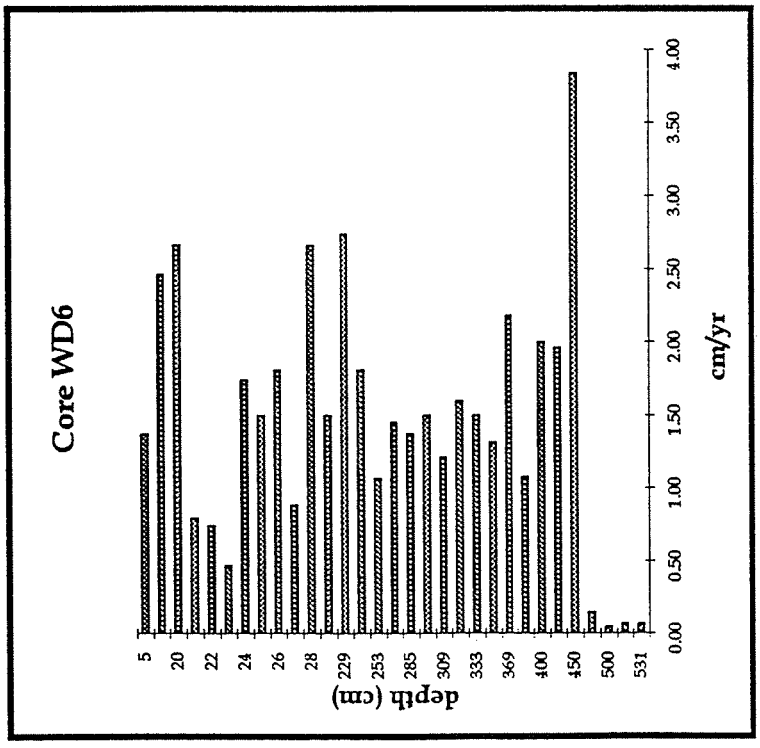

Figure 5. Sedimentation rates vs. depth and time with storm records for Core WD6.

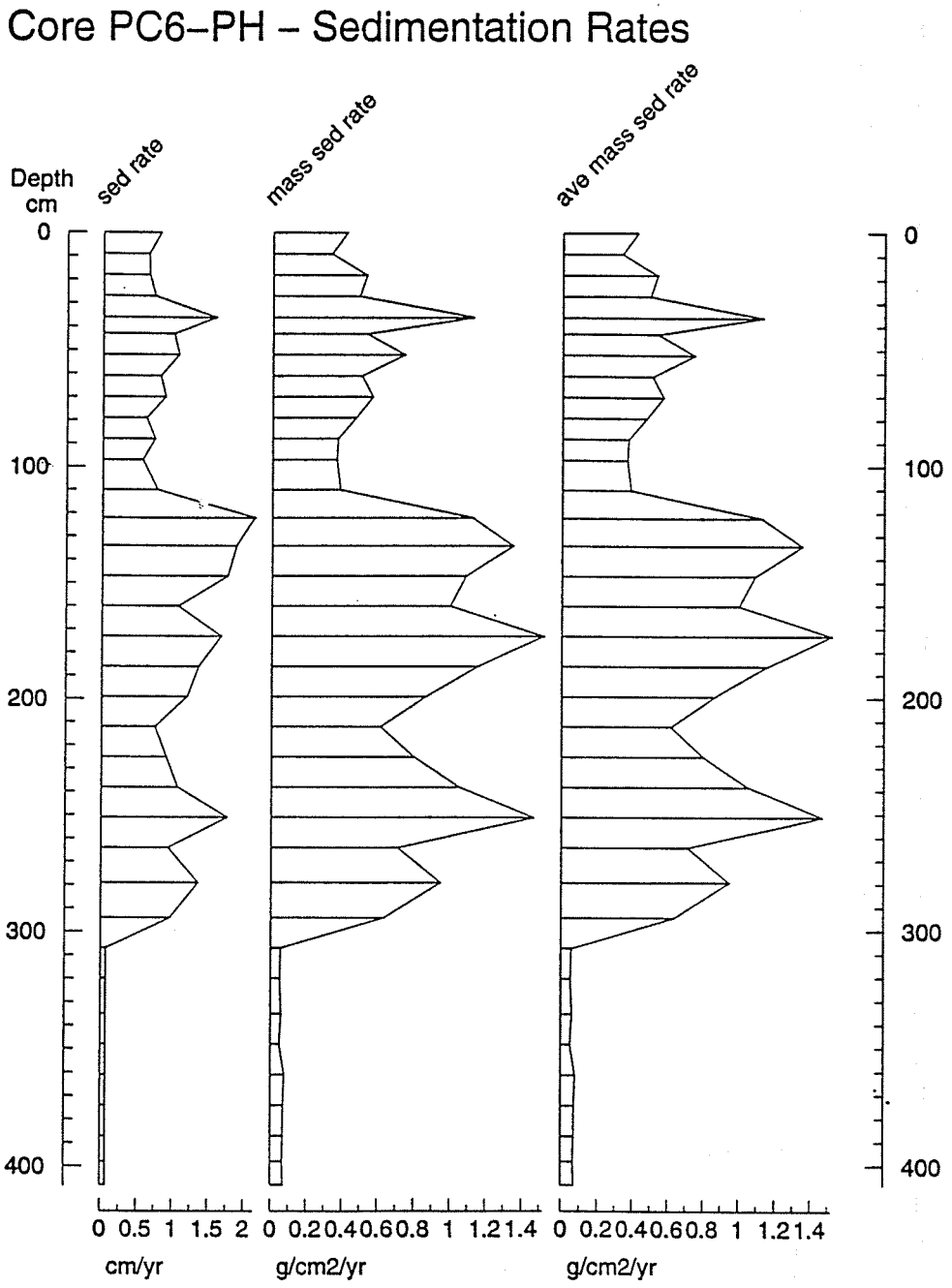

Figure 6. Sedimentation rates in Core PC6-PH.

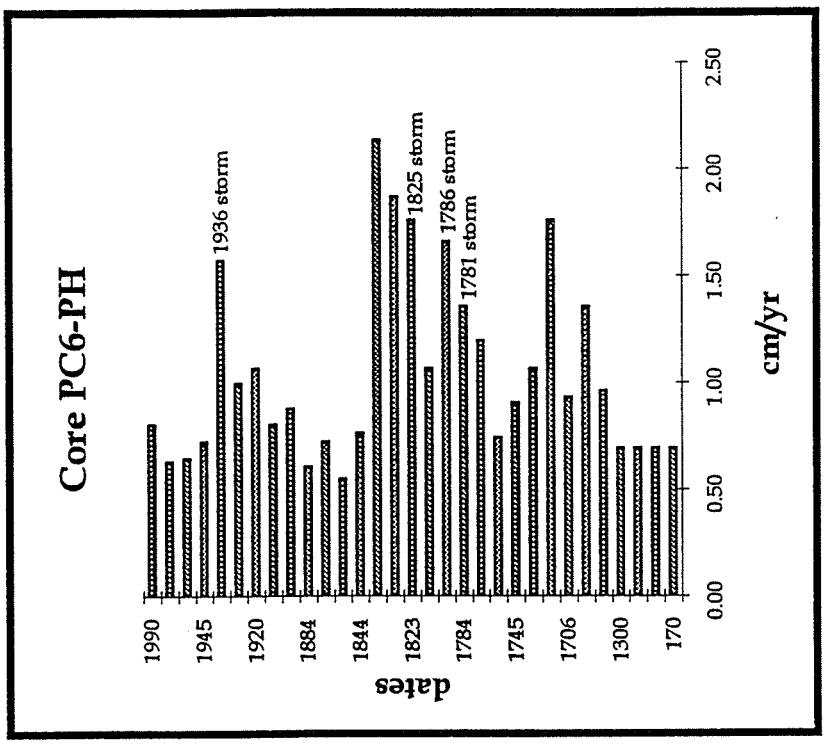

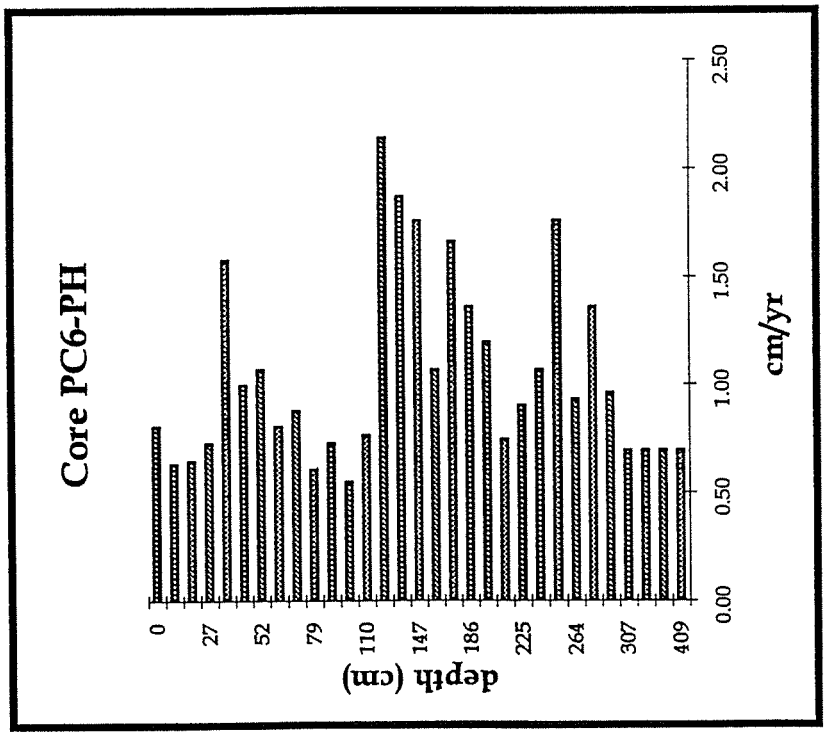

Figure 7. Sedimentation rates vs. depth and time with storm records for Core PC6-PH.

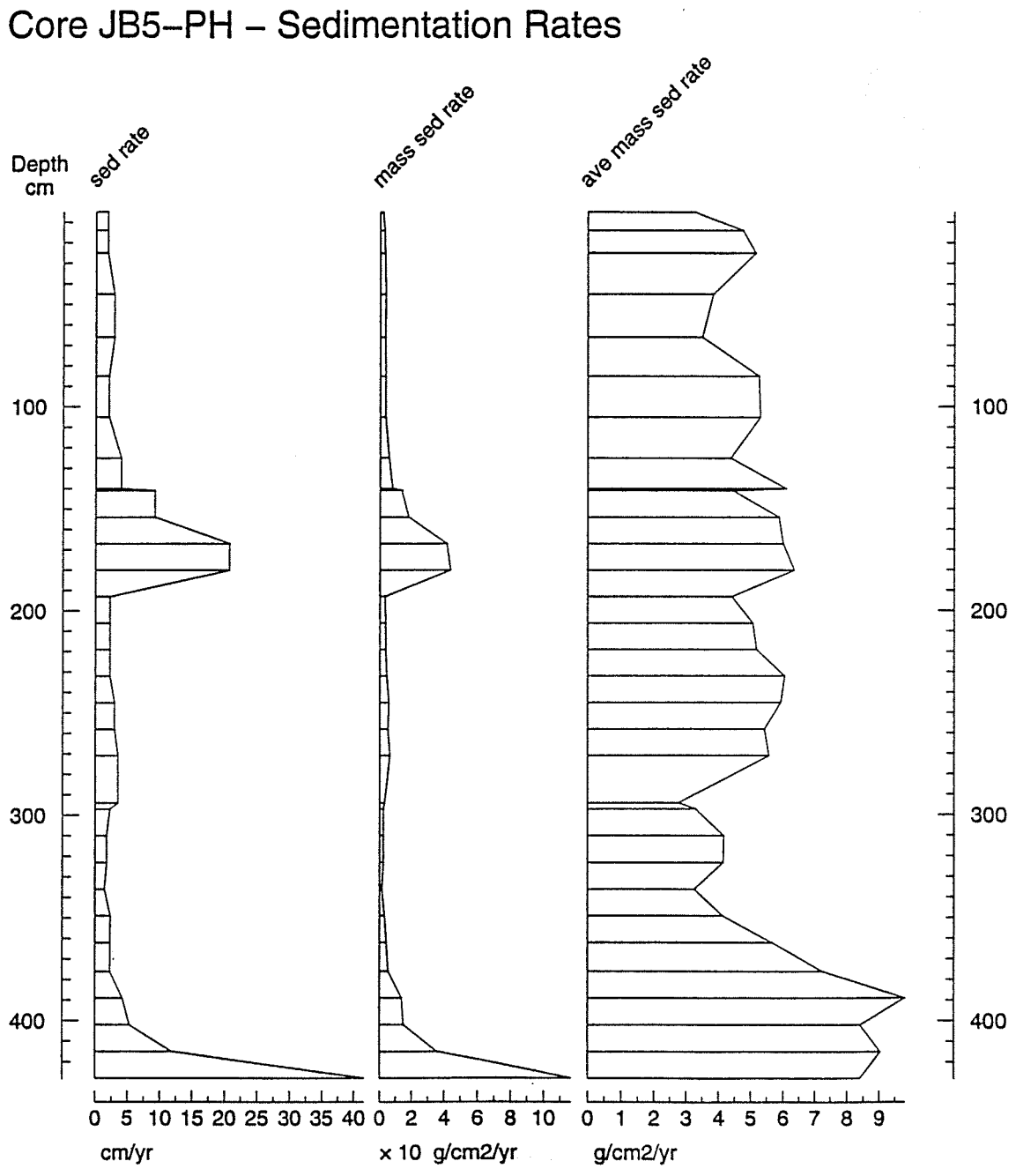

Figure 8. Sedimentation rates in Core JB5-PH.

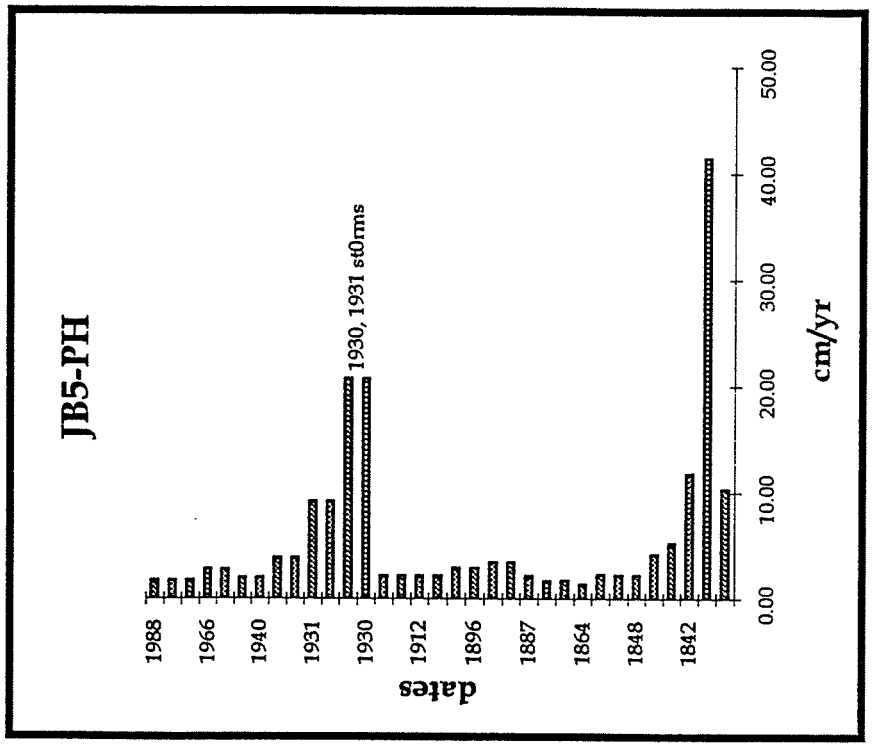

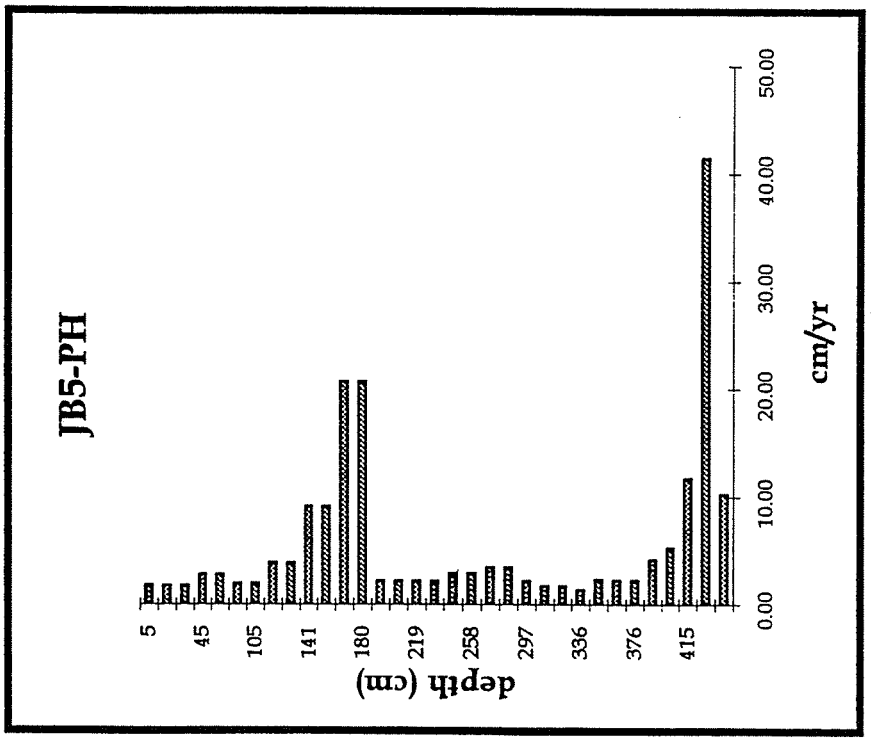

Figure 9. Sedimentation rates vs. depth and time with storm records for Core JB5-PH.

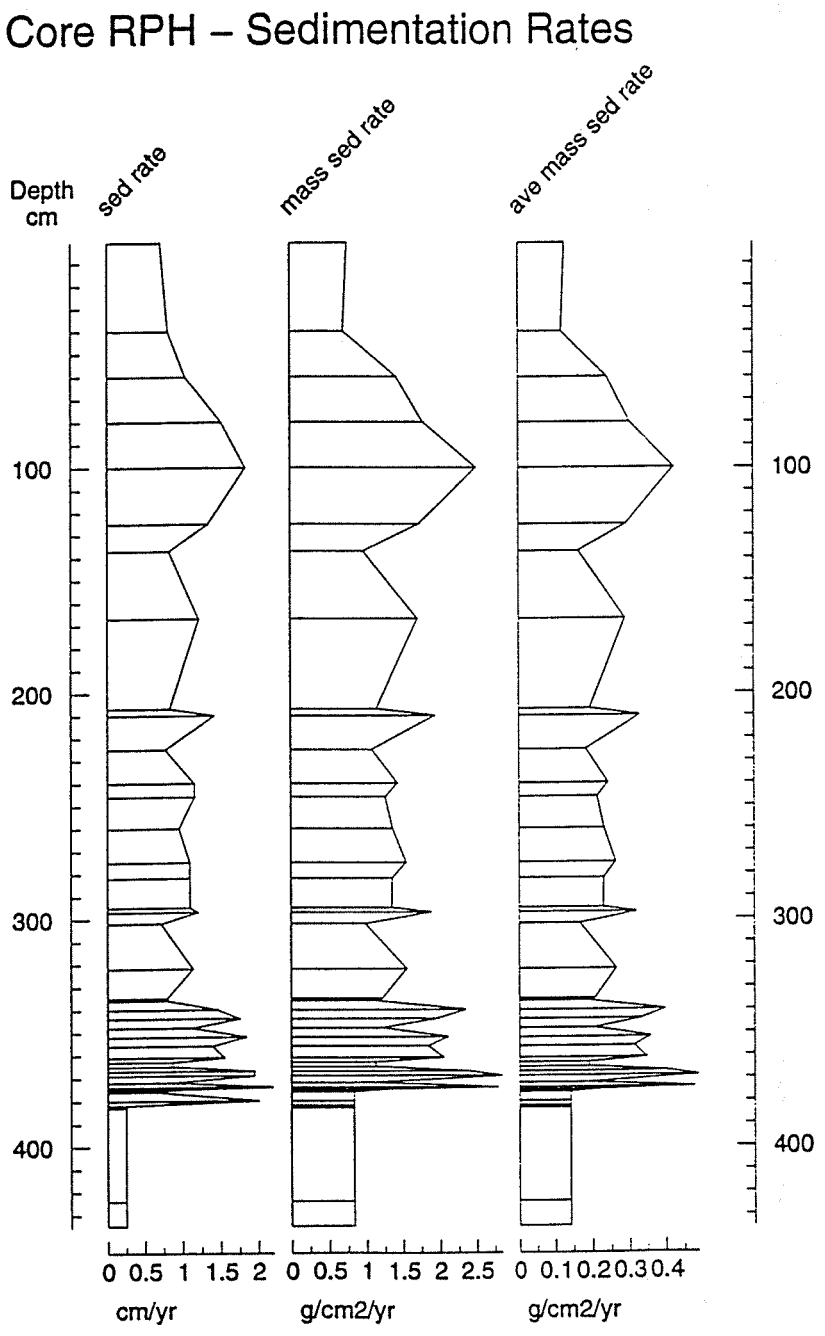

Figure 10. Sedimentation rates in Core RPH.

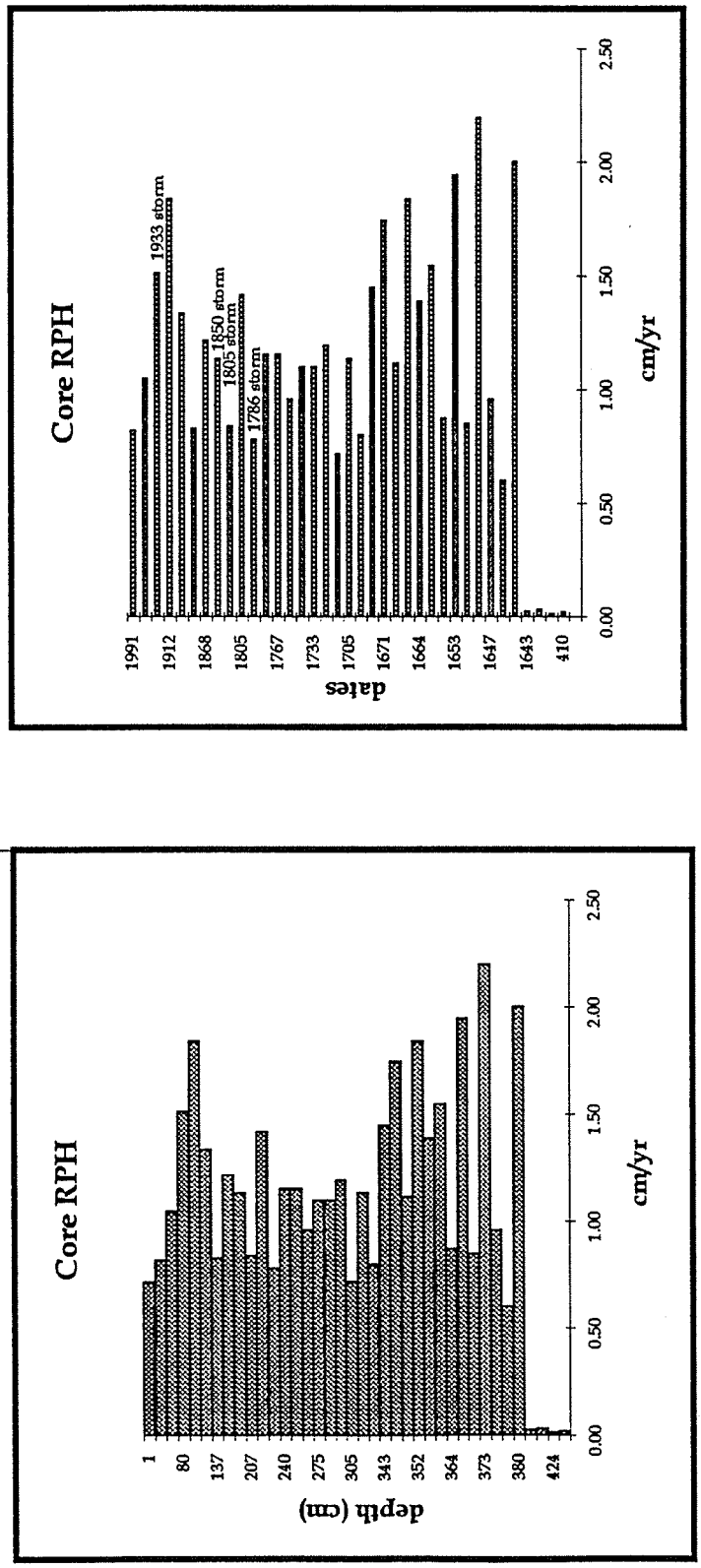

Figure 11. Sedimentation rates vs. depth and time with storm records for Core RPH.

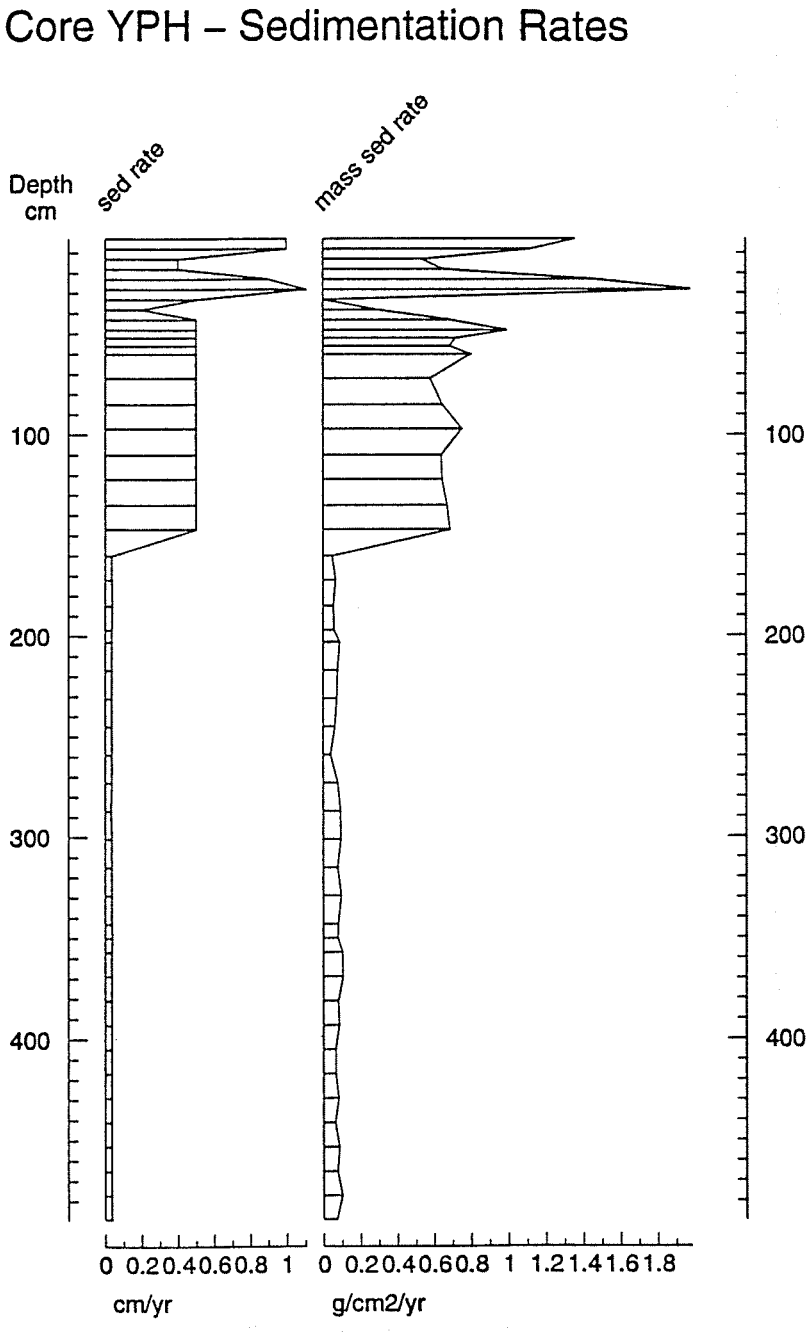

Figure 12. Sedimentation rates in Core YPH.

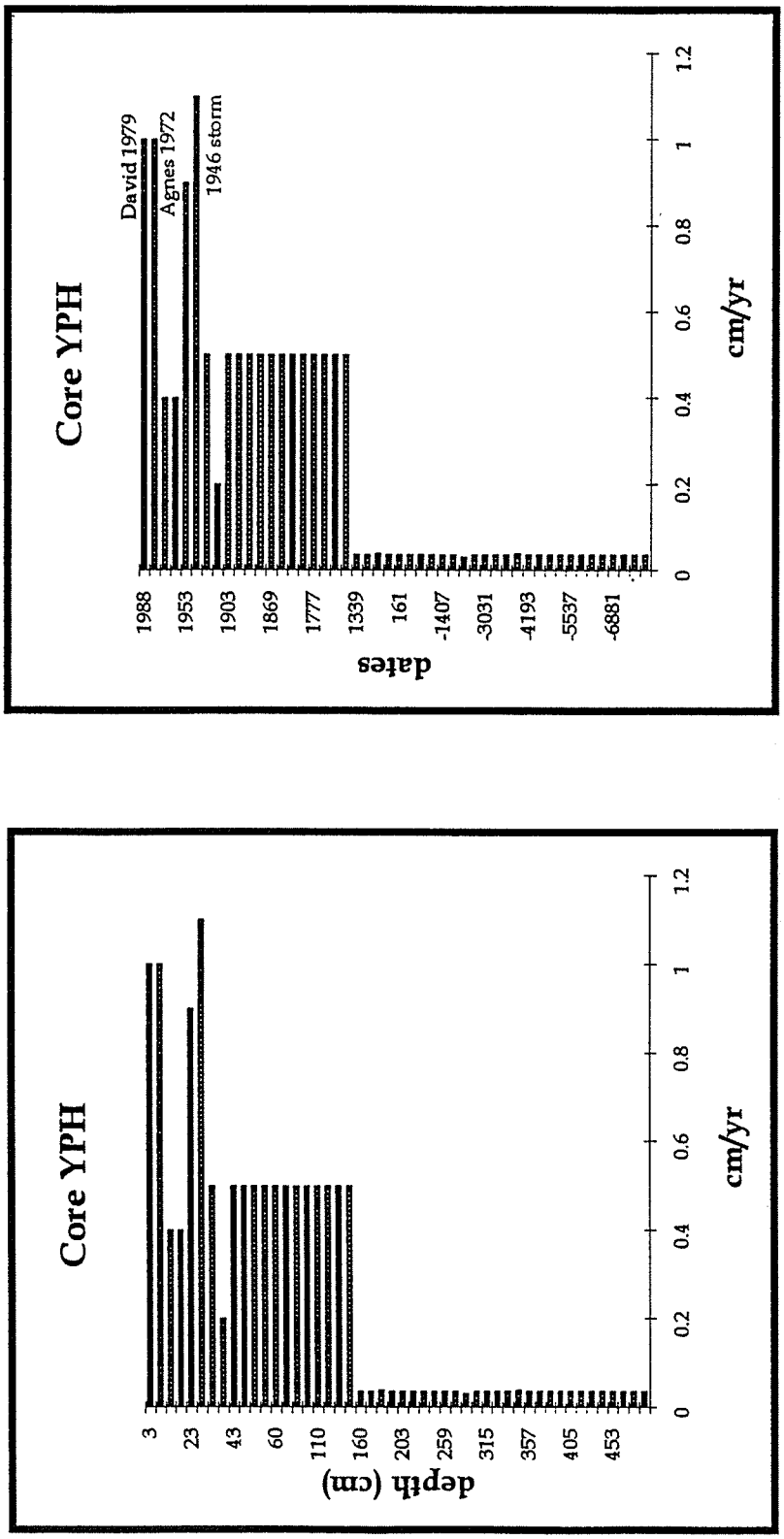

Figure 13. Sedimentation rates vs. depth and time with storm records for Core YPH.

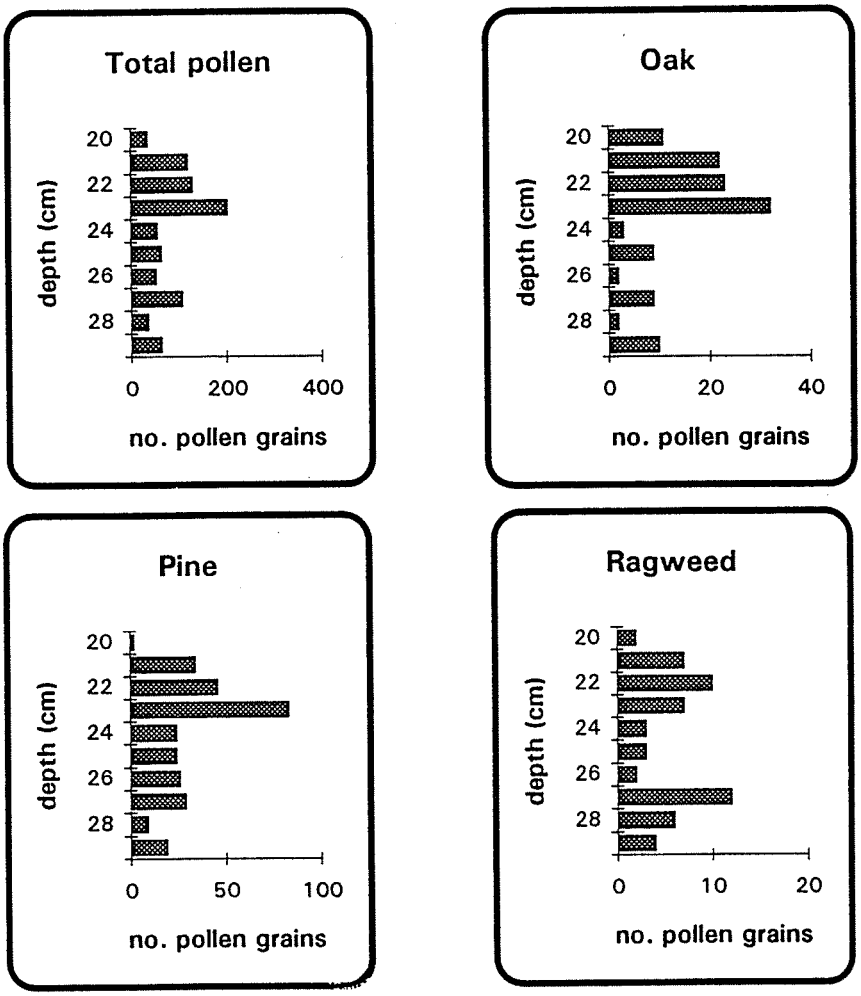

Figure 14. Distributions of some major pollen types in sediment cores.

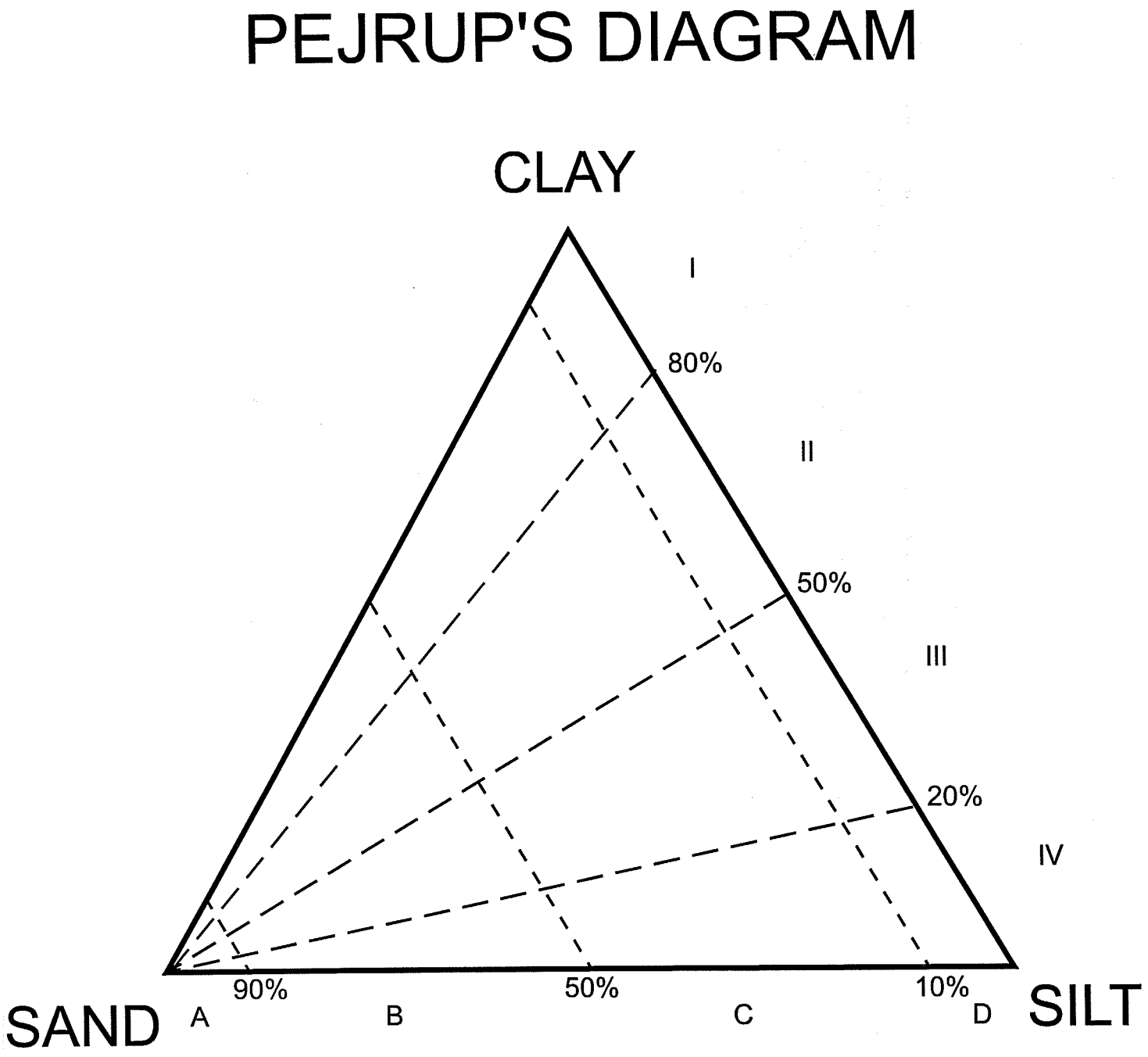

Figure 15. Pejrup's diagram showing classification of sand, silt and clay.

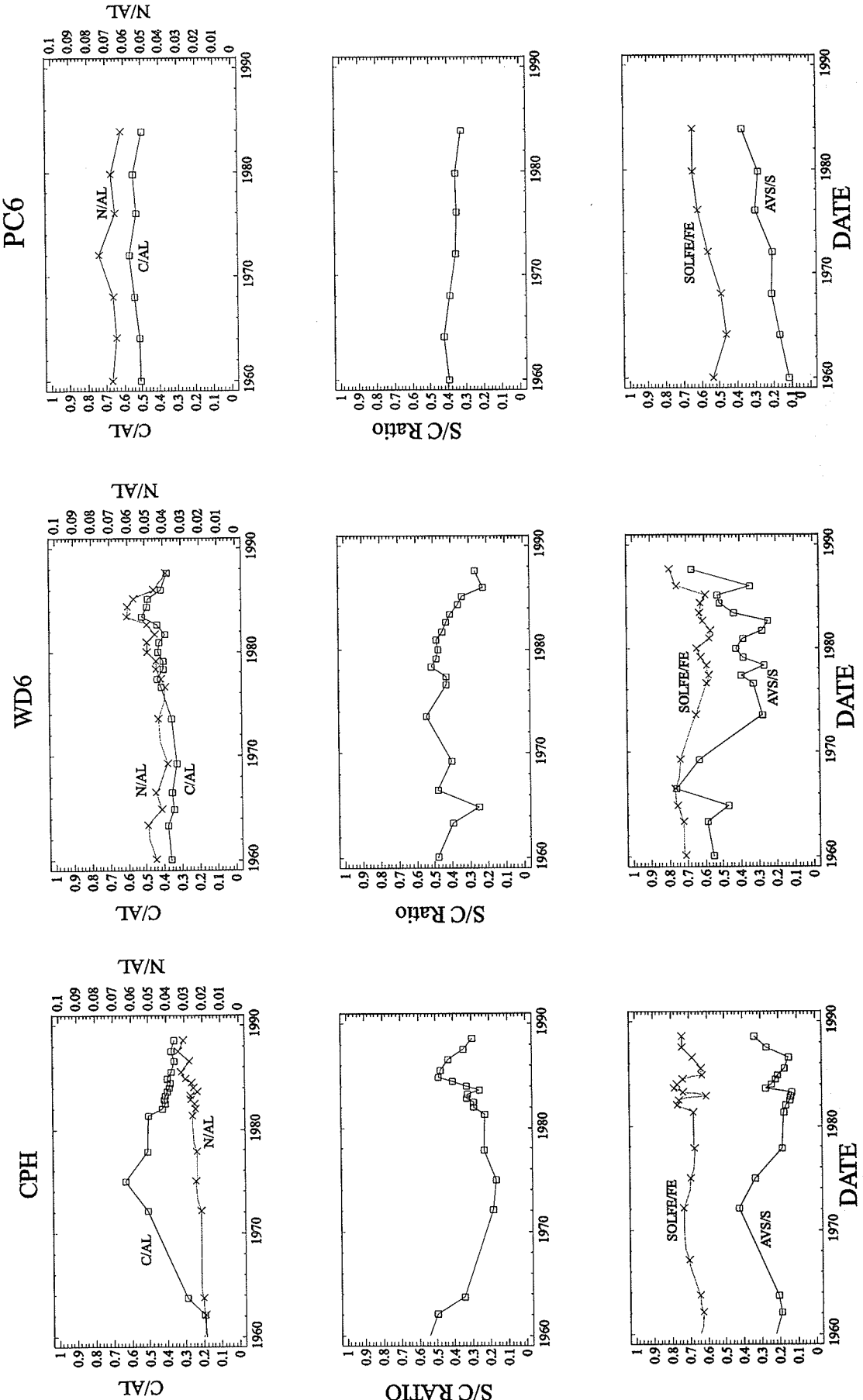

Figure 16. Ratios of chemical species used to interpret geochemical environmental conditions through time.

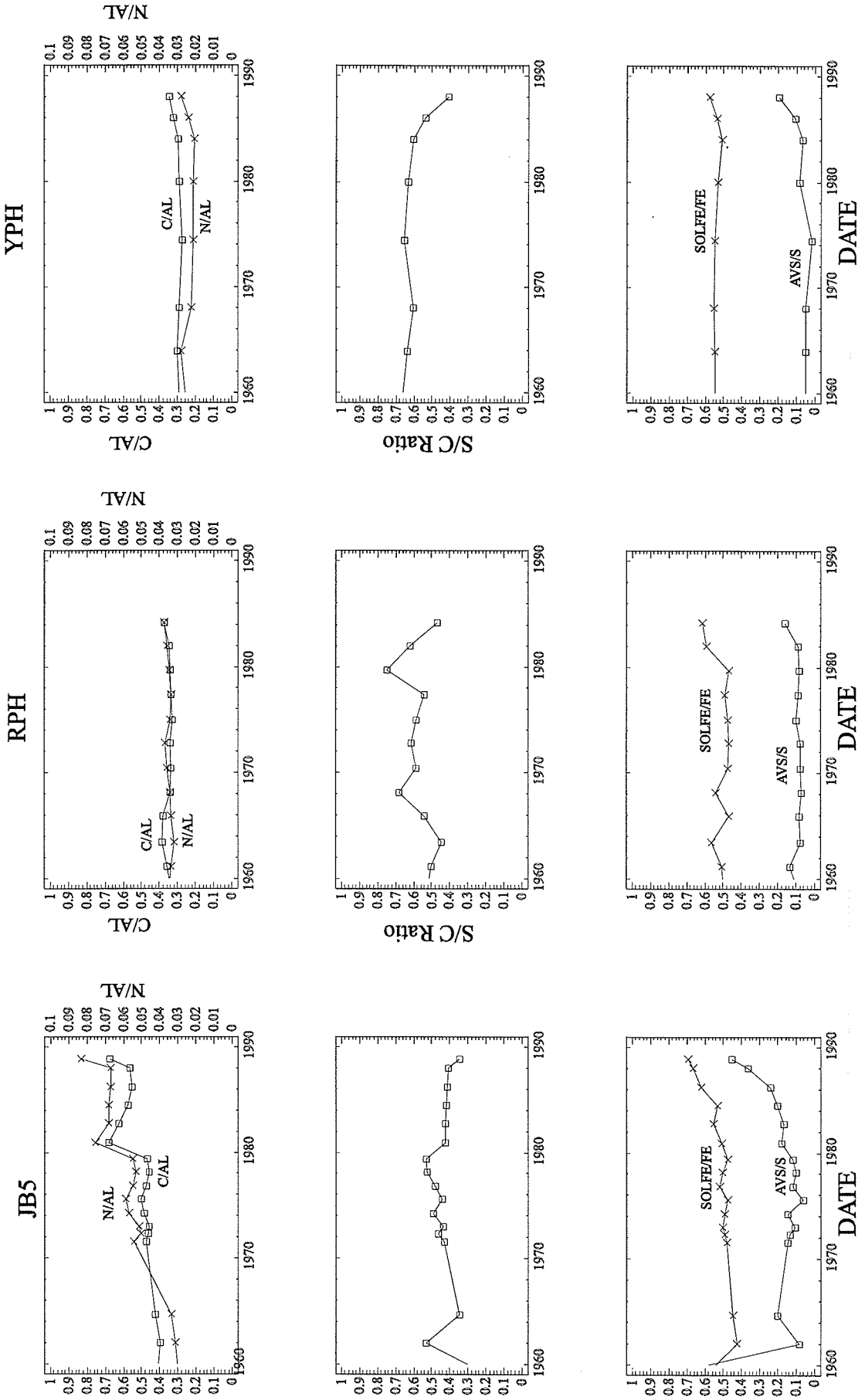

Figure 16 continued.

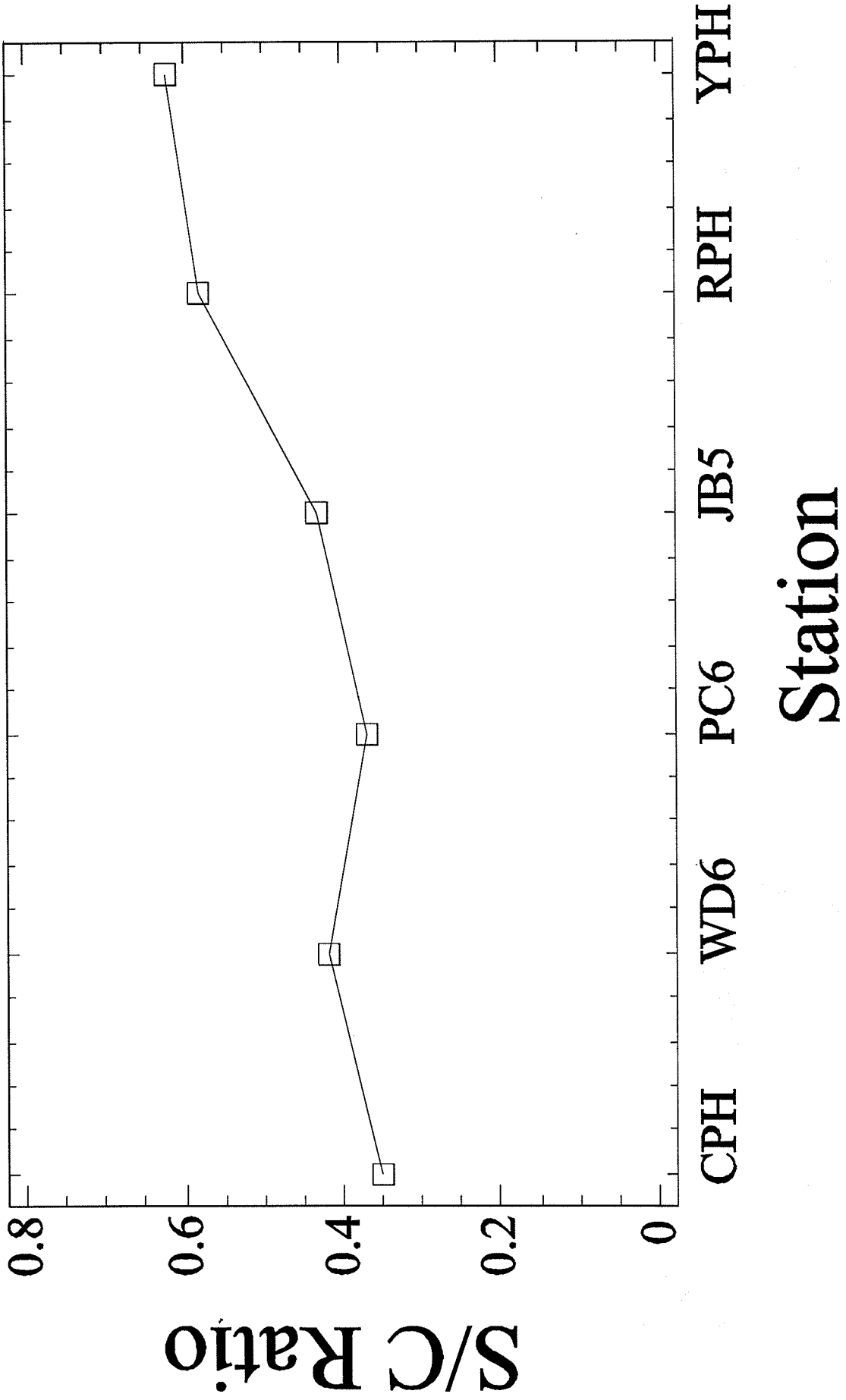

Figure 17. The average S/C ratio in recent sediments for each of the coring locations.

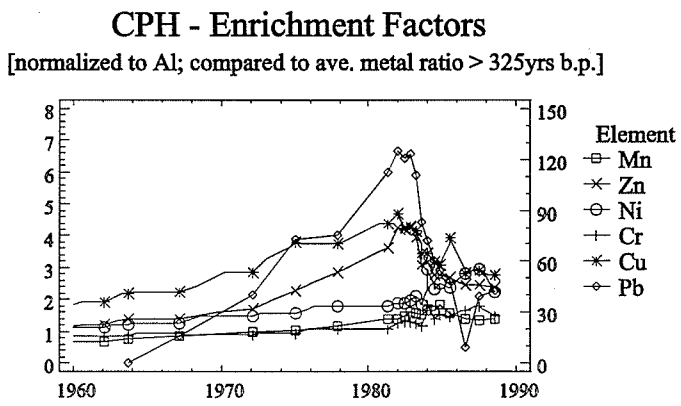

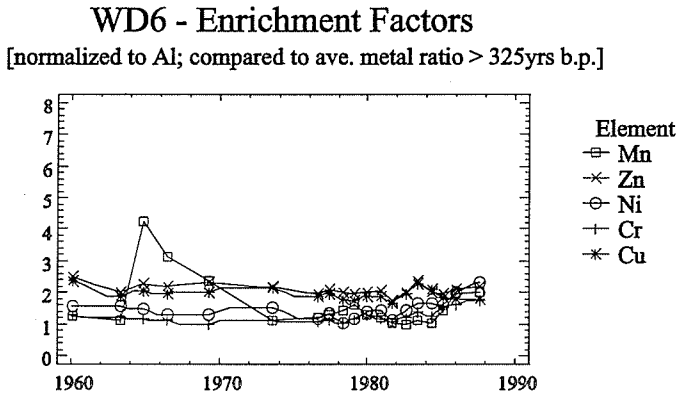

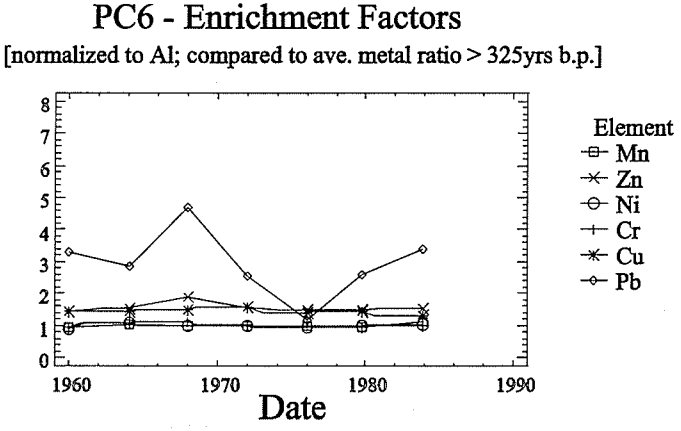

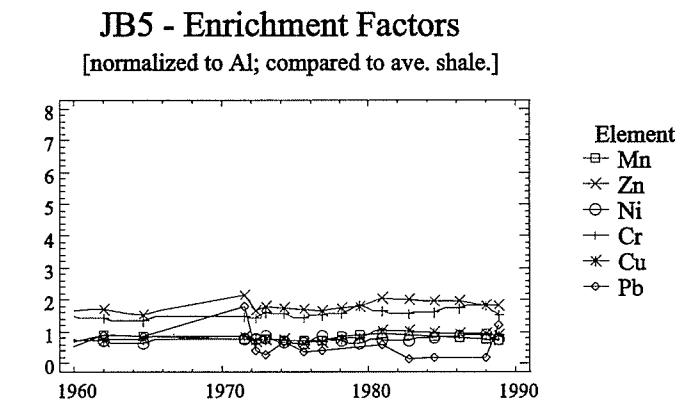

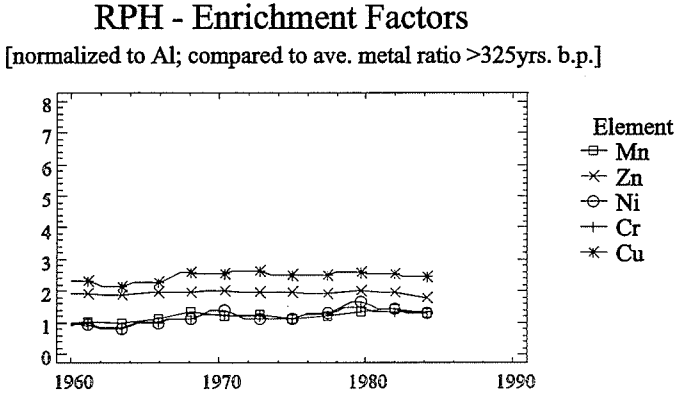

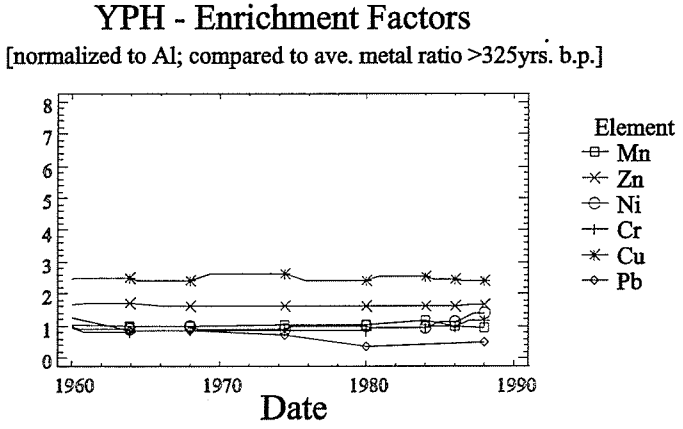

Figure 18. Enrichment factors normalized to Al and referenced to pristine sediments of the same core for all locations.

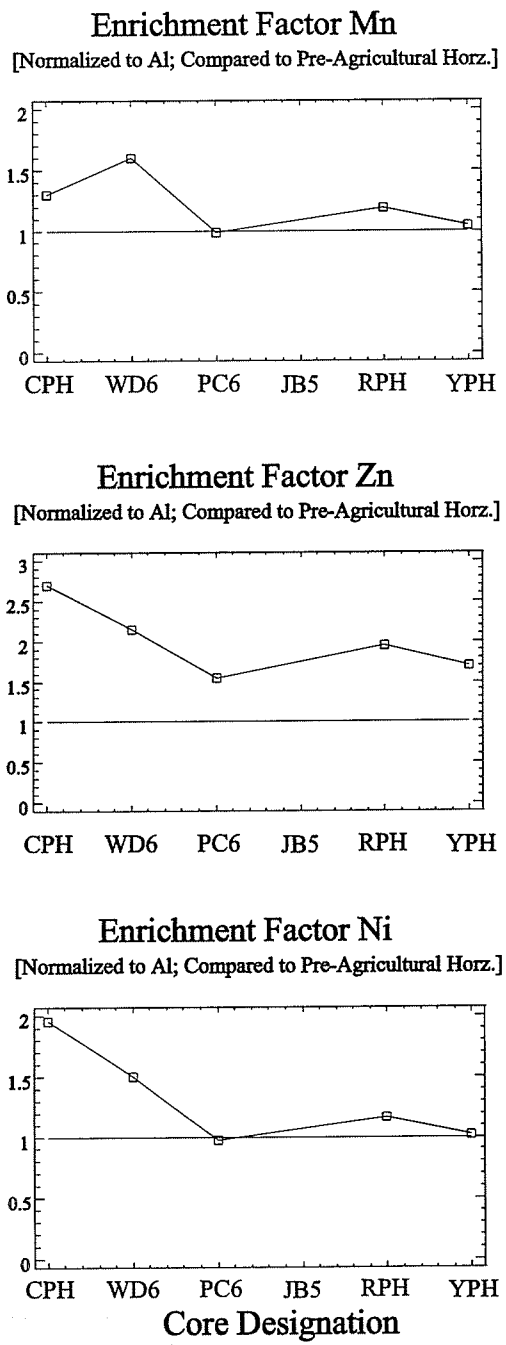

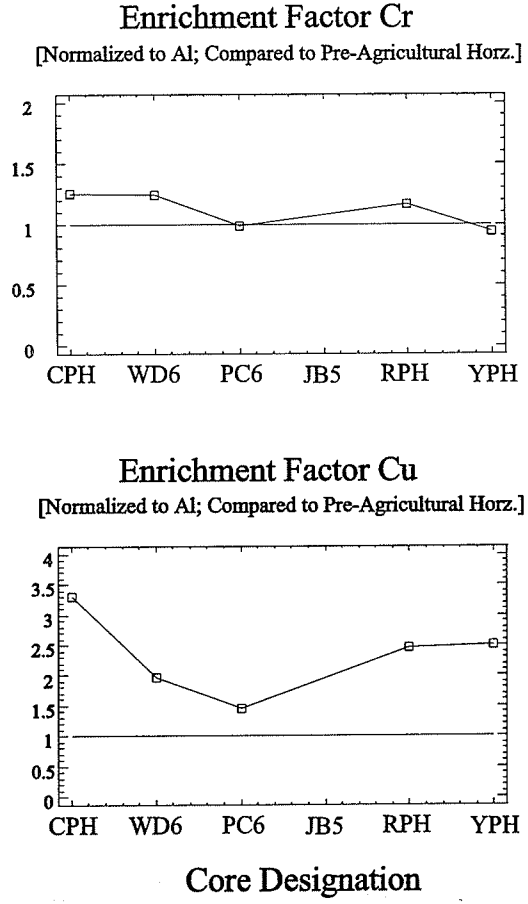

Figure 19. The average enrichment factor for each metal as a function of station location.

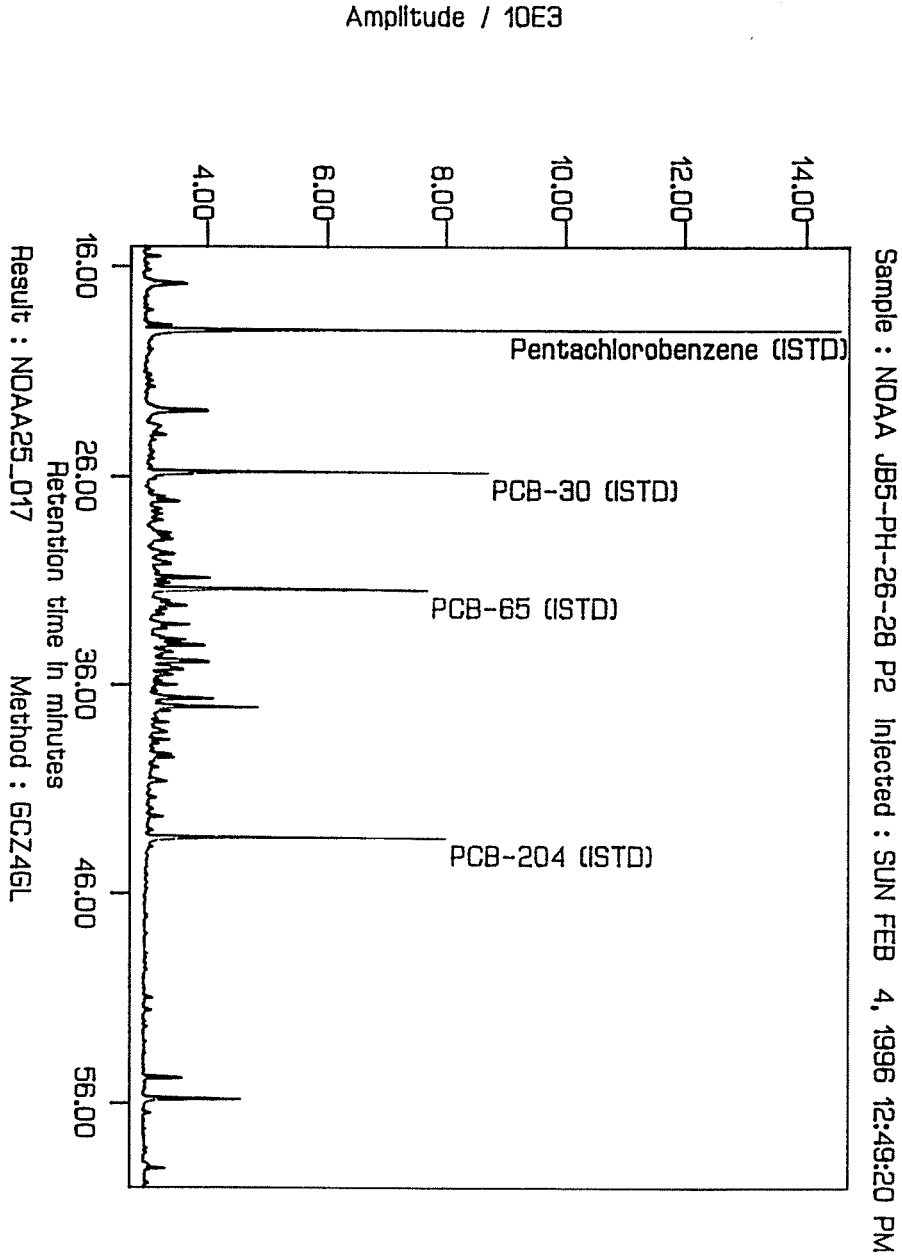

Figure 20. Gas chromatogram of organochlorine contaminants in typical core section.

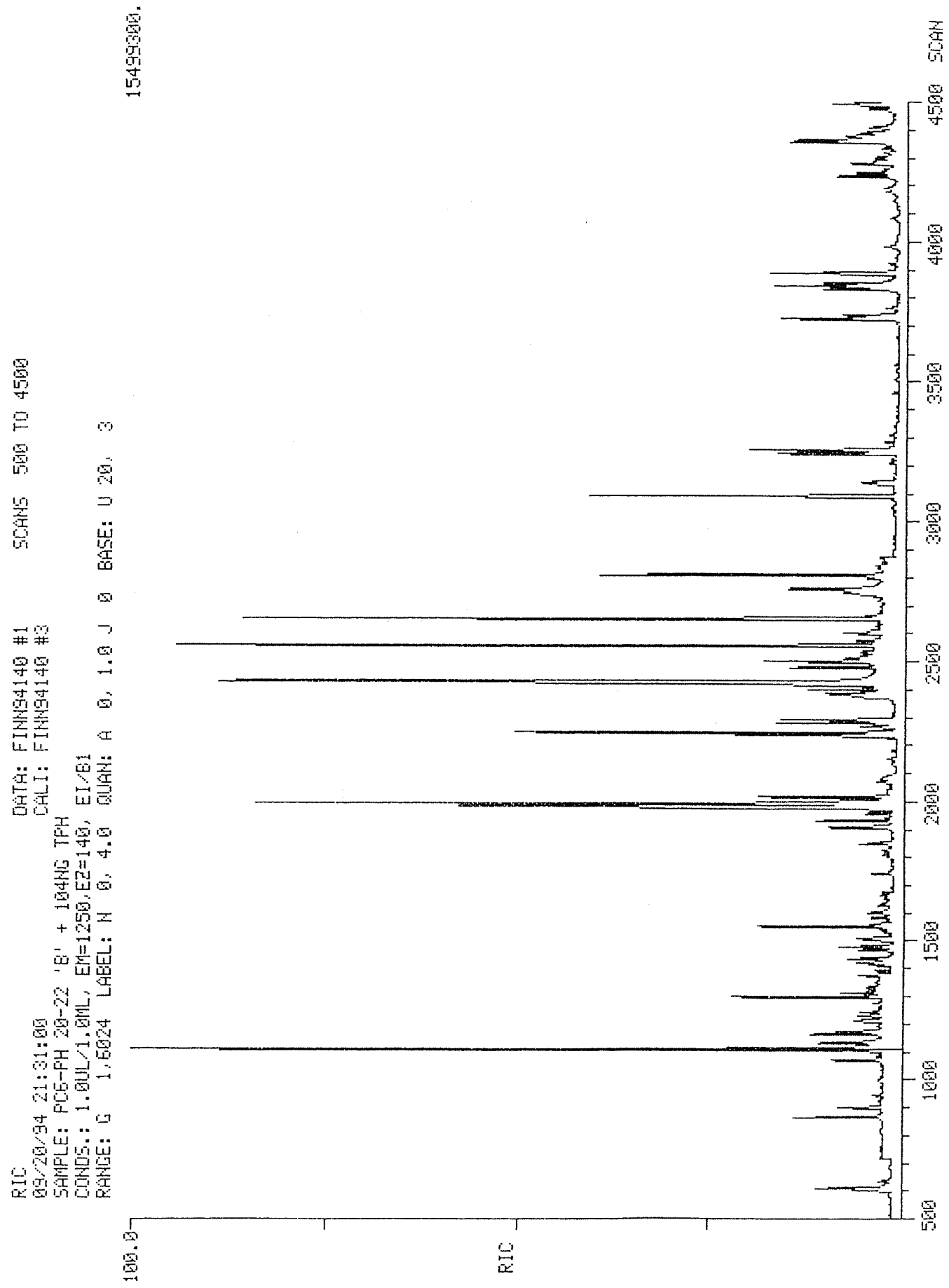

Figure 21. Gas chromatogram of PAH in typical core section.

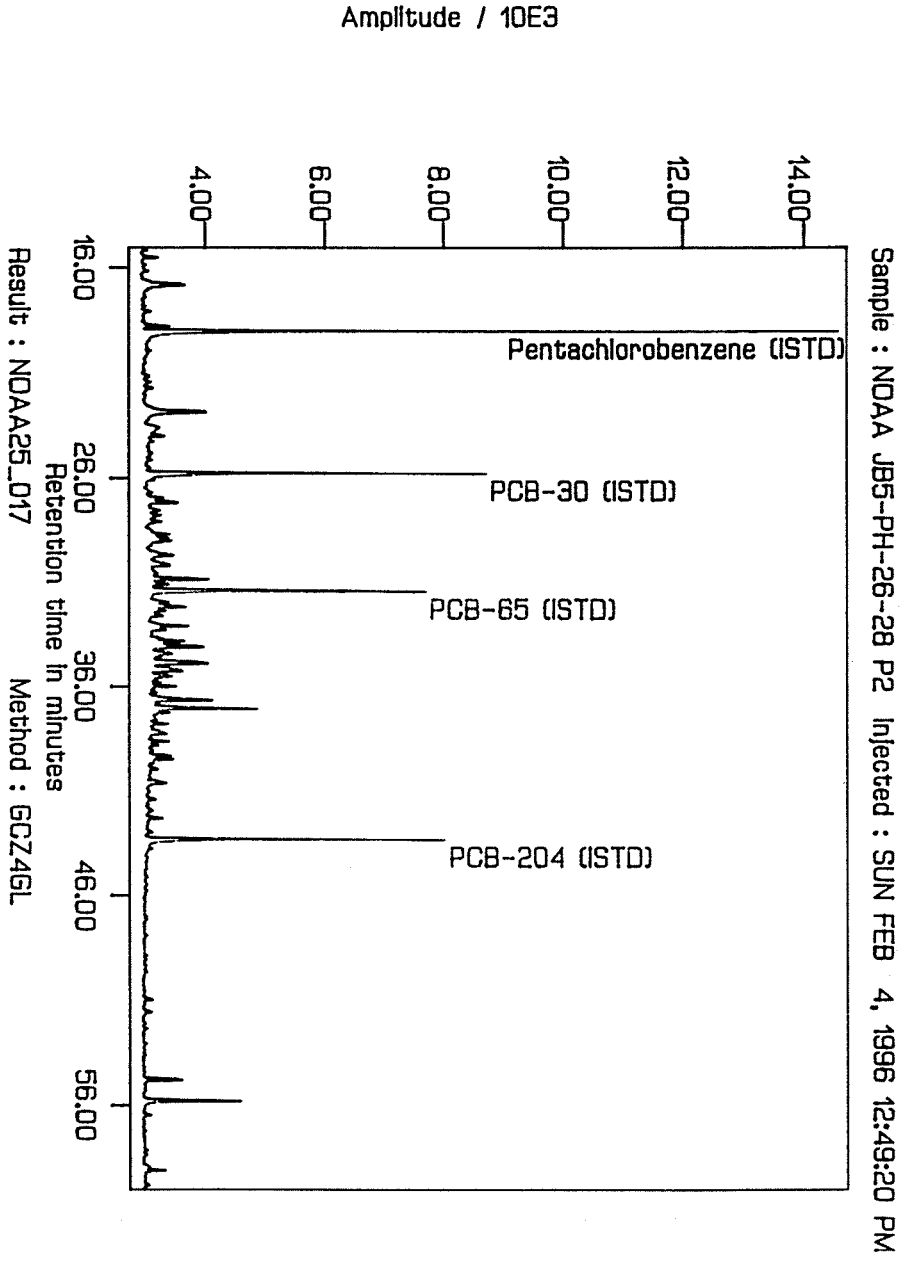

Figure 22. Gas chromatogram of butyltins in typical core section.

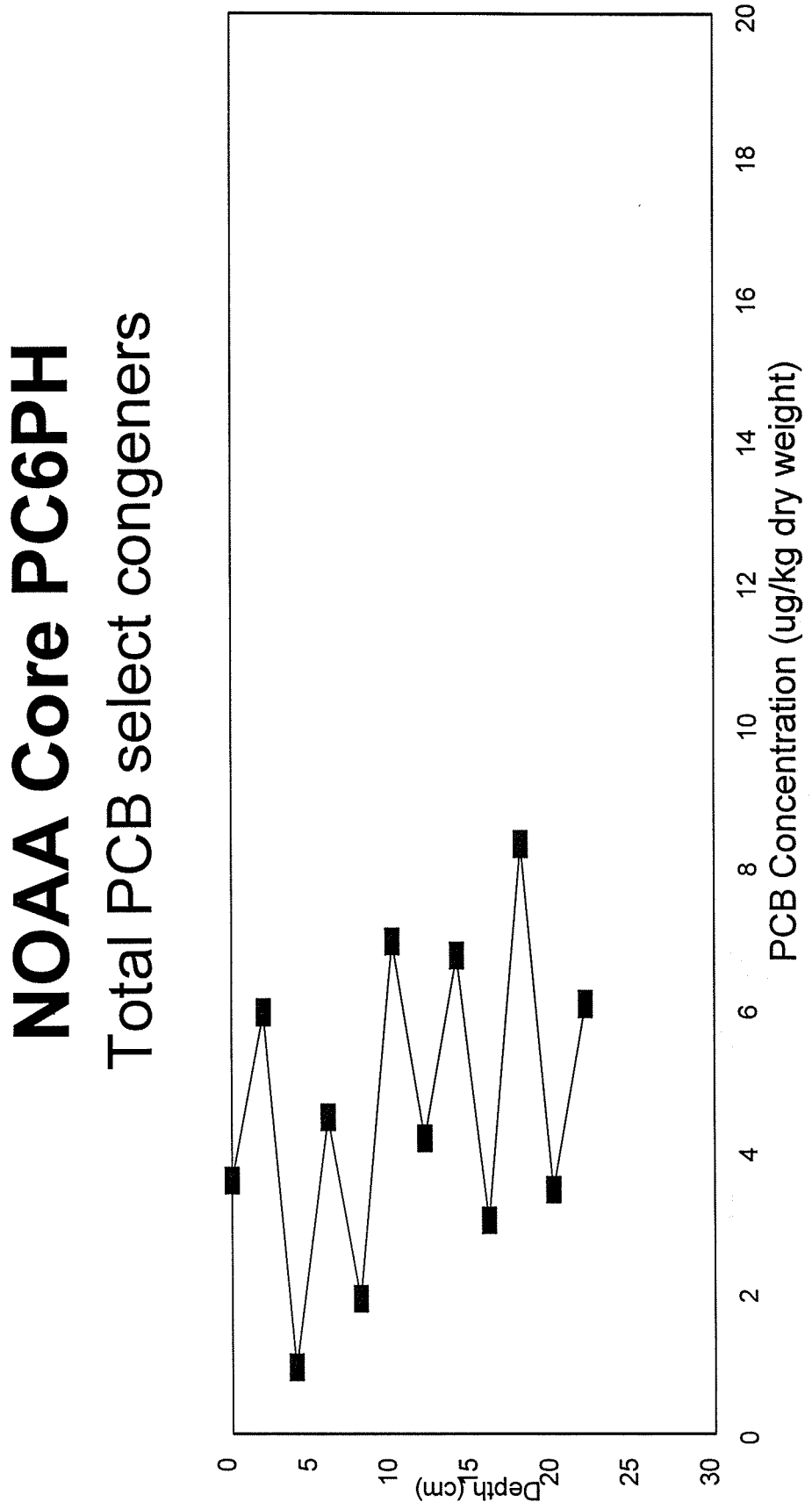

Figure 23. Trends in PCB in Core PC6-PH.

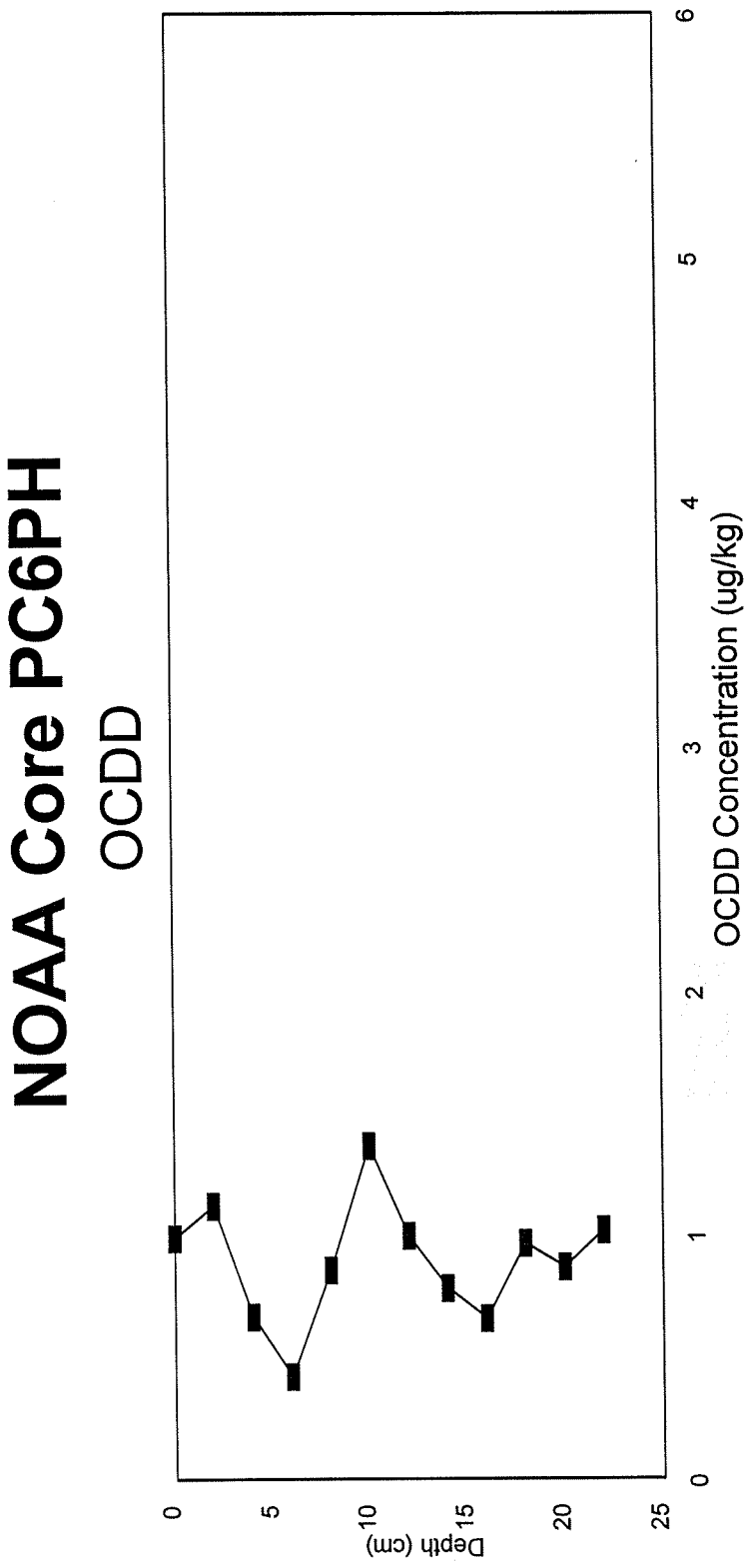

Figure 24. Trends in OCDD in Core PC6-PH.

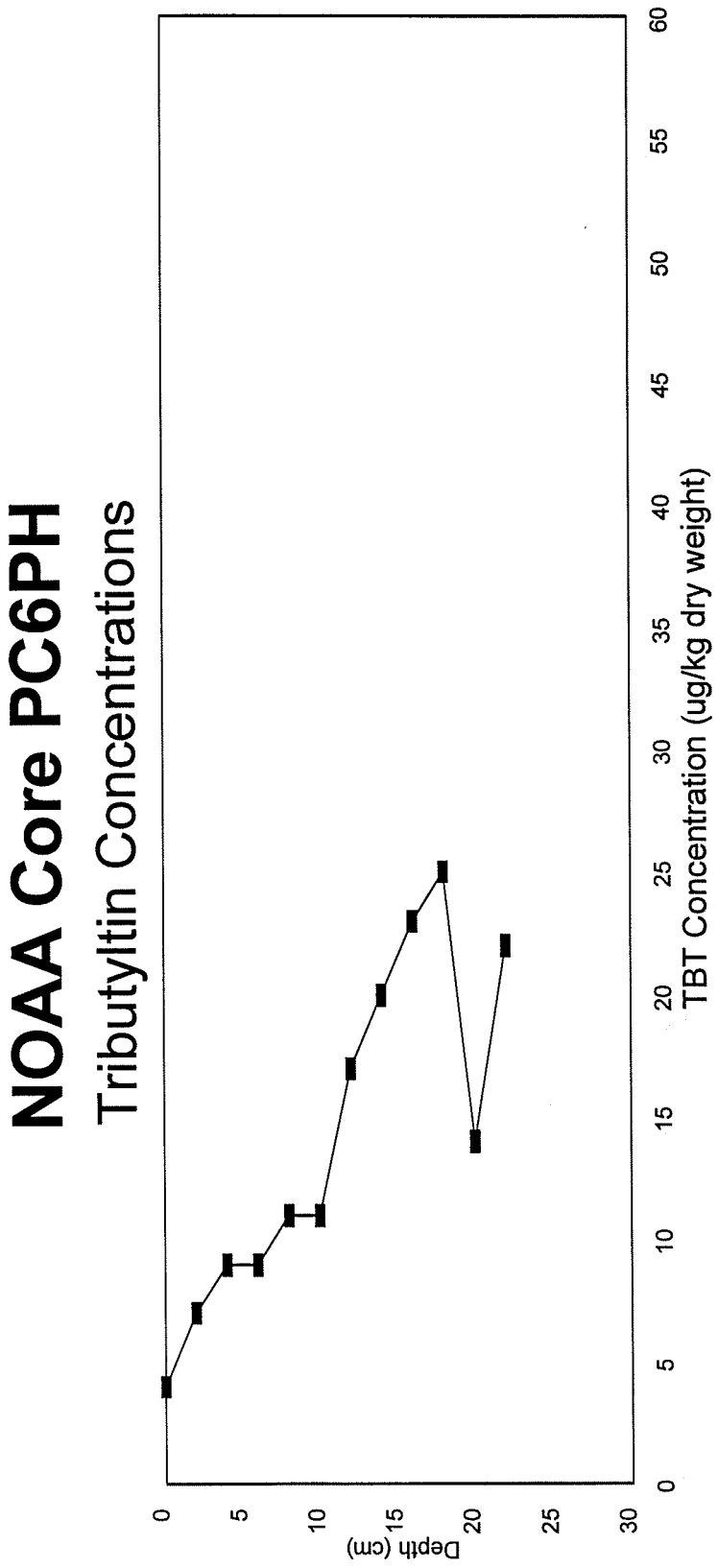

Figure 25. Trends in TBT in Core PC6-PH.

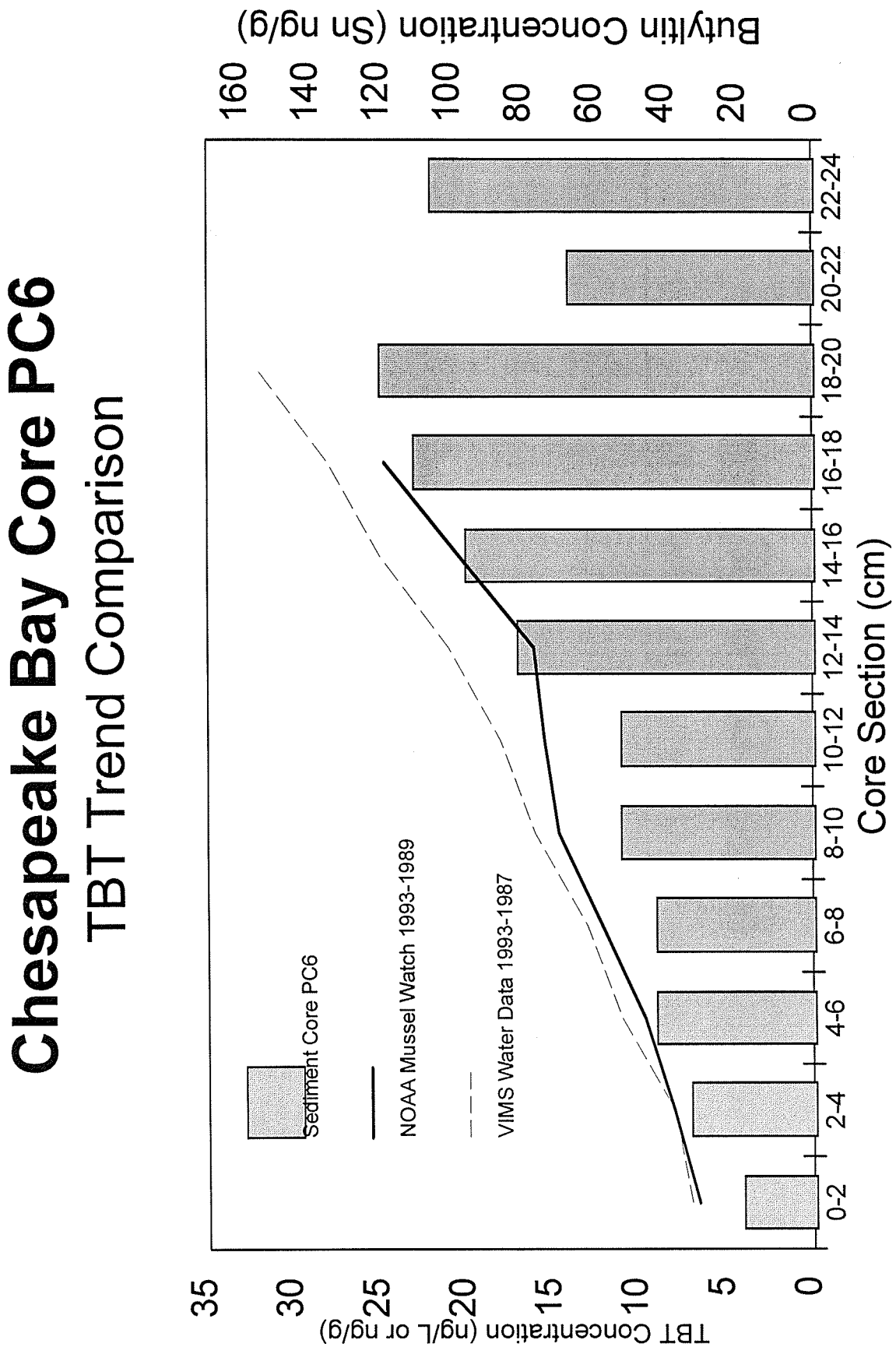

Figure 26. Comparison of TBT trends in water column, shellfish and core data.

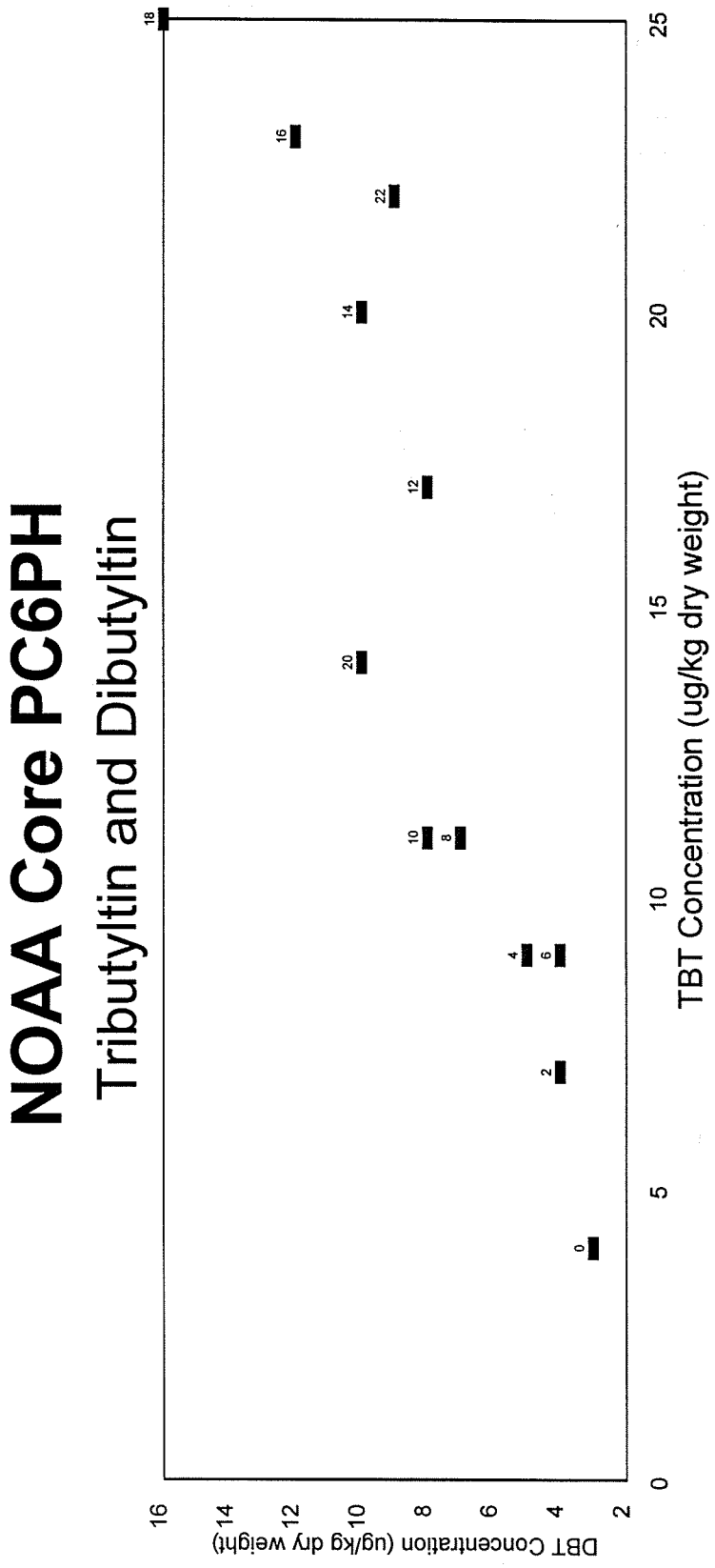

Figure 27. TBT and DBT in Core PC6-PH.

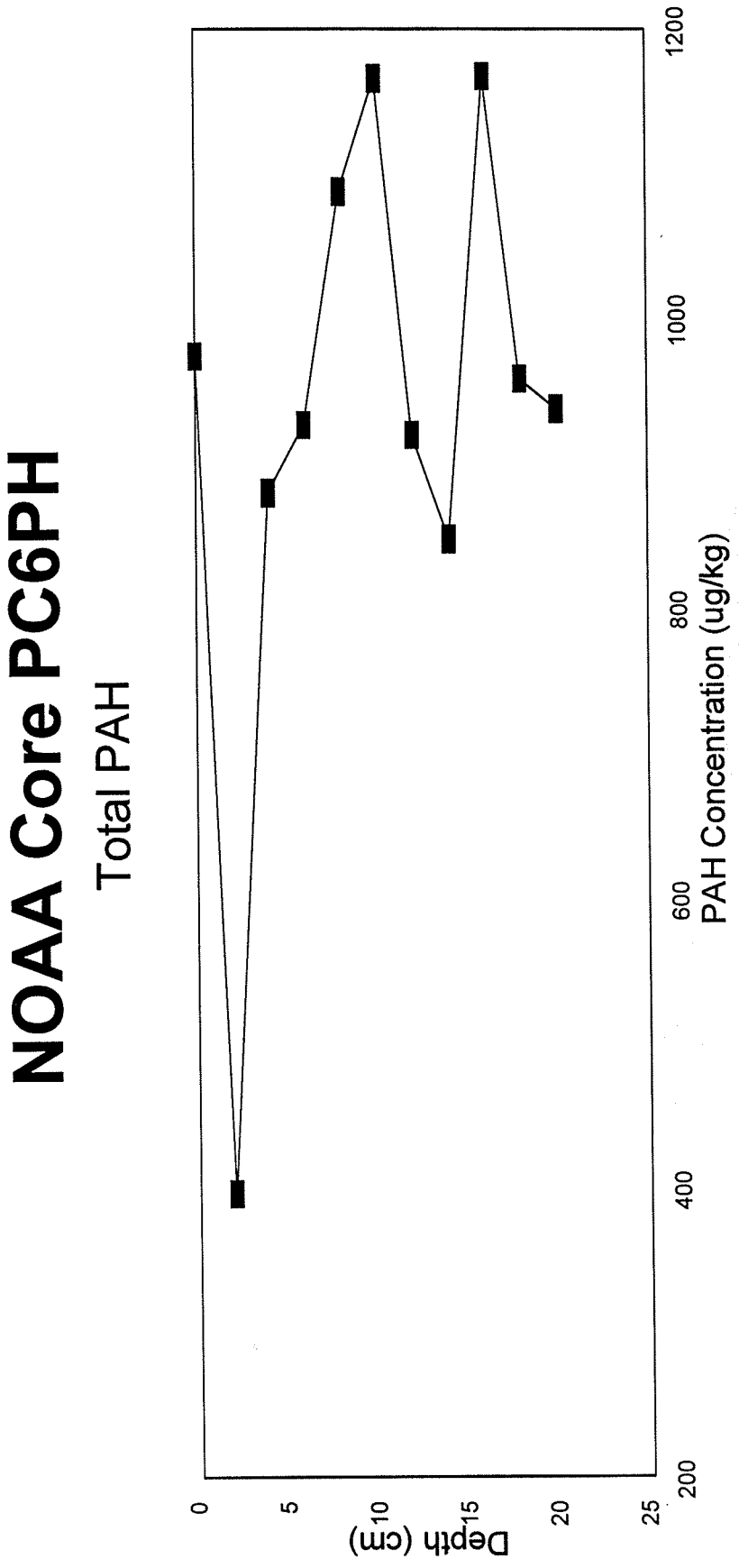

Figure 28. Trends in PAH in Core PC6-PH.

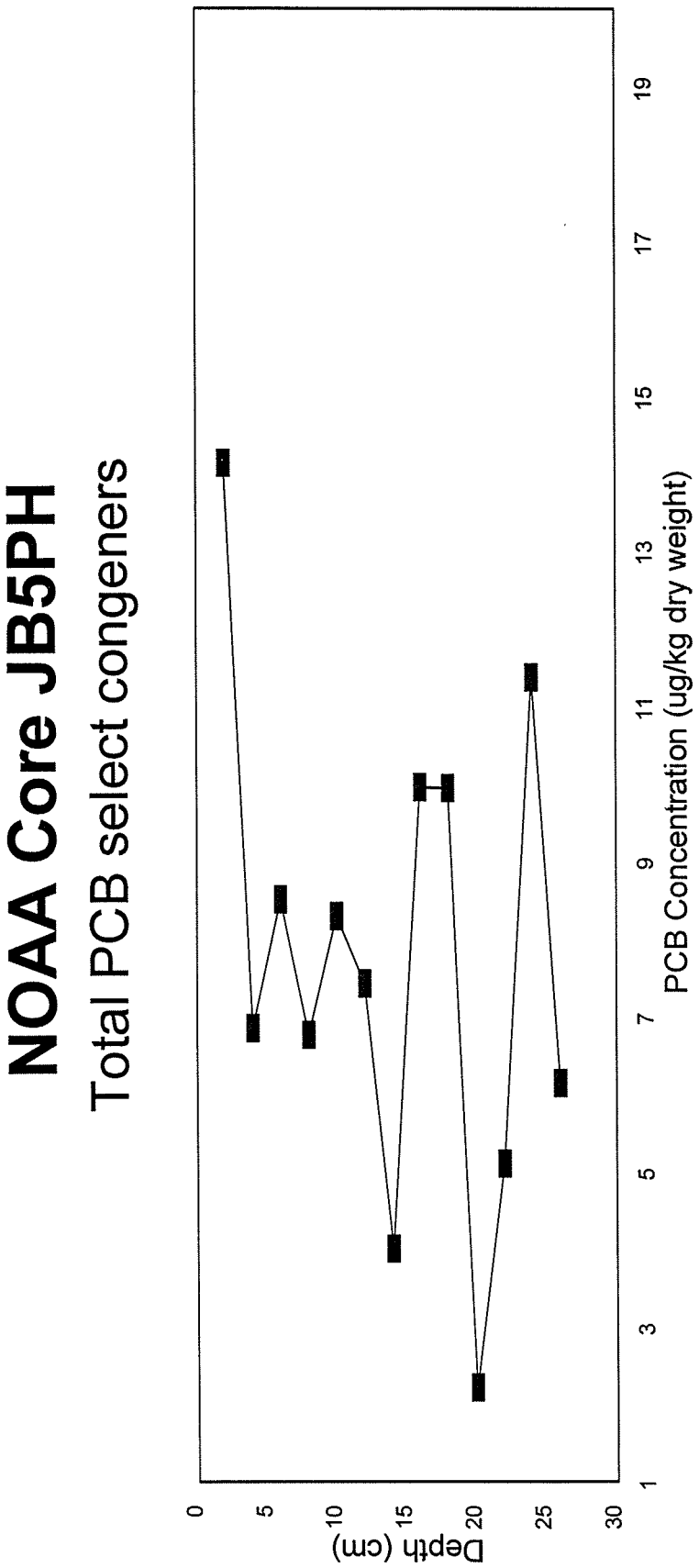

Figures 29. Trends in PCB in Core JB5-PH.

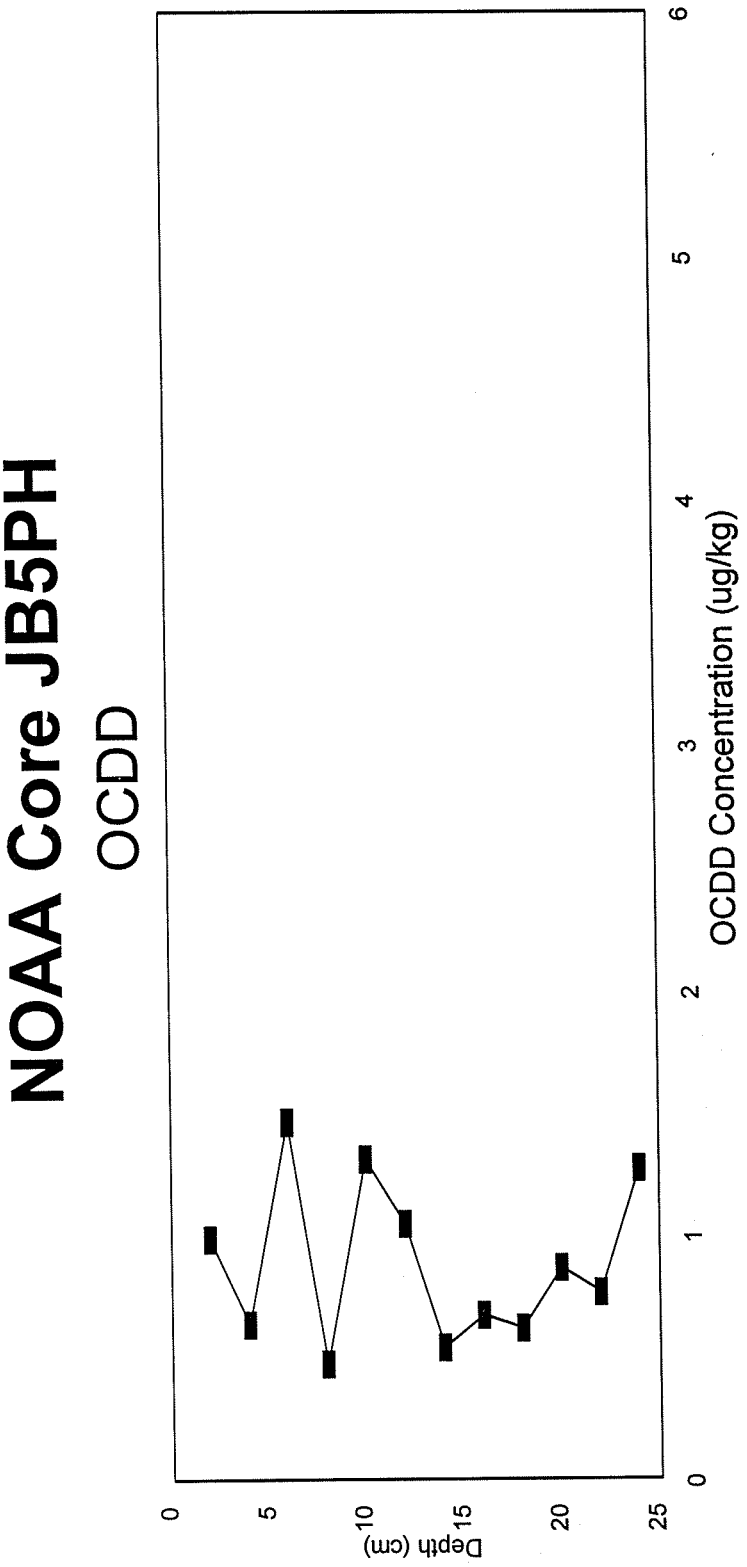

Figure 30. Trends in OCDD in Core JB5-PH.

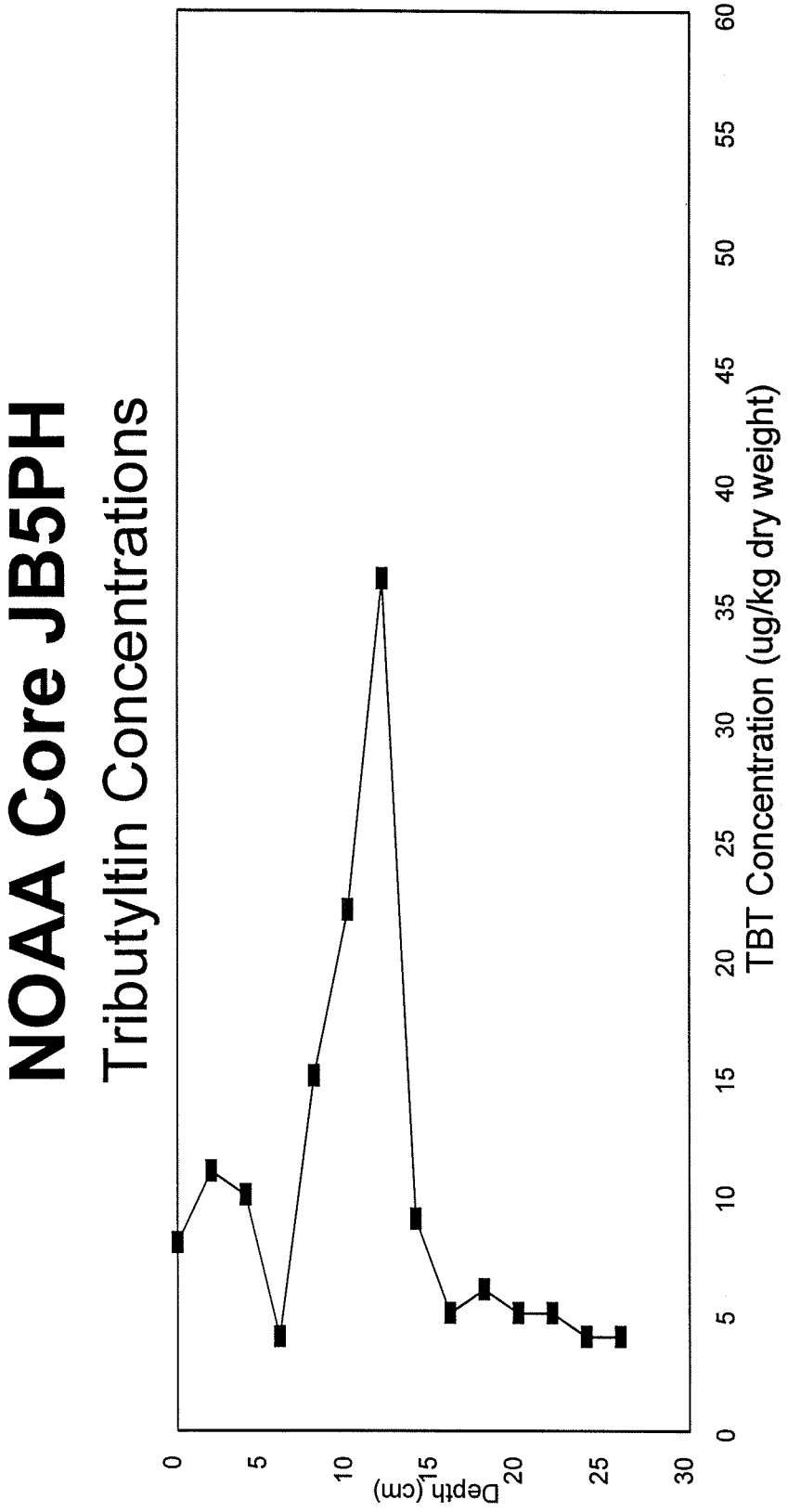

Figure 31. Trends in TBT in Core JB5-PH.

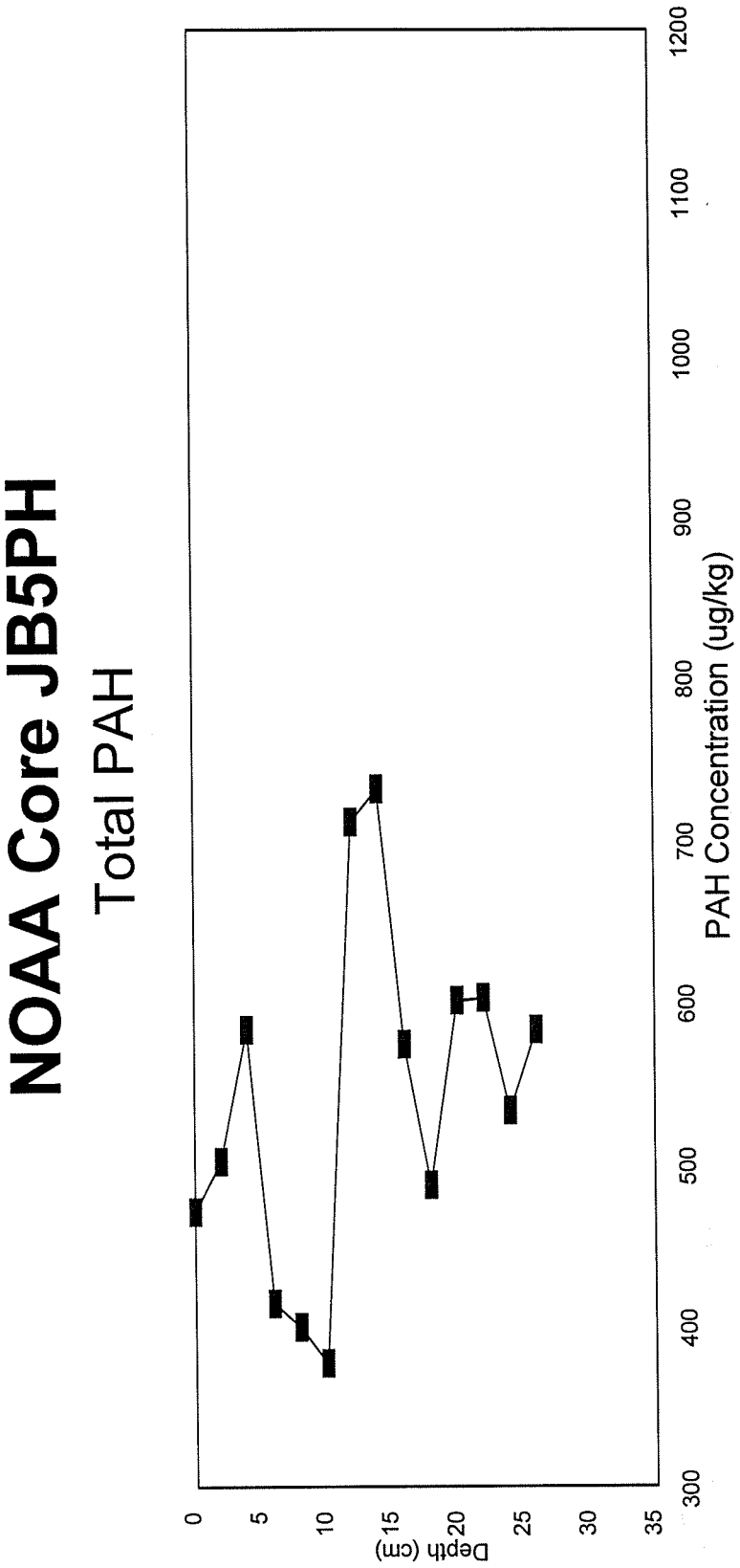

Figure 32. Trends in PAH in Core JB5-PH.

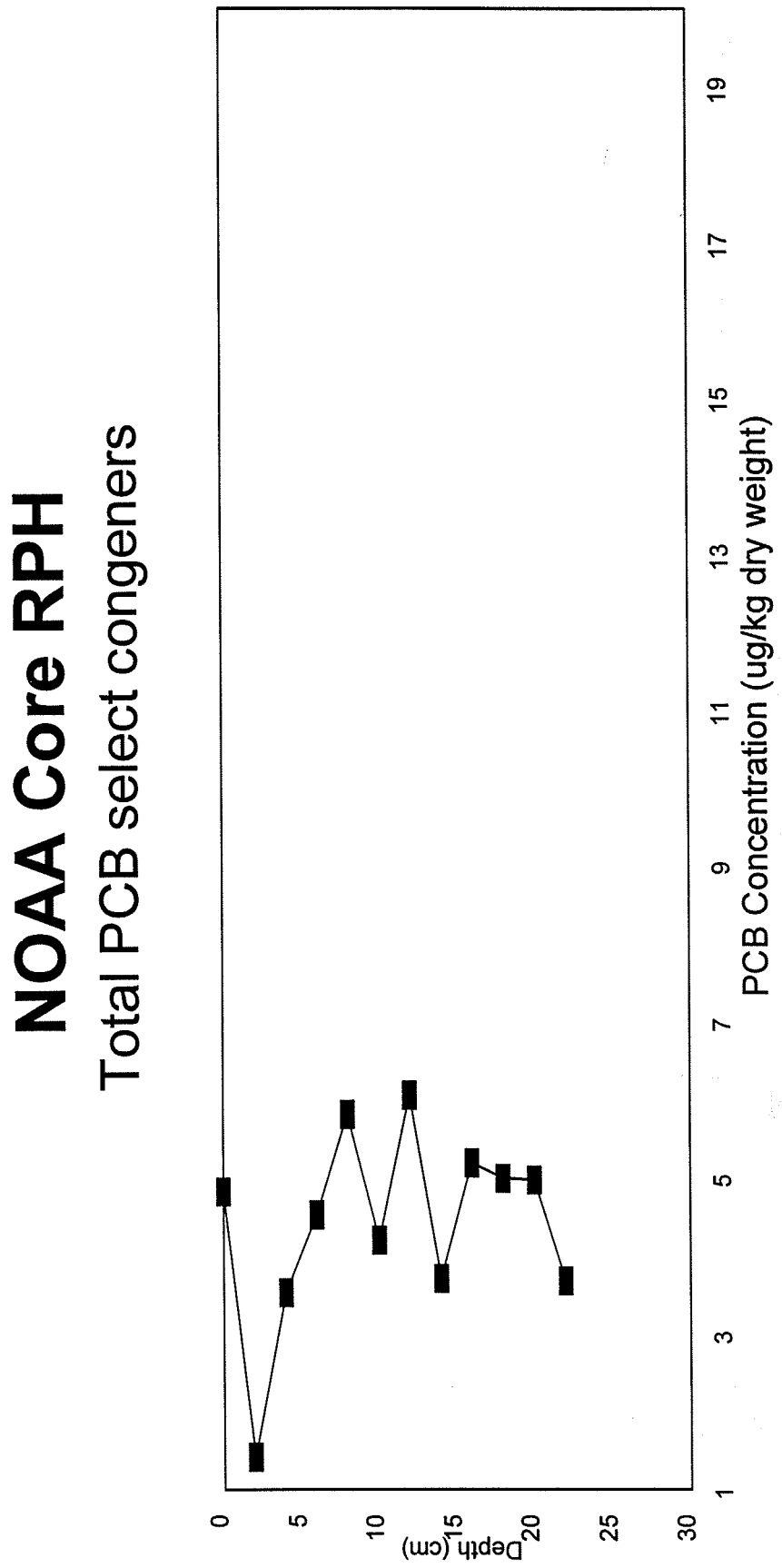

Figure 33. Trends in PCB in Core RPH.

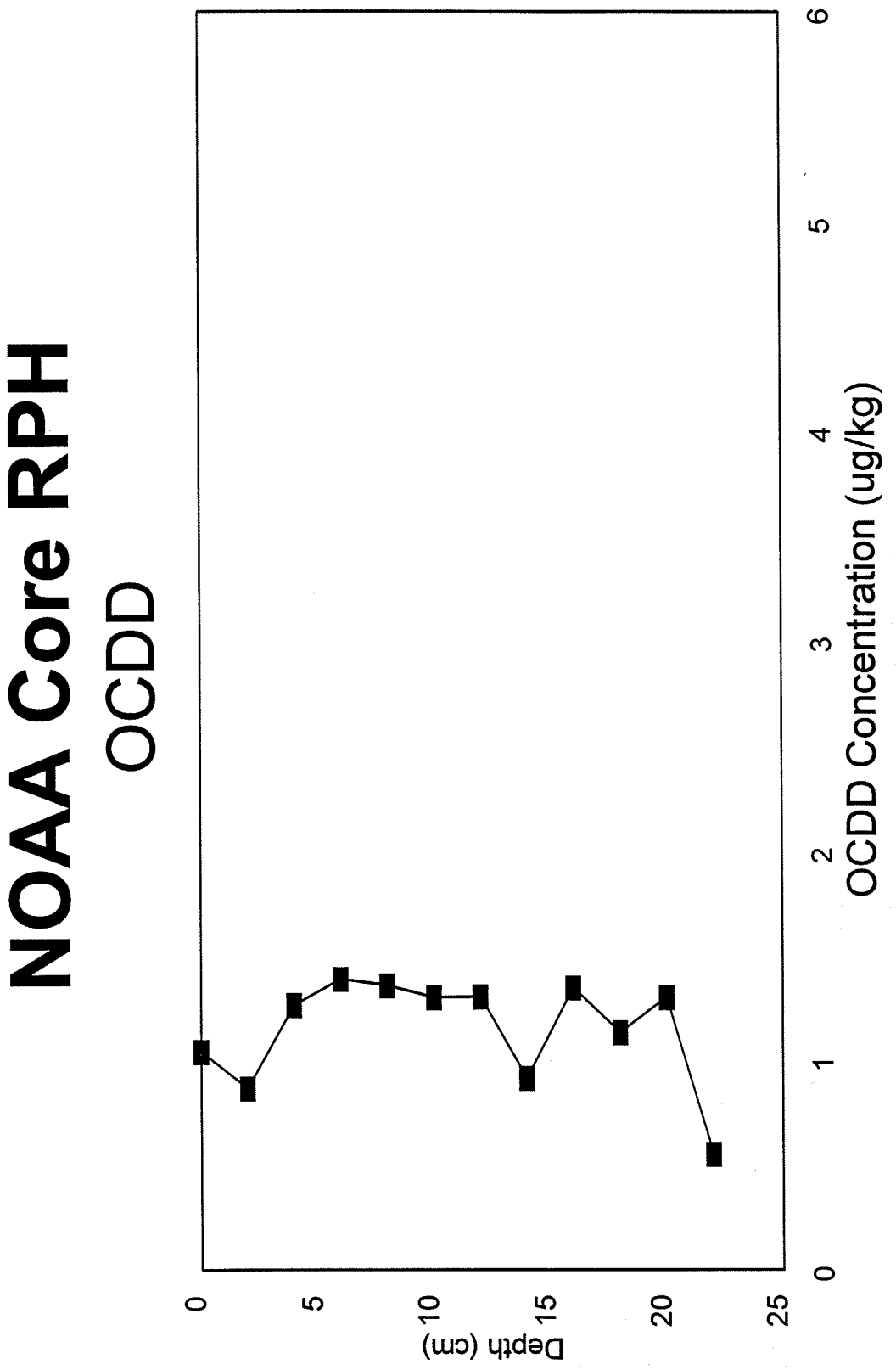

Figure 34. Trends in OCDD in Core RPH.

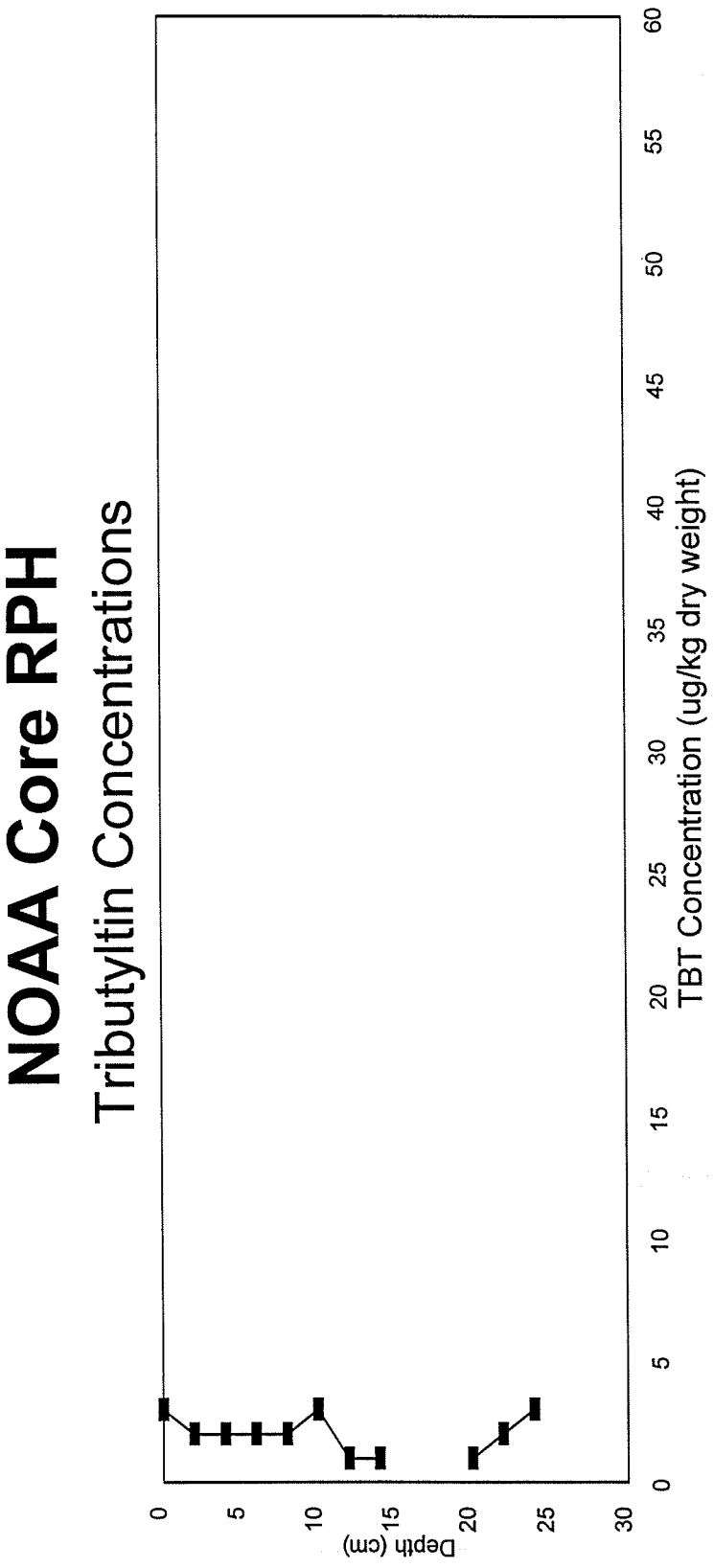

Figure 35. Trends in TBT in Core RPH.

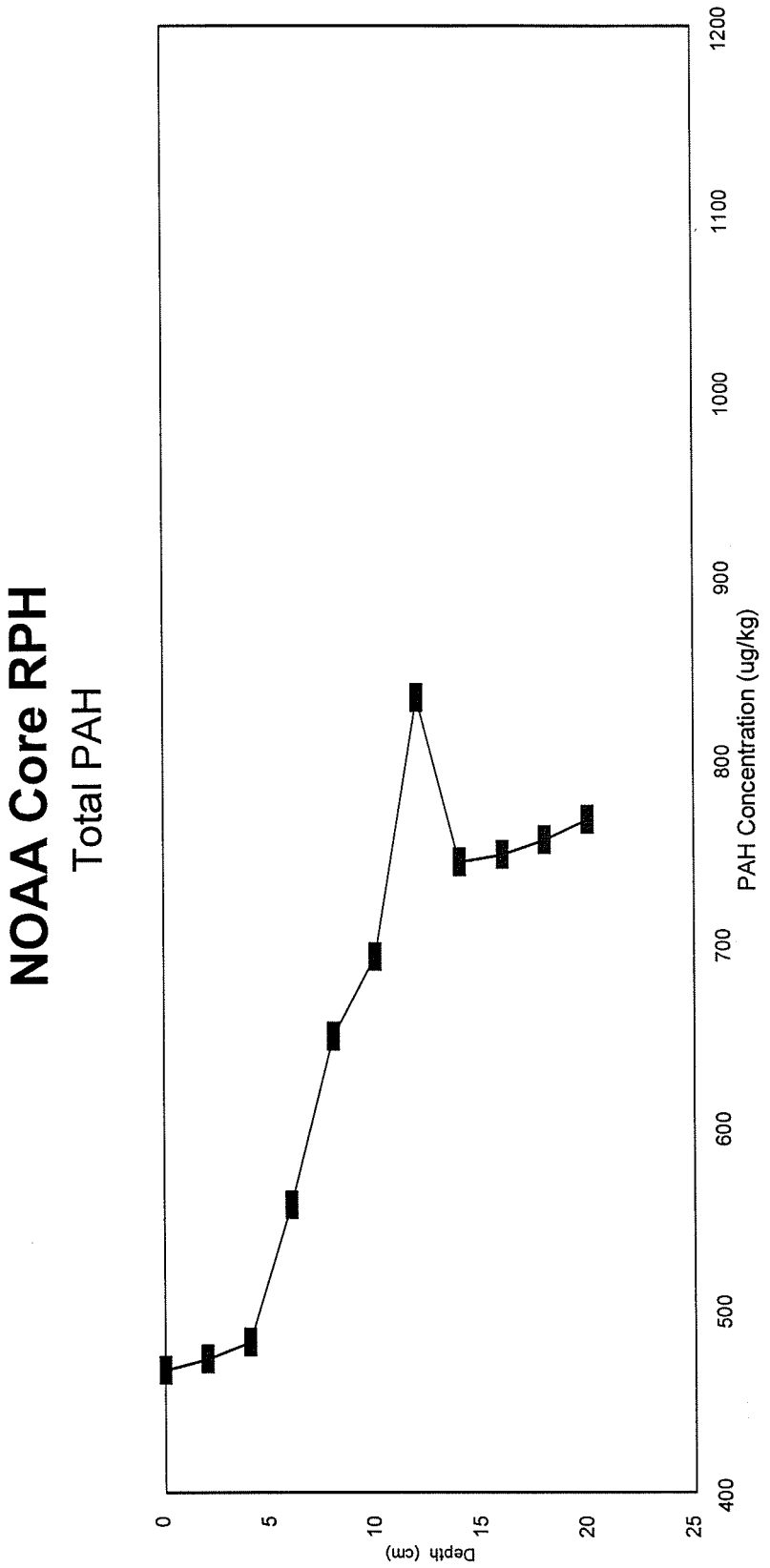

Figure 36. Trends in PAH in Core RPH.

APPENDIX I

This appendix contains the optical scan for each site, and a verbal desciption of each core based on visual and X-ray examination of the cores. The optical scan plots have a grey bar to approximate the color intensity of the sediments.

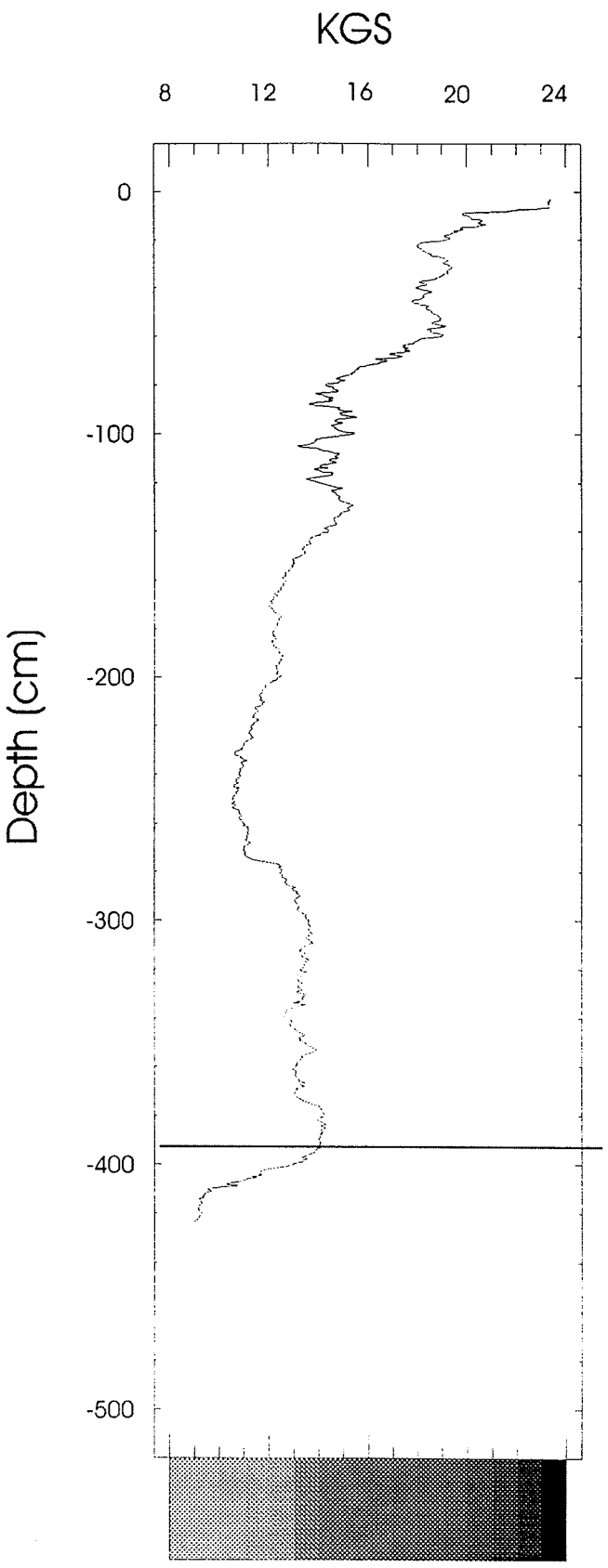

Core CPH
Core length: 426 cm.

Overall: The core is dark near the sediment- water interface and grades into a uniform olive-grey which is maintained from 100cm to the bottom of the core. Physical structures produced by gas are present in the core from 100cm to the bottom.

Specific Features:

10 - 100 cm. - Polycheate burrows abundandant.

11 -17 cm. - Fine layers of coarse sediment with articulated and disarticulated shell assemblages.

156 - 379 cm. - Shell hash occurs throughout this interval with periodic layers of greater concentrations occurring at 156-9, 214-30, 325-337, & 355-67.

379cm - bottom - start of denser material (with thin layers of coaser material at interface confined to a 1 cm thick interval). Larger burrows present.

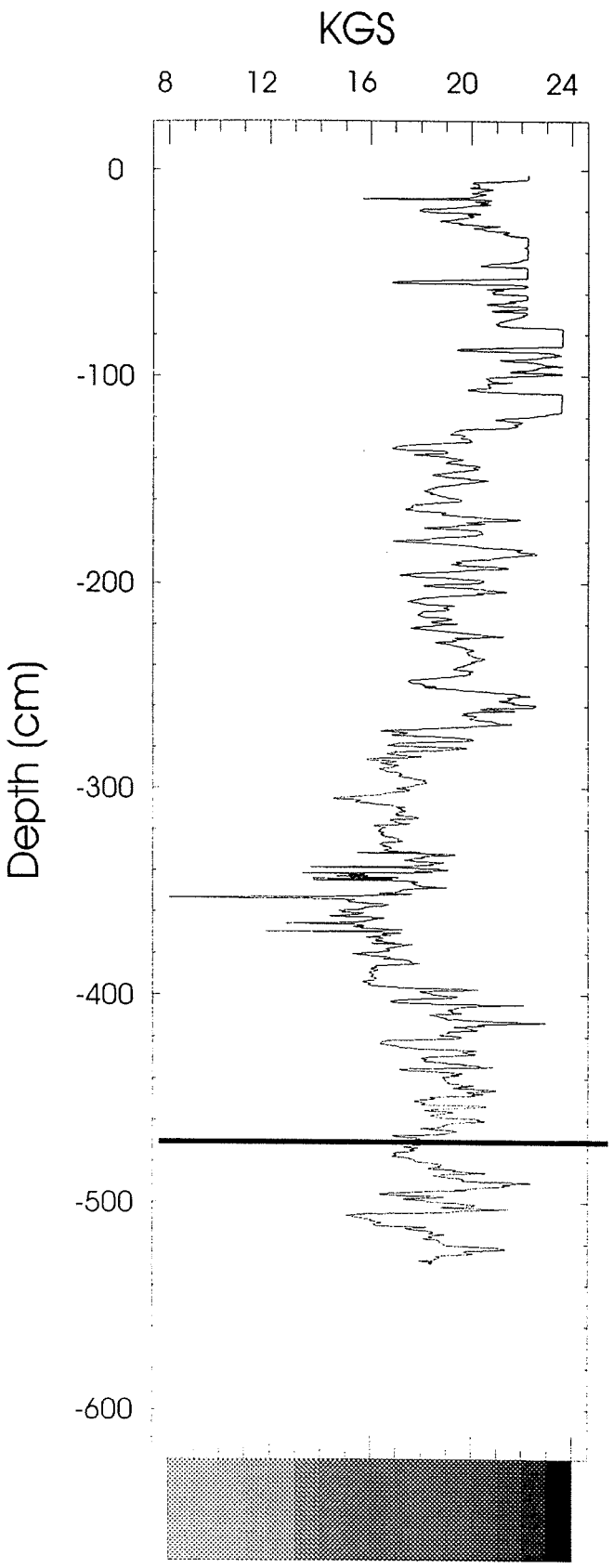

Core WD6

Core length: 520cm.

Overall: The core is very dark/black and highly banded throughout. Physical structures indicative of gas vessicles are present throughout the entire length of the core.

Specific features:

0 - 157cm - Gas vessicles obscure all other sedimentary structures.

157 - 180cm - Burrows present, primarily fine (<1mm dia.) with infrequent larger burrows (>4mm dia.)

197 - 339cm - Sediment appears more compact, gas vessicles have different shape and lower density of occurrence. Laminae (<1mm) of coarser sediment appear sporatically. Burrows absent.

249- 252cm - Shell layer.

274 - 349cm - Burrowing activity present, along with fine laminae.

339- 376cm - Sediment less compact and with higher density of gas vessicles. Shell hash present to a limited extent. Fine burrows present.

376 - 520cm - More compact sediment with lower density of gas vessicles present.

376 - 401cm - Burrows absent, fine laminae present.

401 - 483cm - Burrows present, primarily fine with sporatic ocurrence of larger burrows. Shell layer at 429-31cm. Concentration of laminae at 438-40 & 465 -467.

483- 520cm - Burrows absent, frequency of laminae increase, shell hash increases.

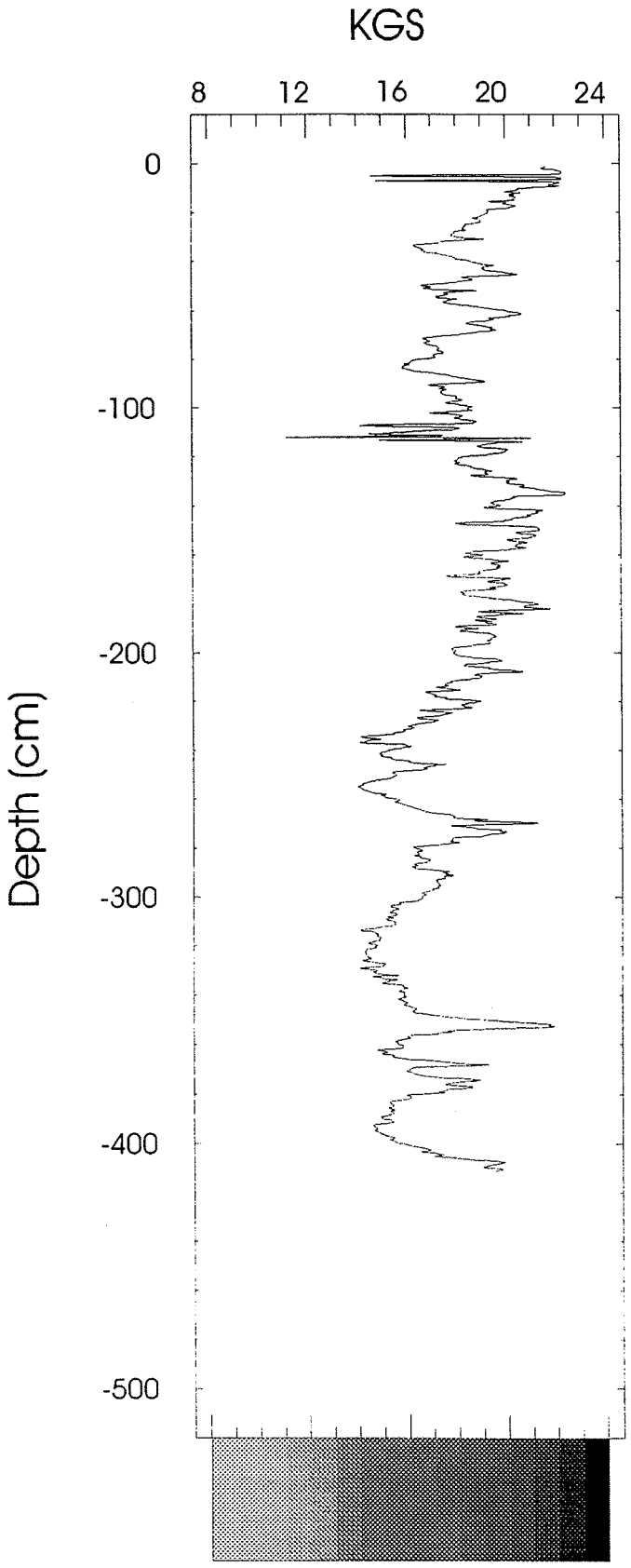

PC6

Core length: 413

Overall: The core shows gas vessicles throughout its entire length. The core is highly banded throughout with dark intervals with lighter bands, and lighter areas with darker bands.

For most of the core (0 - 314cm) gas vessicles obscure physical structures to a greater or lesser extent. Density of gas vessicles is greatest at 0cm and diminishes downward to 239cm; at 239cm gas density is high again and decreases with depth.

Specific features:

10 -11cm. - Shell hash layer

36 -37cm. - Shell hash layer

50 - 106cm. - Large (5mm) gas tubes.

106 - 109cm. - Low gas compact sediment layer

122 - 125cm. - Gas layer: sediment with an extremely high density of gas vessicles.

148 - 151cm. - Gas layer.

157 & 172cm. - Thin shell layers.

201 - 207cm. - Low gas, compact.

207 - 210cm. - Gas layer.

210 - 239cm - Compact sediment , low gas, with sporatic laminae of coarse sediment.

236cm - Shell layer

318 - 413cm. - Compact sediment with low gas density, laminae and burrows (2mm).

364cm. - Shell layer.

369 - 371cm - Old gas layer(?)

380cm. - Shell layer

383 - 413cm - More compact with finer burrows *402cm.* - Shell layer.

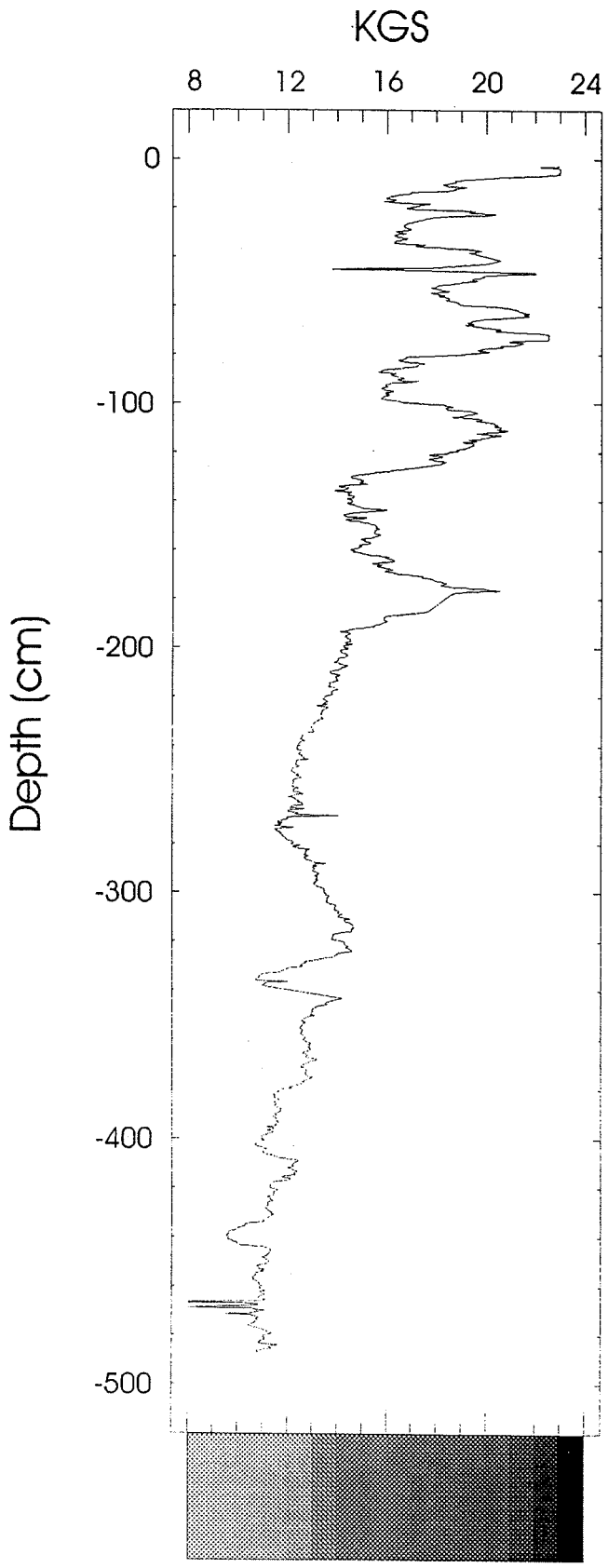

Core JB5
Core length: 489cm.

Overall: Evidence of gas throughout except at the very bottom. Banding is present throughout, but with much much lower frequency than in CPH and WD6. The upper 200cm are the darkest in color, however dark longer intervals are noted in the lighter deeper sediments.

Specific features:

0 - 432cm. - Gas vessicles present to a greater or lesser extent. Fine coarse sediment laminae and thin shell layers frequently present throughout. Evidence of burrows absent.

191 - 193cm. - Gas layer.

234 - 342cm. - High density of gas vessicles which obscure all physical structures.

342 - 489cm. - More compact sediment.

368 - 372cm - Organic debris (peat?) present.

400 - 412cm. - Large burrow (~1cm) infilled with fine grain high water content sediment.

432 - 489cm. - Very hard, coarse grained, dry sediments. No gas present.

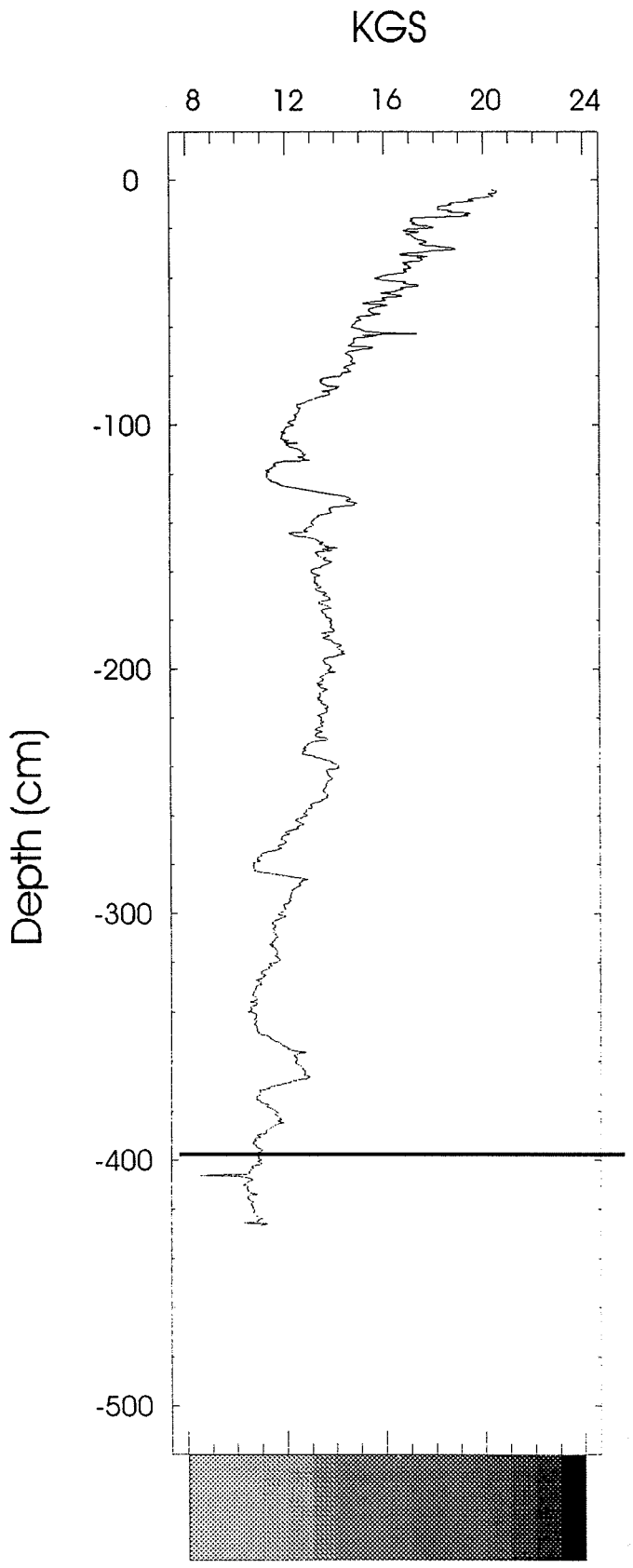

Core RPH
Core length: 442cm.

Overall: Dark near the sediment-water interface, grading rapidly to a uniform grey at 90 - 442cm. Bands occur in the upper 90cm., with sporatic bands in the deeper sediment. Gas vessicles appear starting at 75cm and occur throughout the remainder of the core sporatically; density of occurrence varies from nearly absent to high density.

Specific features:

0 - 9cm. - Highly bioturbated with shell fragments dispersed throughout.

10 - 13cm. - Laminae in compact sediment.

13 - 33cm. - Similar to 0 - 9 cm.

33 - 50cm. - Well laminated compact sediment with no shells

50 - 177cm. - Highly bioturbated, no laminae, with 5mm burrow tubes evident throughout. Gas present at 75cm to th bottom of the core.

177 - 285cm. - Laminae present, lower bioturbation, shell only occurs in one layer at 190cm.

231cm - Distinct layer

282 - 293cm. - Large burrow present, approx. 4cm in diameter.

285 - 442cm - compact well-mixed sediment. Shell layer occurs at 375 - 385cm.

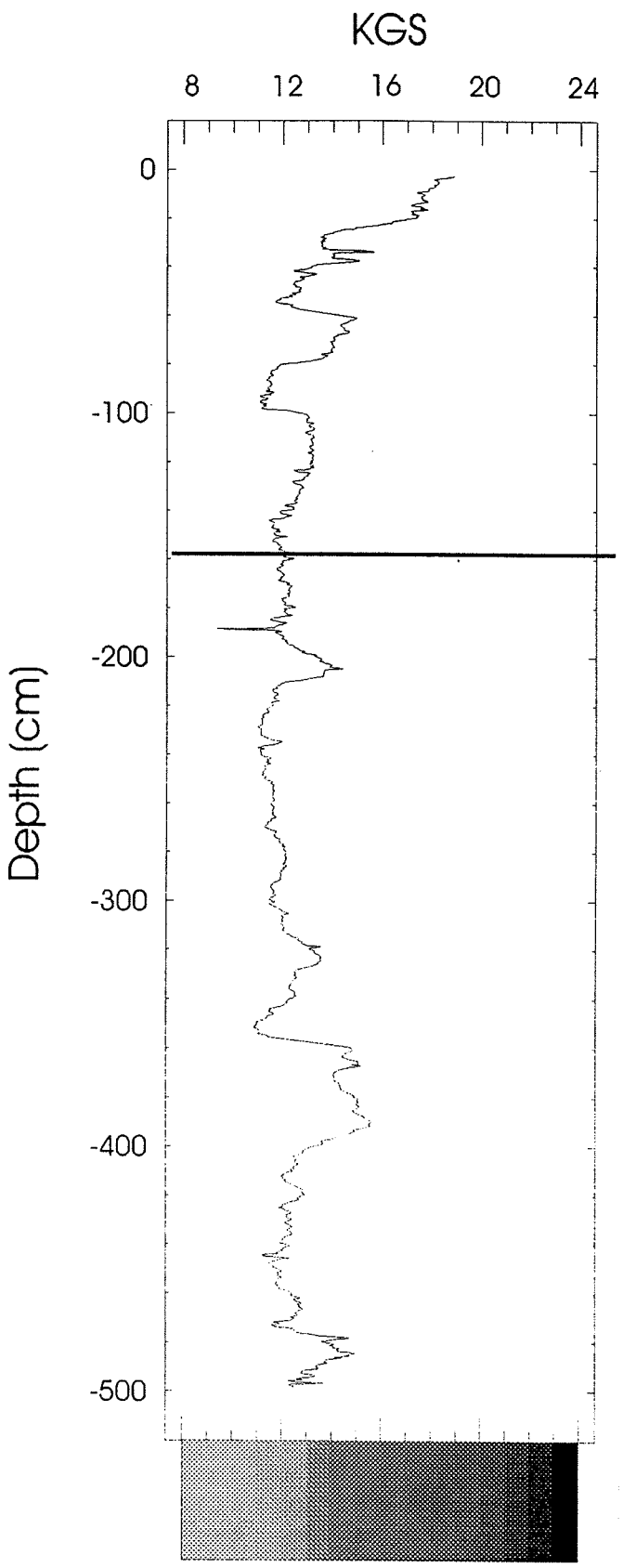

Core YPH
Core length: 510

Overall: Visually uniform grey with minor variations, little or no banding. No gas present. Burrowing evident throughout to a greater or lesser extent. Shell fragments present only near the surface of the core.

Specific Features:

0 - 2cm. - Shell layer; dispersed shell debris to 16cm.

79 - 100cm - Highly laminated sediments with no burrows. Narrow dark bands in a field of lighter colored sediment.

153 - 167cm - Irregular/jagged shaped clasts

167 - 510cm - denser, compact sediments with large burrows.

339 - 340.5cm - Dark band.

464 - 466cm - Light colored Xenoclast

489 - 495cm - A broken light colored xenoclast.

483- 510cm - Distinct change, sediment contains coarse sand and is highly structured as seen visiually.

APPENDIX II

Physical parameters measured on the samples:

STA - Station identifier

DEPTH - Depth interval sampled in the core

yrsbp - Years before present, interpolated from Brush et al. 1996

AVEKGS - The average KGS measurement for the sampled interval

WATER - % water based on total weight of sample

GRAV - % Gravel

SAND - % Sand

SILT - % Silt

CLAY - % Clay

SHEPCLAS - Sherpard's Classification of the sediment

STA	DEPTH	yrsbp	AVEKGS	WATER	GRAV	SAND	SILT	CLAY	SHEPCLAS
CPH	00-02	0		69.7	0	1.6	43.6	54.8	SiCl
CPH	02-04	1.5	18.1	68.0	0	1.2	44.0	54.8	SiCl
CPH	04-06	2.5	17.4	68.5	0	1.2	38.5	60.3	SiCl
CPH	06-08	3.5	17.8	66.5	0	2.4	38.4	59.2	SiCl
CPH	08-10	4.5	17.6	66.6	0	3.1	41.1	55.8	SiCl
CPH	10-12	5.2	17.8	63.7	0	2.3	36.9	60.8	SiCl
CPH	12-14	5.6	17.6	61.6	0	4.0	37.2	58.8	SiCl
CPH	14-16	6	17.3	63.2	0	2.7	39.2	58.1	SiCl
CPH	16-18	6.4	16.9	60.9	0	1.4	37.7	60.9	SiCl
CPH	18-20	6.8	16.2	60.1	0	1.3	36.1	62.6	SiCl
CPH	20-22	7.2	16.2	61.3	0	1.5	35.8	62.7	SiCl
CPH	22-24	7.6	15.9	60.3	0	1.1	36.2	62.7	SiCl
CPH	24-26	8		60.8	0	1.3	39.1	59.6	SiCl
JB5	00-02	0	20.8	84.0	0	0.5	39.5	60.0	SiCl
JB5	02-04	1.2	20.8	85.2	0	0.3	41.7	58.0	SiCl
JB5	04-06	2	20.8	80.5	NS	NS	NS	NS	
JB5	06-08	3.8	20.8	79.5	0	0.7	40.7	58.6	SiCl
JB5	08-10	5.6	20.7	81.0	0	0.4	44.9	54.8	SiCl
JB5	10-12	7.3	19.8	84.4	NS	NS	NS	NS	NS

STA	DEPTH	yrsbp	AVEKGS	WATER	GRAV	SAND	SILT	CLAY	SHEPCLAS
JB5	12-14	9.1	19.2	86.2	NS	NS	NS	NS	NS
JB5	14-16	10.6	18.5	75.3	NS	NS	NS	NS	NS
JB5	16-18	11.9	17.1	75.3	0	0.8	49.1	50.2	SiCl
JB5	18-20	13.2	16.5	77.7					
JB5	20-22	14.4	17.4	80.8	0	0.3	37.9	61.8	SiCl
JB5	22-24	15.8	17.0	77.8	0	0.8	39.8	59.4	SiCl
JB5	24-26	17	16.2	72.5	0	0.7	41.4	58.0	SiCl
JB5	26-28	17.7	15.5	73.5	0	1.5	41.5	57.0	SiCl
JB5	28-30	18.4		74.1	NS	NS	NS	NS	NS
PC6	00-02	0	20.5	83.2	0	0.3	35.6	64.2	SiCl
PC6	02-04	6.1	20.7	80.1	0	0.4	37.0	62.7	SiCl
PC6	04-06	10.2	20.7	76.6	0	0.5	37.3	62.2	SiCl
PC6	06-08	14	20.6	76.2	0	0.5	38.0	61.6	SiCl
PC6	08-10	18	19.5	77.5	0	0.2	38.3	61.5	SiCl
PC6	10-12	22	17.8	73.9	0	0.2	36.9	62.9	SiCl
PC6	12-14	25.9	17.0	75.5	0	0.2	37.8	62.0	SiCl
PC6	14-16	30	17.1	76.3	0	0.2	38.9	61.0	SiCl
PC6	16-18	33.9		73.9	0	0.2	39.3	60.6	SiCl
PC6	18-20	37		75.0	0	0.2	37.5	62.4	SiCl

STA	DEPTH	yrsbp	AVEKGS	WATER	GRAV	SAND	SILT	CLAY	SHEPCLAS
PC6	20-22	39		76.5	0	0.2	39.9	59.9	SiCl
PC6	22-24	41		76.5	0	0.2	36.8	63.0	SiCl
RPH	00-02	0	21.5	73.0	0	3.3	52.4	44.3	ClSi
RPH	02-04	2.9	19.7	69.2	0	7.2	56.3	36.5	ClSi
RPH	04-06	5.8	15.7	65.2	0	2.7	51.1	46.2	ClSi
RPH	06-08	8	16.6	64.8	0	1.4	46.7	51.9	SiCl
RPH	08-10	10.3	15.7	75.8	0	1.0	49.4	49.7	SiCl
RPH	10-12	12.6	16.0	63.8	0	0.7	47.6	51.7	SiCl
RPH	12-14	15	15.9	69.2	0	0.4	46.5	53.1	SiCl
RPH	14-16	17.2	16.6	65.4	0	0.5	47.7	51.8	SiCl
RPH	16-18	19.6	16.4	67.1	0	0.2	42.6	57.2	SiCl
RPH	18-20	21.9	16.2	67.4	0	0.3	43.6	56.1	SiCl
RPH	20-22	24.1	16.3	68.1	0	1.0	48.0	51.1	SiCl
RPH	22-24	26.5	16.0	63.7	0	1.1	46.0	52.8	SiCl
RPH	24-26	28.8		70.5	NS	NS	NS	NS	NS
WD6	00-02	0		79.2	0	0.3	19.5	80.2	Cl
WD6	02-04	2.4		76.6	0	0.5	21.9	77.7	Cl
WD6	04-06	4		76.6	0	2.1	31.7	66.2	SiCl
WD6	06-08	4.9		75.1	0	2.1	36.0	61.9	SiCl

STA	DEPTH	yrsbp	AVEKGS	WATER	GRAV	SAND	SILT	CLAY	SHEPCLAS
WD6	08-10	5.7		79.5	0	1.1	35.4	63.5	SiCl
WD6	10-12	6.6		80.5	0	0.8	36.1	63.2	SiCl
WD6	12-14	7.4		78.2	0	1.6	37.8	60.6	SiCl
WD6	14-16	8.3		74.7	0	2.0	40.1	57.9	SiCl
WD6	16-18	9.1		78.4	0	0.5	32.2	67.3	SiCl
WD6	18-20	10		81.0	0	0.5	30.5	69.1	SiCl
WD6	20-22	10.9		79.3	0	0.9	34.2	65.0	SiCl
WD6	22-24	11.7		77.5	0	0.9	33.7	65.4	SiCl
WD6	24-26	12.6		76.4	NS	NS	NS	NS	NS
WD6	26-28	13.4		75.9	NS	NS	NS	NS	NS
YPH	00-02	0	21.5	69.1	0	3.0	39.8	57.1	SiCl
YPH	02-04	2	20.2	68.5	0	3.0	41.2	55.7	SiCl
YPH	04-06	4	17.9	66.5	0	2.9	41.8	55.4	SiCl
YPH	06-08	6	16.8	65.5	0	1.7	40.3	58.0	SiCl
YPH	08-10	10	15.2	77.6	0	2.6	41.6	55.9	SiCl
YPH	10-12	15.6	15.0	64.5	0	3.3	41.6	55.2	SiCl
YPH	12-14	22	15.0	63.2	0	3.6	39.6	56.8	SiCl
YPH	14-16	26.1	15.4	63.8	0	3.4	38.8	57.8	SiCl
YPH	16-18	30.1	15.7	63.7	0	3.7	39.3	57.0	SiCl

STA	DEPTH	yrsbp	AVEKGS	WATER	GRAV	SAND	SILT	CLAY	SHEPCLAS
YPH	18-20	33	16.0	63.5	0.07	4.8	41.0	54.2	SiCl
YPH	20-22	34.9	15.3	59.7	NS	NS	NS	NS	NS
YPH	22-24	37	14.8	55.5	NS	NS	NS	NS	NS
YPH	24-26	39		55.0	NS	NS	NS	NS	NS

APPENDIX III

List of the measured nutrient and chemical species:

STA - Station identifier

DEPTH - Depth interval (cm) of sample

yrsbp - Interpolated years before present

N - Total Nitrogen (%)

C - Total Carbon (%)

S - Total Sulfur (%)

SOLFE - Soluble Iron (%)

AVS - Acid Volatile Sulfur (%)

STA	DEPTH	yrsbp	N	C	S	SOLFE	AVS
CPH	00-02	0	0.260	2.84	0.606	3.37	0.145
CPH	02-04	1.5	0.228	2.64	0.782	3.30	0.262
CPH	04-06	2.5	0.250	2.77	0.953	3.15	0.254
CPH	06-08	3.5	0.202	2.67	1.146	2.95	0.169
CPH	08-10	4.5	0.259	3.08	1.453	3.10	0.243
CPH	10-12	5.2	0.236	3.16	1.528	3.19	0.321
CPH	12-14	5.6	0.208	3.03	1.237	3.61	0.272
CPH	14-16	6	0.204	3.17	1.038	3.82	0.250
CPH	16-18	6.4	0.190	3.28	0.855	3.83	0.233
CPH	18-20	6.8	0.198	3.02	0.973	3.37	0.125
CPH	20-22	7.2	0.210	3.25	1.073	2.94	0.143
CPH	22-24	7.6	0.208	3.41	0.993	3.94	0.138
CPH	24-26	‘8	0.199	3.50	1.024	3.83	0.166
JB5	00-02	0	0.495	4.07	1.289	2.49	0.558
JB5	02-04	1.2	0.481	3.91	1.351	2.52	0.614
JB5	04-06	2	0.407	3.44	1.393	2.73	0.509
JB5	06-08	3.8	0.396	3.28	1.355	2.36	0.324
JB5	08-10	5.6	0.398	3.36	1.419	1.90	0.287
JB5	10-12	7.3	0.374	3.44	1.468	1.92	0.249
JB5	12-14	9.1	0.399	3.59	1.518	1.72	0.271
JB5	14-16	10.6	0.325	2.79	1.478	1.83	0.175
JB5	16-18	11.9	0.320	2.77	1.453	1.97	0.147
JB5	18-20	13.2	0.339	2.95	1.423	1.92	0.170
JB5	20-22	14.4	0.356	3.06	1.357	1.81	0.083
JB5	22-24	15.8	0.362	3.08	1.522	1.98	0.218
JB5	24-26	17	0.322	2.87	1.253	2.04	0.132
JB5	26-28	17.7	0.317	2.91	1.352	1.89	0.186
JB5	28-30	18.4	0.339	2.94	1.270	1.86	0.184

STA	DEPTH	yrsbp	N	C	S	SOLFE	AVS
PC6	00-02	0	0.443	3.55	1.158	2.43	0.463
PC6	02-04	6.1	0.407	3.30	1.077	2.51	0.402
PC6	04-06	10.2	0.430	3.50	1.260	2.38	0.359
PC6	06-08	14	0.415	3.37	1.180	2.41	0.353
PC6	08-10	18	0.449	3.48	1.255	2.13	0.262
PC6	10-12	22	0.403	3.33	1.299	1.90	0.279
PC6	12-14	25.9	0.409	3.25	1.381	1.90	0.232
PC6	14-16	30	0.445	3.40	1.343	1.99	0.159
PC6	16-18	33.9	0.423	3.35	1.343	1.64	0.136
PC6	18-20	37	0.424	3.25	1.353	1.73	0.146
PC6	20-22	39	0.399	3.22	1.407		0.164
PC6	22-24	41	0.367	3.29	1.472	1.75	
RPH	00-02	0	0.279	2.50	0.927	1.98	0.343
RPH	02-04	2.9	0.225	2.34	0.947	2.27	0.260
RPH	04-06	5.8	0.235	2.33	1.099	2.44	0.180
RPH	06-08	8	0.232	2.26	1.407	2.59	0.125
RPH	08-10	10.3	0.233	2.27	1.699	2.06	0.140
RPH	10-12	12.6	0.224	2.27	1.224	2.08	0.113
RPH	12-14	15	0.234	2.25	1.322	2.06	0.134
RPH	14-16	17.2	0.251	2.32	1.420	2.04	0.115
RPH	16-18	19.6	0.238	2.25	1.314	1.95	0.103
RPH	18-20	21.9	0.241	2.40	1.635	2.51	0.124
RPH	20-22	24.1	0.232	2.64	1.435	2.02	0.119
RPH	22-24	26.5	0.217	2.65	1.188	2.14	0.096
RPH	24-26	28.8	0.236	2.51	1.258	2.07	0.173

STA	DEPTH	yrsbp	N	C	S	SOLFE	AVS
WD6	00-02	0	0.357	3.36	1.139	3.85	0.712
WD6	02-04	2.4	0.329	3.25	0.873	4.15	0.585
WD6	04-06	4	0.349	3.20	0.724	3.59	0.253
WD6	06-08	4.9	0.368	3.18	1.086	2.51	0.569
WD6	08-10	5.7	0.411	3.40	1.229	2.55	0.631
WD6	10-12	6.6	0.383	3.30	1.341	2.69	0.583
WD6	12-14	7.4	0.344	3.05	1.306	2.53	0.323
WD6	14-16	8.3	0.302	2.64	1.193	2.19	0.336
WD6	16-18	9.1	0.331	2.86	1.387	2.46	0.536
WD6	18-20	10	0.340	2.97	1.412	2.68	0.601
WD6	20-22	10.9	0.326	2.98	1.448	2.66	0.562
WD6	22-24	11.7	0.315	2.88	1.490	2.44	0.402
WD6	24-26	12.6	0.287	3.00	1.284	2.37	0.510
WD6	26-28	13.4	0.280	2.98	1.286	2.35	0.425
YPH	00-02	0	0.196	2.41	1.154	2.42	0.057
YPH	02-04	2	0.193	2.38	0.971	2.42	0.188
YPH	04-06	4	0.169	2.31	1.236	2.25	0.135
YPH	06-08	6	0.153	2.18	1.311	2.18	0.087
YPH	08-10	10	0.162	2.20	1.390	2.15	0.115
YPH	10-12	15.6	0.163	2.11	1.378	2.35	0.022
YPH	12-14	22	0.166	2.18	1.322	2.24	0.065
YPH	14-16	26.1	0.207	2.28	1.448	2.22	0.078
YPH	16-18	30.1	0.194	2.22	1.462	2.32	0.073
YPH	18-20	33	0.208	2.32	1.516	2.41	0.089
YPH	20-22	34.9	0.196	2.22	1.431	2.25	0.074
YPH	22-24	37	0.170	1.98	1.272	2.18	0.062
YPH	24-26	39	0.171	1.93	1.344	2.05	0.045

APPENDIX IV

a. Major elements: Fe(%), Si(%), Al(%), Mn(ppm)
b. Trace metals (ppm): Cd, Cr, Cu, Ni, Pb, Zn
c. Trace metals measured by Artesian (ppm): Hg, As

STA	DEPTH	yrsbp	Al (%)	Si (%)	Fe (%)	Mn
CPH	00-02	0	7.23	29.2	3.98	894
CPH	02-04	1.5	7.37	29.3	4.47	891
CPH	04-06	2.5	7.42	29.5	4.27	874
CPH	06-08	3.5	7.43	29.6	4.34	888
CPH	08-10	4.5	8.17	26.7	4.90	1096
CPH	10-12	5.2	7.95	27.7	5.10	1251
CPH	12-14	5.6	7.99	27.7	4.93	1132
CPH	14-16	6	8.16	27.6	4.99	1163
CPH	16-18	6.4	8.27	28.1	4.91	1086
CPH	18-20	6.8	7.39	29.1	4.60	999
CPH	20-22	7.2	7.84	28.1	4.89	1079
CPH	22-24	7.6	8.35	27.5	5.23	1054
CPH	24-26	8	8.21	26.7	5.01	984
JB5	00-02	0	8.23	24.1	3.72	517
JB5	02-04	1.2	5.80	23.9	3.64	435
JB5	04-06	2	6.09	25.1	4.12	505
JB5	06-08	3.8	5.92	26.0	3.82	505
JB5	08-10	5.6	5.83	26.0	3.57	519
JB5	10-12	7.3	5.48	25.2	3.46	530
JB5	12-14	9.1	5.27	24.3	3.40	540
JB5	14-16	10.6	5.94	27.8	3.86	567
JB5	16-18	11.9	6.03	28.4	3.90	561
JB5	18-20	13.2	6.19	27.4	3.71	486
JB5	20-22	14.4	6.08	26.7	3.81	462
JB5	22-24	15.8	6.35	27.4	4.02	501
JB5	24-26	17	6.26	27.8	4.05	512
JB5	26-28	17.7	6.28	27.4	3.83	524
JB5	28-30	18.4	6.22	27.4	3.86	500

STA	DEPTH	yrsbp	Al (%)	Si (%)	Fe (%)	Mn
PC6	00-02	0	6.31	25.6	3.67	477
PC6	02-04	6.1	6.64	26.6	3.87	616
PC6	04-06	10.2	6.42	27.0	3.69	494
PC6	06-08	14	6.39	26.6	3.88	531
PC6	08-10	18	6.11	26.5	3.76	497
PC6	10-12	22	6.13	26.7	3.88	509
PC6	12-14	25.9	6.35	27.1	4.10	549
PC6	14-16	30	6.69	27.0	3.70	534
PC6	16-18	33.9	6.69	27.4	3.80	527
PC6	18-20	37	6.47	27.0	3.86	522
PC6	20-22	39	6.57	26.8	3.91	497
PC6	22-24	41	6.56	25.7	4.06	470
RPH	00-02	0	6.20	27.1	3.94	493
RPH	02-04	2.9	5.97	28.3	3.57	457
RPH	04-06	5.8	6.25	28.5	3.95	504
RPH	06-08	8	6.49	27.7	4.40	582
RPH	08-10	10.3	6.67	27.6	4.38	554
RPH	10-12	12.6	6.71	28.4	4.23	500
RPH	12-14	15	6.82	28.5	4.31	479
RPH	14-16	17.2	6.79	28.8	4.34	520
RPH	16-18	19.6	6.68	28.6	4.13	503
RPH	18-20	21.9	7.01	27.7	4.63	576
RPH	20-22	24.1	6.90	25.9	4.28	481
RPH	22-24	26.5	6.83	27.0	3.78	410
RPH	24-26	28.8	6.98	27.7	4.05	439

STA	DEPTH	yrsbp	Al (%)	Si (%)	Fe (%)	Mn
WD6	00-02	0	8.10	25.7	5.04	1378
WD6	02-04	2.4	8.53	25.7	5.25	1818
WD6	04-06	4	7.70	26.7	4.76	1598
WD6	06-08	4.9	6.51	27.7	4.24	996
WD6	08-10	5.7	6.89	29.2	4.13	763
WD6	10-12	6.6	6.38	24.7	4.31	766
WD6	12-14	7.4	6.97	27.1	4.17	742
WD6	14-16	8.3	6.75	28.6	3.90	753
WD6	16-18	9.1	6.70	28.0	4.32	855
WD6	18-20	10	6.90	27.2	4.19	948
WD6	20-22	10.9	7.39	27.1	4.29	1260
WD6	22-24	11.7	7.13	28.2	4.16	1086
WD6	24-26	12.6	6.90	28.3	4.13	941
WD6	26-28	13.4	7.20	28.3	4.00	930
YPH	00-02	0	7.07	28.1	4.23	485
YPH	02-04	2	6.91	27.6	4.19	464
YPH	04-06	4	7.06	27.2	4.19	493
YPH	06-08	6	7.41	28.6	4.28	606
YPH	08-10	10	7.61	28.3	4.06	558
YPH	10-12	15.6	7.70	28.6	4.31	574
YPH	12-14	22	7.48	29.1	4.05	532
YPH	14-16	26.1	7.48	28.7	4.05	521
YPH	16-18	30.1	7.58	28.6	4.25	548
YPH	18-20	33	7.03	28.2	4.26	552
YPH	20-22	34.9	6.87	28.9	4.34	571
YPH	22-24	37	6.99	30.1	4.27	537
YPH	24-26	39	7.04	30.4	4.10	500

APPENDIX IV b.

STA	DEPTH	yrsbp	Cd	Cr	Cu	Ni	Pb	Zn
CPH	00-02	0	BD	118	37.6	64.0	32.1	231
CPH	02-04	1.5	0.337	150	41.1	76.5	28.7	244
CPH	04-06	2.5	0.279	184	43.1	101.2	26.9	252
CPH	06-08	3.5	0.118	174	42.0	96.0	6.2	252
CPH	08-10	4.5	0.024	166	64.1	89.4	36.0	306
CPH	10-12	5.2	0.138	171	48.7	91.8	39.3	308
CPH	12-14	5.6	0.370	153	50.7	85.6	43.6	309
CPH	14-16	6	0.345	209	56.2	111.4	53.5	358
CPH	16-18	6.4	0.342	133	57.3	69.8	62.5	356
CPH	18-20	6.8	0.032	131	61.4	71.6	74.1	405
CPH	20-22	7.2	0.672	141	66.9	71.8	87.7	467
CPH	22-24	7.6	BD	150	70.1	72.5	91.7	494
CPH	24-26	8	0.177	145	77.3	70.9	93.5	486
JB5	00-02	0	0.172	101	30.1	39.4	8.9	127
JB5	02-04	1.2	0.384	101	29.5	37.2	17.6	127
JB5	04-06	2	0.167	126	31.6	46.9	2.7	132
JB5	06-08	3.8	0.493	118	31.6	43.2	BD	138
JB5	08-10	5.6	0.429	105	32.8	39.8	2.5	136
JB5	10-12	7.3	0.534	98	32.1	33.0	1.7	132
JB5	12-14	9.1	0.330	99	31.1	33.4	7.5	129

STA	DEPTH	yrsbp	Cd	Cr	Cu	Ni	Pb	Zn
JB5	14-16	10.6	0.168	125	26.7	31.2	BD	128
JB5	16-18	11.9	BD	108	25.5	36.8	BD	126
JB5	18-20	13.2	BD	108	23.5	44.4	6.5	124
JB5	20-22	14.4	BD	100	21.7	33.9	5.6	125
JB5	22-24	15.8	0.404	112	27.6	37.5	10.6	131
JB5	24-26	17	BD	113	27.1	45.0	4.7	132
JB5	26-28	17.7	0.296	101	25.0	40.7	6.8	123
JB5	28-30	18.4	0.251	105	29.2	39.9	28.1	158
PC6	00-02	0	BD	102	30.9	47.4	11.6	151
PC6	02-04	6.1	0.210	111	29.9	49.5	12.8	154
PC6	04-06	10.2	0.077	105	31.9	46.6	9.5	145
PC6	06-08	14	BD	109	31.5	43.3	4.2	145
PC6	08-10	18	0.444	107	33.4	43.7	8.9	146
PC6	10-12	22	0.444	115	31.7	45.3	16.4	172
PC6	12-14	25.9	0.078	117	31.6	49.2	10.4	148
PC6	14-16	30	BD	105	33.3	44.4	12.6	146
PC6	16-18	33.9	0.370	101	33.9	44.8	20.3	147
PC6	18-20	37	0.616	104	35.2	49.8	15.1	149
PC6	20-22	39	0.483	99	34.1	38.5	21.5	150
PC6	22-24	41	BD	100	29.8	36.3	10.6	148

STA	DEPTH	yrsbp	Cd	Cr	Cu	Ni	Pb	Zn
RPH	00-02	0	0.259	157	19.4	69.8	8.7	107
RPH	02-04	2.9	BD	84	16.3	22.8	10.7	98
RPH	04-06	5.8	BD	138	19.9	52.2	14.9	105
RPH	06-08	8	0.064	145	21.4	59.8	9.3	120
RPH	08-10	10.3	BD	161	22.6	70.1	14.6	126
RPH	10-12	12.6	BD	139	21.8	56.6	19.3	120
RPH	12-14	15	0.028	127	22.2	50.0	18.2	124
RPH	14-16	17.2	0.385	138	23.3	48.0	15.9	125
RPH	16-18	19.6	BD	140	22.1	59.3	9.5	124
RPH	18-20	21.9	0.188	131	23.7	50.9	17.3	129
RPH	20-22	24.1	BD	120	20.7	44.4	9.7	127
RPH	22-24	26.5	0.077	99	18.9	34.9	11.3	119
RPH	24-26	28.8	BD	115	21.2	41.7	21.7	126
WD6	00-02	0	BD	249	38.5	128.7	13.2	212
WD6	02-04	2.4	BD	207	39.9	110.7	25.3	236
WD6	04-06	4	0.027	174	35.7	86.4	13.1	203
WD6	06-08	4.9	BD	137	31.5	58.8	15.8	162
WD6	08-10	5.7	0.300	120	37.6	64.4	19.4	175
WD6	10-12	6.6	0.176	126	37.9	59.4	19.8	189
WD6	12-14	7.4	BD	117	36.1	56.6	13.8	176

STA	DEPTH	yrsbp	Cd	Cr	Cu	Ni	Pb	Zn
WD6	14-16	8.3	BD	102	29.1	43.1	10.2	147
WD6	16-18	9.1	0.201	109	32.7	54.4	11.1	172
WD6	18-20	10	0.136	126	33.6	54.6	14.1	175
WD6	20-22	10.9	BD	122	33.4	48.9	21.9	183
WD6	22-24	11.7	0.098	106	32.9	40.7	19.4	180
WD6	24-26	12.6	0.219	110	35.6	51.6	12.3	181
WD6	26-28	13.4	0.291	107	34.9	47.5	21.0	177
YPH	00-02	0	0.088	121	28.8	46.0	5.1	137
YPH	02-04	2	0.213	139	23.3	51.3	3.8	131
YPH	04-06	4	BD	124	24.4	42.7	BD	132
YPH	06-08	6	0.047	120	26.3	37.2	BD	138
YPH	08-10	10	0.030	112	25.8	40.4	3.1	140
YPH	10-12	15.6	BD	117	28.3	37.8	6.0	142
YPH	12-14	22	0.281	111	25.1	39.3	6.8	139
YPH	14-16	26.1	0.387	109	26.2	36.4	6.9	145
YPH	16-18	30.1	0.248	123	26.3	40.4	10.4	144
YPH	18-20	33	0.292	121	27.1	39.5	13.4	148
YPH	20-22	34.9	0.227	120	26.4	41.2	8.1	143
YPH	22-24	37	0.200	115	23.2	39.6	2.9	137
YPH	24-26	39	0.215	111	23.1	34.2	2.8	131

APPENDIX IV c.

STA	DEPTH	yrsbp	As	Hg
CPH	00-02	0	3.05	BD
CPH	02-04	1.5	3.97	BD
CPH	04-06	2.5	4.24	BD
CPH	06-08	3.5	4.2	0.166
CPH	08-10	4.5	3.31	BD
CPH	10-12	5.2	2.71	BD
CPH	12-14	5.6	2.9	BD
CPH	14-16	6	3.98	0.215
CPH	16-18	6.4	4.75	0.192
CPH	18-20	6.8	3.79	0.234
CPH	20-22	7.2	4.47	0.271
CPH	22-24	7.6	NS	NS
CPH	24-26	8	NS	NS
JB5	00-02	0	5.85	BD
JB5	02-04	1.2	4.9	BD
JB5	04-06	2	5.7	BD
JB5	06-08	3.8	4.89	BD
JB5	08-10	5.6	5.93	BD
JB5	10-12	7.3	6.23	BD
JB5	12-14	9.1	5.9	BD
JB5	14-16	10.6	4.44	BD
JB5	16-18	11.9	5.15	BD
JB5	18-20	13.2	5.21	BD
JB5	20-22	14.4	9.18	BD
JB5	22-24	15.8	4.78	BD
JB5	24-26	17	4.81	BD
JB5	26-28	17.7	2.22	BD
JB5	28-30	18.4	6.43	1.26

STA	DEPTH	yrsbp	As	Hg
PC6	00-02	0	4.72	BD
PC6	02-04	6.1	5.35	BD
PC6	04-06	10.2	4.65	BD
PC6	06-08	14	4.52	BD
PC6	08-10	18	5.23	BD
PC6	10-12	22	6.06	BD
PC6	12-14	25.9	4.77	BD
PC6	14-16	30	4.28	BD
PC6	16-18	33.9	4.92	BD
PC6	18-20	37	5.08	BD
PC6	20-22	39	4.12	BD
PC6	22-24	41	6.66	BD
RPH	00-02	0	5.02	BD
RPH	02-04	2.9	5.82	BD
RPH	04-06	5.8	6.11	BD
RPH	06-08	8	6.11	BD
RPH	08-10	10.3	4.63	BD
RPH	10-12	12.6	7.4	BD
RPH	12-14	15	6.52	BD
RPH	14-16	17.2	6.31	BD
RPH	16-18	19.6	BD	BD
RPH	18-20	21.9	5.85	BD
RPH	20-22	24.1	4.54	BD
RPH	22-24	26.5	6.06	BD
RPH	24-26	28.8	NS	NS

STA	DEPTH	yrsbp	As	Hg
WD6	00-02	0	5.4	BD
WD6	02-04	2.4	4.66	BD
WD6	04-06	4	8.57	BD
WD6	06-08	4.9	7.58	BD
WD6	08-10	5.7	7.71	BD
WD6	10-12	6.6	5.03	BD
WD6	12-14	7.4	6.76	BD
WD6	14-16	8.3	6.64	BD
WD6	16-18	9.1	7.56	BD
WD6	18-20	10	6.23	BD
WD6	20-22	10.9	4.96	BD
WD6	22-24	11.7	7.3	BD
WD6	24-26	12.6	6.74	BD
WD6	26-28	13.4	5.64	BD
YPH	00-02	0	5.33	BD
YPH	02-04	2	5.78	BD
YPH	04-06	4	5.98	BD
YPH	06-08	6	5.52	BD
YPH	08-10	10	6.67	BD
YPH	10-12	15.6	5.76	BD
YPH	12-14	22	6.06	BD
YPH	14-16	26.1	6.87	BD
YPH	16-18	30.1	8.63	BD
YPH	18-20	33	8.04	BD
YPH	20-22	34.9	NS	NS
YPH	22-24	37	NS	NS
YPH	24-26	39	NS	NS